2017

In Search of Antarctica's Last Vegetation Refugium Within the McMurdo Dry Valleys

David Rau

Louisiana State University and Agricultural and Mechanical College

IN SEARCH OF ANTARCTICA'S LAST VEGETATION REFUGIUM WITHIN THE MCMURDO DRY VALLEYS

A Thesis

Submitted to the Graduate Faculty of the
Louisiana State University and
Agricultural and Mechanical College
in partial fulfillment of the
requirements for the degree of
Master of Science

in

The Department of Geology and Geophysics

by
David Rau
B.S., Louisiana State University, 2014
May 2017

ACKNOWLEDGEMENTS

I wish to extend my gratitude to everyone who has contributed to make this study possible. I would like to thank my major advisor, Dr. Warny; my committee members, Dr. Bart and Dr. Doran for providing guidance. Thanks are extended to Boston University for collecting samples and providing the sedimentological expertise to this project. I am grateful for results from a pilot study conducted by Dr. Warny and Dr. Askin that provided invaluable guidance and additional results for this project. I am grateful for the aid I received from the Polar Geospatial Center and the Environmental Research and Assessment organizations. I am grateful for my peers in the CENEX office at Louisiana State University for their help and moral boost. Funding for this project was provided by NSF OPP CAREER Grant #1048343 to SW.

TABLE OF CONTENTS

LIST OF TABLES

LIST OF FIGURES

LIST OF PLATES

ABSTRACT

The McMurdo Dry Valleys, a hyper-arid cold polar desert located within the Transantarctic Mountains was once covered by vegetation. An in depth study of surface samples of various Neogene age, acquired throughout the Valleys, provide insight to the location of one of Antarctica's last vegetation refugia. Boston University's Antarctic Research Group has collected 82 surface samples from paleo lake sediments on 14 expeditions spanning 22 years in the McMurdo Dry Valleys. The ages of the samples are still not fully constrained, but 8 regions where samples were collected have been interpreted to range between 16.95 ± 0.17 to 4 Ma old (Marchant, pers. comm.). Results show the palynomorph assemblage diversity is low with a terrestrial assemblage dominated by southern beech *Nothofagus* spp. (fusca group), and the nonterrestrial assemblage is dominated by ice-indicative acritarch *Leiosphaeridia* spp. with some samples containing spores of the fresh water algae Zygnemataceae. Based on palynological concentrations recovered, the Victoria Valley and Beacon Valley may have been the site for vegetation refugia. Samples collected from Victoria Valley have concentrations ranging from 252.1 to 5191.1 gdw^{-1} and nonterrestrial derived palynomorph concentrations ranging from 735.6 to 2386.1 gdw^{-1}. The Central Beacon Valley has a terrestrial-derived palynomorph concentration of 131.8 to 675.3 gdw^{-1}. These concentration ranges are higher than other sample locations analyzed for this study such as the Olympus Range, Taylor Valley, and valleys located in the Asgard Range, with samples concentrations that are barren to 17.4 gdw^{-1} for the Olympus Range, barren to 1.4 gdw^{-1} for Taylor Valley, and barren to 39.6 gdw^{-1} sites in the Asgard Range. Based on the present study, the Victoria Valley and Beacon Valley regions acted as refugia for isolated pockets of vegetation to survive around the Mid-Miocene and >8.07±0.06 Ma based on their palynomorph assemblages and concentrations. These sites potentially were ideal locations where geological processes such as erosion and transportation did not influence the geologic record, thus preserving these sites. The results in this study provide detailed information to be utilized for future expeditions into the region to precisely time vegetation's demise within the McMurdo Dry Valleys.

CHAPTER 1: INTRODUCTION

The Transantarctic Mountains are a physiological and geological boundary between the East and West Antarctic continental blocks. They extend 4,500 km from the Ross Sea to the Weddell Sea (Anderson, 1996). Glacier ice extends over much of the Transantarctic Mountains, however there are areas predominately free of ice. This study focuses on palynology of surface sediment samples from the McMurdo Dry Valleys, a region within Victoria Land that lies 100 km to the west of McMurdo Station and McMurdo Sound, between the East Antarctic Ice sheet and the Ross Sea within the Transantarctic Mountains. The McMurdo Dry Valleys (Figure 1) cover an area approximately 22,700 km^2 of which 4,500 km^2 is ice-free. This makes it the largest ice-free area in Antarctica (Levy, 2013). Sections of the Dry valleys remain ice-free because the Transantarctic Mountains block ice flow into the region from the nearby Polar Plateau (Doran et al., 1994). Today, the region is classified as a hyper-arid and cold-polar desert with temperatures ranging from -1°C to -40°C and precipitation ranging from 5 to 400 mm weq (Doran et al. 2002; Fountain et al. 2009). Very Little is currently known about the on land late Miocene and Early Pliocene vegetation history within the region. This study aims to answer three research questions that characterize part of the Cenozoic history of the region: where can the last remnants of vegetation be found in the dry valleys, what types of vegetation existed during the final stages, and when did the vegetation exist and shift to its current state of rare angiosperms, lichens, mosses, liverworts, or lack of vegetation. To answer these questions, the first in depth surface sample palynological analysis of the McMurdo Dry Valleys was conducted.

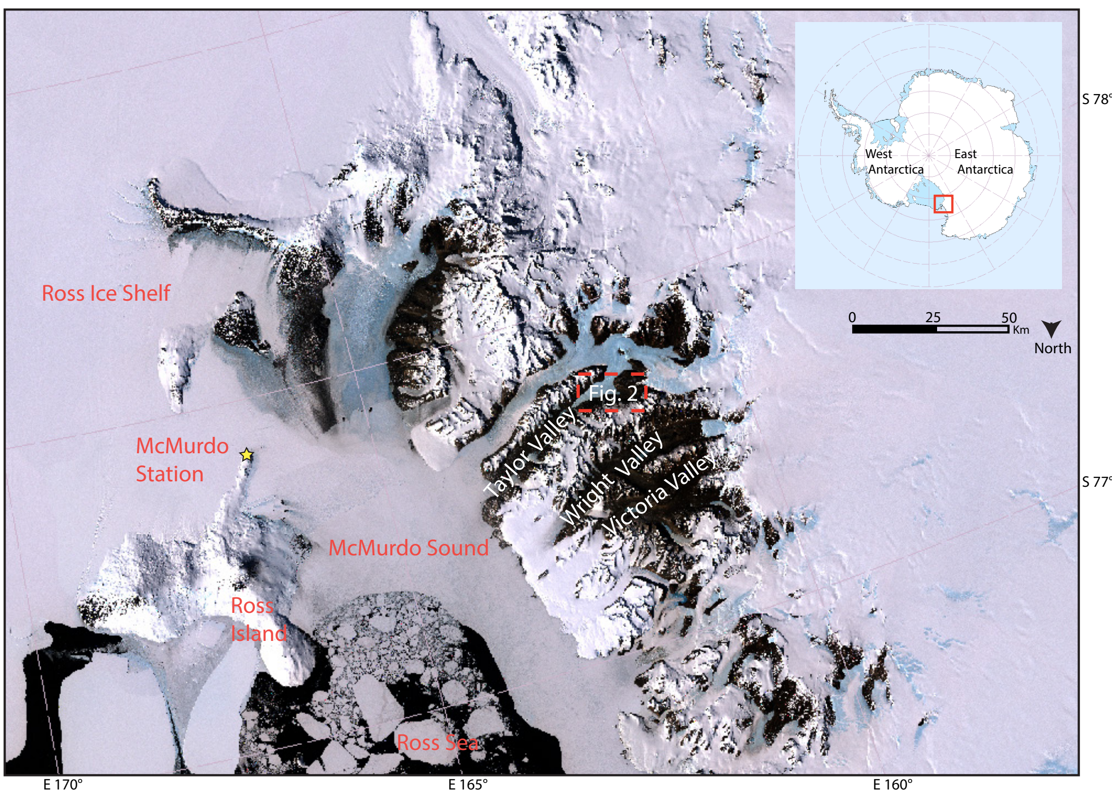

Figure 1: Landsat Image Mosaic Of Antarctica (LIMA) satellite image of the McMurdo Dry Valleys showing an overview of the study region, surrounding area, and the location of Figure 2 within Taylor Valley (Geomap App, 2017).

1.1 Geologic History

The McMurdo Dry Valleys basement rock is composed of pre-Cambrian to Paleozoic age granites and gneisses, which were produced and metamorphosed during the Cambrian-Ordovician Ross Orogeny. Outcrops of the basement rock can be observed below 800 m elevation near the Ross Sea coast and in the central portions of the McMurdo Dry Valleys (Marchant and Head, 2007). An unconformity called the Kukri Peneplain eroded into the basement rock (Barrett, 1981). The bedrock consists of flat lying Devonian to Triassic age sandstones, siltstones, and conglomerates that make up the Beacon Supergroup (Marchant and Head, 2007). Thick deposits of a Jurassic age intrusive sills called the Ferrar Dolerite is present throughout the Beacon Supergroup ranging from 200 to 300 m in thickness as can been seen in Figure 2 (Elliot and Fleming, 2004). Jurassic aged Kirkpatrick Basalt overlay and cap the Beacon Supergroup (Barrett, 1981). It appears that many of the Cretaceous Cenozoic units deposited after the deposition of the Beacon Supergroup have been largely eroded. A 160 Ma time gap occurs in most of

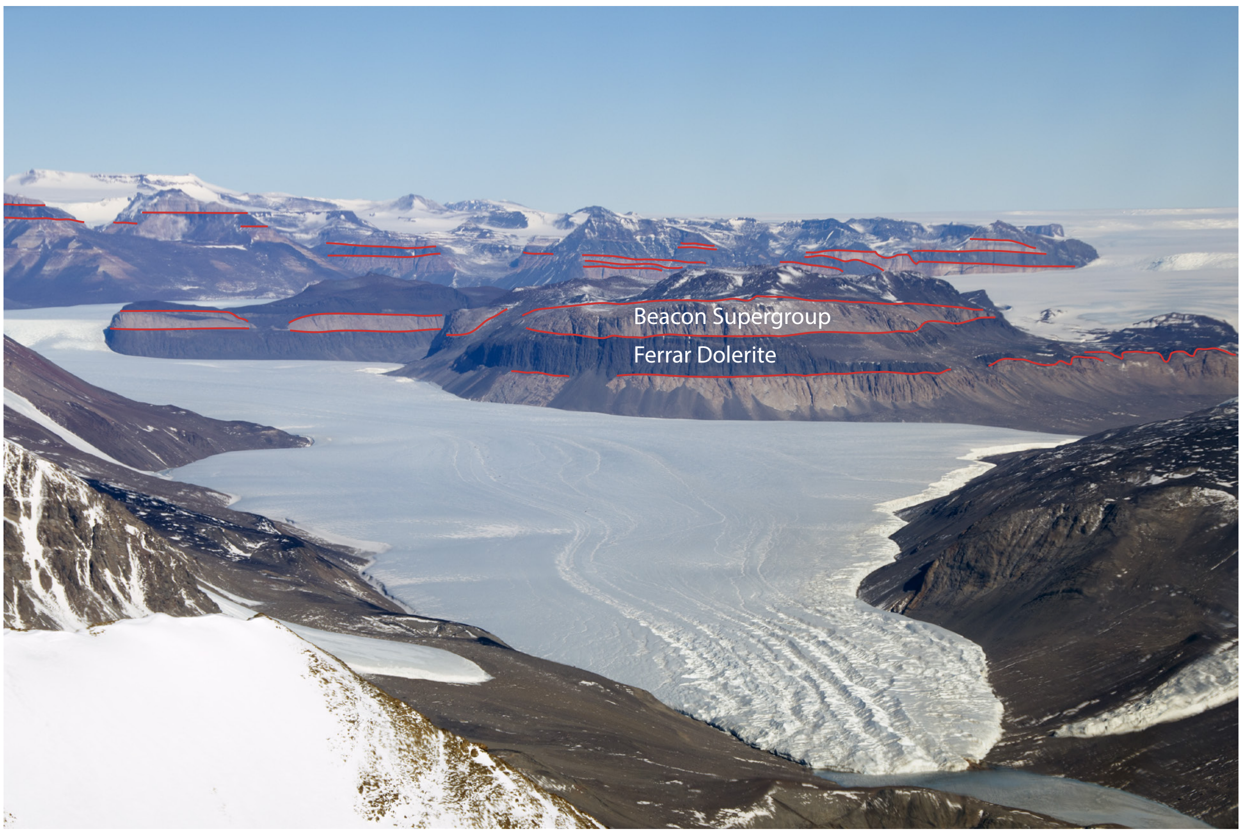

Figure 2: Aerial photograph overlooking Taylor Glacier within Taylor Valley. Two geologic features of the region, the Beacon Supergroup and the Ferrar Dolerite, are visible and outlined. The Beacon supergroup is composed of the lighter colored unit, and the Ferrar Dolerite sill is composed of the darker intruded layer (NASA, 2013).

the geologic record of the McMurdo Dry Valleys. The area remained active, with for instance the eruptions of alkaline basalts during the early Miocene. Volcanic activity still occurs today on the nearby Ross Island, and volcanic ash deposits have been found throughout the region (Armstrong, 1978; Marchant et al, 1996). The geologic record outcropping within the McMurdo Dry Valleys has very few Cenozoic units preserved (Thomson et al., 1991), but we know that extensive deposition occurred as thick Cenozoic sedimentary units have been recovered from the nearby basins. Figure 3 shows the location of some of these recent drilling project, e.g., CRP, DVDP, MSSTS, CIROS, and ANDRILL drilling projects off the McMurdo Dry Valley coast, and two

DVDP drill sites located in Taylor Valley. CIROS-1, CRP, and ANDRILL SMS have drilled portions of the geologic record from the Oligocene to the Pleistocene (Harwood et al., 1998; Roberts et al., 2003; Acton et al., 2008). Thomson et al. (1991) have attributed the missing geologic record to glacial erosion by Pliocene and Pleistocene ice sheets in that Ross sector of Antarctica.

Figure 3: Modified Overview ASMA No. 2 McMurdo Dry Valleys map showing sample site locations and nearby drill program locations (ERA, 2017).

The genesis of the Transantarctic Mountains is problematic and various studies and models have been done to try and explain its formation and timing (Anderson, 1999). One study by Fitzgerald et al. (1986) proposes a passive rift model to account for quick large uplift of the Transantarctic Mountains. Their study suggests that the Ross Orogeny is the source for

a shallow crustal penetrative detachment zone, which explains subsidence in the Ross Sea and uplift in the Transantarctic Mountains. Stern and Ten Brink's (1989) model represents East and West Antarctica's lithosphere as a cantilevered elastic beam that can move freely with respect to the lithosphere boundary. The study suggests that the Terror Rift was the source for depression to the East of the Transantarctic Mountains and subsequent flexure. However, later studies argue that the Terror Rift is not extensive enough to support Stern and Ten Brink's 1989 model (Cooper and Davey, 1987; Ten Brick et al., 1993). Ten Brink et al. (1993) interpreted that the formation of the Transantarctic Mountain originated from thermal buoyancy.

Apatite fission-track studies have been done to understand the timing of the uplift within the Transantarctic Mountains. Fission Track studies are a radiometric dating technique where spontaneous decay of uranium-238 creates damage marks or tracks minerals and glass that can be analyzed to interpret the age of the clast. The uplift has been interpreted to initiate in the Early to Middle Eocene around 55-50 million years ago (Gleadow and Fitzgerald, 1987; Fitzgerald and Gleadow, 1988; Fitzgerald, 1992). The range of uplift has been interpreted to be 4.8 to 6 km with a rate of uplift averaging 100 m/Ma (Gleadow and Fitzgerald, 1987; Fitzgerald and Gleadow, 1990; Fitzgerald, 1992). Behrendt and Cooper (1991) argue that the Transantarctic Mountains have been rising at 1 km/Ma periodically with the most recent uplift event occurring in the mid-Pliocene. Fitzgerald (1994) interprets that the Transantarctic Mountains are composed of discrete blocks that can have different rates of uplift, and that the apatite fission-track data cannot confirm or deny high uplift rates in the Pliocene.

1.2 Paleoenvironment History

Before the Eocene/Oligocene Transition (33.9 Ma), Antarctica had a relatively rich diversity of vegetation (Askin, 1992, 1997, 2000; Truswell and MacPhail, 2009, Warny and Askin, 2011a; Anderson et al., 2011; Feakins et al., 2014; Griener et al., 2013; Griener et al., 2015; Griener and Warny, 2015). At that time, the Ross Sea region likely experienced mean annual temperature greater than 10°C and precipitation rates greater than 1000 mm/yr, suggesting that the winter conditions were hospitable enough to support temperate rainforests (Francis et al., 2008, Warny and Askin, 2011a; Pross et al., 2012; Feakins et al., 2014). At the Eo-Oligocene boundary, the abrupt increase in $\delta_{18}O$ values and a decrease in pCO_2 concentrations known from offshore records (DeConto and Pollard, 2003; Zachos et al., 2008; Pagani et al., 2011) are known to coincide with the first major growth of the Antarctic Ice Sheet (Zachos et al., 2001). Palynological studies conducted in Antarctica targeting strata that are younger than 35 Ma show the gradual disappearance of vegetation (Askin and Raine, 2000; Raine and Askin, 2001; Prebble et al., 2006; Warny and Askin, 2011b; Anderson et al., 2011). This abrupt decline of terrestrial palynomorph concentration around the Eocene-Oligocene (E-O) boundary also attests to the drastically cooling conditions (Warny and Askin 2011a,b; Feakins et al., 2014). Griener et al. (2013) analysis of $\delta_{13}C$ of *Nothofagus* pollen grains indicates that the climate not only was getting colder, but moisture availability decreased dramatically at that time as well. There are a few exceptions to the general post E-O boundary cooling trend, in particular around 15.7 Ma when vegetation was able to recolonize the Ross Sea region during the Mid-Miocene Climatic Optimum (Warny et al., 2009; Levy et al., 2016). Warny et al. (2009) have estimated land temperatures to rise up to 10°C and sea-surface temperatures ranged from 0 to 11.5 °C based on palynomorph assemblage they recovered. Feakins et al. (2012) conducted a hydrogen isotopic analysis of leaf wax extracted from the same samples as those studied by Warny et al. (2009), and their results indicated that available moisture increased briefly but sharply around 15.8 Ma and that moisture availability was one of the factors that allowed for vegetation re-colonization during the Mid Miocene Climatic Optimum in the Ross Sea region.

The post E-O boundary vegetation up to the middle Miocene is characterized by tundra with prostrate woody plants located within secluded shelters (Raine, 1998; Askin and Raine, 2000; Warny et al., 2009). The post MMCO demise of the vegetation in Antarctica occurred at different times depending on location. Lewis et al. (2008) provided strong evidences that the

McMurdo Dry Valleys was able to support vegetation up to at least 13.85 Ma while the Antarctic Peninsula was able to support vegetation until 12.8 Ma (Warny and Askin, 2011b; Anderson et al., 2011), but these dates are based on only two sites. Very little is known on the Late Miocene and Pliocene vegetation and when exactly the vegetative cover evolved to its current state of essentially only lichens, mosses and liverworts. This study presents the first in-depth palynological surface sample analyses of the Dry Valleys. The objective is to locate, characterize, and time the history of the final vegetation cover that existed in the Dry Valleys.

CHAPTER 2: MATERIAL AND METHODS

Eighty-two paleo lake sediment samples were collected for our palynological analysis. Boston University's Antarctic Research Group acquired the samples over the course of 22 years and 14 expeditions (Figure 4). The samples for this study were gathered from 18 different locations, which include various Olympus Range locations, Mount Flemming, various Asgard Range locations, Beacon Valley region, Arena Valley, Catspaw Glacier, Stocking Glacier, Miers Divide, Rhone Platform, Bulls Pass, and Victoria Valley. The on-land stratigraphic record for the McMurdo Dry Valleys is not well known. Personal Communication with Dr. David Marchant of Boston University has provided precise interpreted dates for regions of the McMurdo Dry Valleys (shown in Table 1). These ages range from 16.95 ± 0.17 Ma at the Dry Valley coast to roughly 4 Ma for till in the upper Beacon Valley.

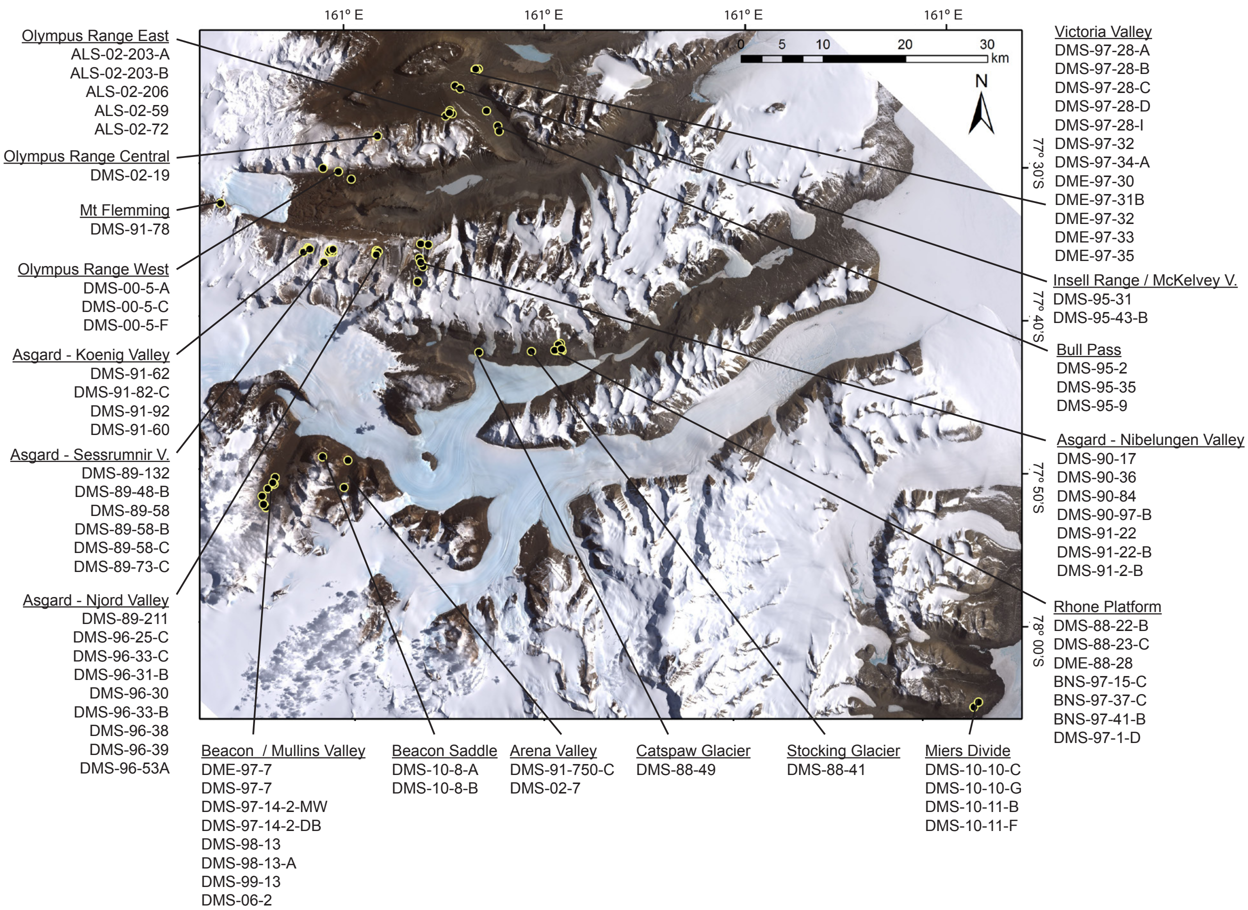

Figure 4: Satellite map showing the sample site locations of palynological samples gathered by Boston University's Antarctic Research Group throughout the McMurdo Dry Valleys (Boston University, 2015).

The samples were sent to Global Geolab Limited for palynological processing. The processing included acid digestion, heavy liquid separation, controlled oxidation, and slide mounting. During the acid digestion phase, 25-55 grams of the sample was exposed to a 10% hydrochloric acid solution and to a 70% hydrofluoric acid solution to dissolve the carbonate and siliceous matrix. The next step consisted in utilizing 25 ml of $ZnBr_2$ (density of 2 g/ml) to separate the microfossils from the residue. The supernatant was then decanted and exposed to 3 ml of Schultze reagent (mixture of $KClO_3$ and HNO_3) and placed in a hot plate to briefly oxidize the residue for the ease of identification. The final step was to mount the residue onto a microscope slide by mixing

the residue with glycerin and placing them onto a glass slide with a cover slip.

Figure 5 and Table 1 presents a summary of all available and interpreted data associated with this study, and places the study samples in a global climate contex along with Lewis et al. 2008 and Warny et al. 2009 studies.

Table 1: Summary table containing Sample ID, Sample Region, Sample GIS Latitude/Longitude, modern values for altitude, temperature, and precipitation, the inferred age of each sample, the basis for the age inference, and the Terrestrial Palynomorph Concentration (TCC) and Marine and Freshwater Palynomorph Concentration (MCC).

Sample ID	Sample Region	Latitude	Longitude	Altitude (m)	Temp. (°C)	Precipitation (mm weq)	Inferred age	Basis	TCC (GDW^-1)	MCC (GDW^-1)
				Modern Val.	Modern Val.	Modern Val.				
DMS-10-10-C	Royal Society Range	-78.09	164.269	500 ± 50m	-7	100	16.95 ± 0.17	Argon 40/39 date on interbedded ash	1.4	0
DMS-10-10-G	Royal Society Range	-78.09	164.269	500 ± 50m	-7	100	16.95 ± 0.17	Argon 40/39 date on interbedded ash	0	0
DMS-10-11-B	Royal Society Range	-78.09	164.269	500 ± 50m	-7	100	16.95 ± 0.17	Argon 40/39 date on interbedded ash	1.4	0
DMS-10-11-F	Royal Society Range	-78.09	164.269	599 ± 50m	-7	100	16.95 ± 0.17	Argon 40/39 date on interbedded ash	0.8	0
DMS-94-004	Miers Divide	-78.084	164.292	500 ± 50m	-7	100	16.95 ± 0.17	Argon 40/39 date on interbedded ash	0	0
DME-91-60	Asgard Range - Koenig Valley	-77.597	160.81	1475 ± 50m	-20	100	13.67±0.10	Correlated with Argon 40/39 date on nearby ash	107.9	0
DMS-91-62	Asgard Range - Koenig Valley	-77.596	160.801	1475 ± 50m	-20	100	>13.56 Ma	Strat correlation	0.9	0
DMS-91-82-C	Asgard Range - Koenig Valley	-77.597	160.805	1475 ± 50m	-20	100	>13.56 Ma	Strat correlation	642.7	304.6
DMS-91-92	Asgard Range - Koenig Valley	-77.6	160.779	1475 ± 50m	-20	100	>13.56 Ma	Strat correlation	1.3	0
DME-96-30	Asgard Range - Njord Valley	-77.6	161.151	1675 ± 50m	-20	100	13.67±0.10	Correlated with Argon 40/39 date on nearby ash	9.2	0
DME-96-31B	Asgard Range - Njord Valley	-77.6	161.148	1675 ± 50m	-20	100	13.67±0.10	Correlated with Argon 40/39 date on nearby ash	4.3	3.5
DME-96-33B	Asgard Range - Njord Valley	-77.6	161.151	1675 ± 50m	-20	100	13.67±0.10	Correlated with Argon 40/39 date on nearby ash	39.6	0
DME-96-38	Asgard Range - Njord Valley	-77.601	161.156	1675 ± 50m	-20	100	13.67±0.10	Correlated with Argon 40/39 date on nearby ash	4	0
DME-96-39	Asgard Range - Njord Valley	-77.601	161.158	1675 ± 50m	-20	100	13.67±0.10	Correlated with Argon 40/39 date on nearby ash	1.2	0.2
DME-96-53A	Asgard Range - Njord Valley	-77.604	161.149	1675 ± 50m	-20	100	13.67±0.10	Correlated with Argon 40/39 date on nearby ash	0.4	0.2
DMS-02-11-B	Asgard Range - Njord Valley	-77.616	161.382	1675 ± 50m	-20	100	>14.8 Ma	Strat correlation	0.3	0
DMS-89-211	Asgard Range - Njord Valley	-77.604	161.146	1675 ± 50m	-20	100	14.55 ± 0.06	Argon 40/39 date on interbedded ash	0.3	0
DMS-96-25-C	Asgard Range - Njord Valley	-77.6	161.149	1675 ± 50m	-20	100	13.67±0.10	Argon 40/39 date on interbedded ash	0.5	0
DMS-96-33-C	Asgard Range - Njord Valley	-77.6	161.149	1675 ± 50m	-20	100	13.67±0.10	Argon 40/39 date on interbedded ash	0	0
DMS-90-17	Asgard Range - Nibelungen Valley	-77.593	161.373	1675 ± 50m	-20	100	>14.8 Ma	Strat correlation	0	0
DMS-90-36	Asgard Range - Nibelungen Valley	-77.594	161.413	1675 ± 50m	-20	100	10.08 ± 0.17 Ma	Argon 40/39 date on interbedded ash	0.8	0
DMS-90-84	Asgard Range - Nibelungen Valley	-77.618	161.385	1675 ± 50m	-20	100	>13.56 Ma	Strat correlation	0.4	0
DMS-90-97-B	Asgard Range - Nibelungen Valley	-77.609	161.365	1675 ± 50m	-20	100	>13.56 Ma	Strat correlation	1.2	0
DMS-91-2-B	Asgard Range - Nibelungen Valley	-77.613	161.373	1675 ± 50m	-20	100	>14.8 Ma	Strat correlation	0.5	0
DMS-91-22	Asgard Range - Nibelungen Valley	-77.634	161.355	1675 ± 50m	-20	100	15.01 ± 0.02	Argon 40/39 date on interbedded ash	0.6	0
DMS-91-22-B	Asgard Range - Nibelungen Valley	-77.634	161.355	1675 ± 50m	-20	100	>15.01 ± 0.02	Argon 40/39 date on interbedded ash	0.7	0
DMS-89-132	Asgard Range - Sessrumnir Valley	-77.612	160.88	1500 ± 50m	-20	100	10.12 ± 0.13	Argon 40/39 date on interbedded ash	0.2	0
DMS-89-48-B	Asgard Range - Sessrumnir Valley	-77.601	160.906	1500 ± 50m	-20	100	>13.56 Ma	Strat correlation	0.9	0
DMS-89-58	Asgard Range - Sessrumnir Valley	-77.601	160.928	1500 ± 50m	-20	100	>13.56 Ma	Strat correlation	1.5	0
DMS-89-58-B	Asgard Range - Sessrumnir Valley	-77.6	160.92	1500 ± 50m	-20	100	>14.8 Ma	Strat correlation	0.4	0
DMS-89-58-C	Asgard Range - Sessrumnir Valley	-77.599	160.913	1500 ± 50m	-20	100	>14.8 Ma	Strat correlation	0.6	0
DMS-89-73-C	Asgard Range - Sessrumnir Valley	-77.598	160.929	1500 ± 50m	-20	100	>13.56 Ma	Strat correlation	0	0
DMS-91-78	Mt. Flemming	-77.545	160.365	1700 ± 50m	-20	100	>14.8 Ma	Strat correlation	4.1	0
DMS-95-2	Bull Pass	-77.465	161.767	575 ± 50m	-8	100	Presumed Middle Miocene	Strat correlation	0	0
DMS-95-35	Bull Pass	-77.449	161.711	575 ± 50m	-8	100	Presumed Middle Miocene	Strat correlation	1.1	1.5
DMS-95-9	Bull Pass	-77.471	161.774	575 ± 50m	-8	100	Presumed Middle Miocene	Strat correlation	0	0
DMS-02-19	Olympus Range (Boreas site)	-77.475	161.163	1400 ± 50m	-20	200	14.07 ± 0.05 Ma	Strat correlation with dated ash in nearby lacustrine sediments	0.9	1.6
ALS-02-203-A	Olympus Range (East)	-77.448	161.527	1375 ± 50m	-20	200	14.07 ± 0.05 Ma	Strat correlation with dated ash in nearby lacustrine sediments	0.9	0
ALS-02-203-B	Olympus Range (East)	-77.448	161.527	1375 ± 50m	-20	200	14.07 ± 0.05 Ma	Strat correlation with dated ash in nearby lacustrine sediments	0.3	0
ALS-02-206	Olympus Range (East)	-77.452	161.538	1375 ± 50m	-20	200	14.07 ± 0.05 Ma	Strat correlation with dated ash in nearby lacustrine sediments	0	0.4
ALS-02-59	Olympus Range (East)	-77.454	161.506	1375 ± 50m	-20	200	14.07 ± 0.05 Ma	Strat correlation with dated ash in nearby lacustrine sediments	2.2	0
ALS-02-72	Olympus Range (East)	-77.45	161.524	1375 ± 50m	-20	200	14.07 ± 0.05 Ma	Strat correlation with dated ash in nearby lacustrine sediments	0.2	0
DMS-00-5-A	Olympus Range (West)	-77.509	160.886	1350 ± 50m	-15	100	> 10 Ma	Strat correlation	0.4	0
DMS-00-6-C	Olympus Range (West)	-77.513	160.962	1350 ± 50m	-15	100	> 10 Ma	Strat correlation	2.1	0
DMS-00-8-F	Olympus Range (West)	-77.522	161.028	1350 ± 50m	-6	50	> 10 Ma	Strat correlation	12.9	0
DMS-95-31	Insell Range/ McKelvey Valley	-77.421	161.555	575 ± 50m	-9	100	Presumed Middle Miocene	Strat correlation	4.2	0.4
DMS-95-43-B	Insell Range/ McKelvey Valley	-77.424	161.579	575 ± 50m	-9	100	Presumed Middle Miocene	Strat correlation	0.6	0.3
DME-97-30	Victoria Valley	-77.404	161.66	575 ± 50m	-5	200	Presumed Middle Miocene	Ash yet to be dated	1292	735.6
DME-97-31B	Victoria Valley	-77.405	161.659	575 ± 50m	-5	200	Presumed Middle Miocene	Ash yet to be dated	5017.6	2247.5
DME-97-32	Victoria Valley	-77.404	161.656	575 ± 50m	-5	200	Presumed Middle Miocene	Ash yet to be dated	0	0
DME-97-33	Victoria Valley	-77.405	161.662	575 ± 50m	-5	200	Presumed Middle Miocene	Ash yet to be dated	31.4	1.4
DME-97-35	Victoria Valley	-77.403	161.658	575 ± 50m	-5	200	Presumed Middle Miocene	Ash yet to be dated	27.4	2
DMS-97-28-A	Victoria Valley	-77.403	161.66	575 ± 50m	-5	200	Presumed Middle Miocene	Ash yet to be dated	5159.1	2386.1
DMS-97-28-B	Victoria Valley	-77.403	161.66	575 ± 50m	-5	200	Presumed Middle Miocene	Ash yet to be dated	29	3
DMS-97-28-C	Victoria Valley	-77.404	161.663	575 ± 50m	-5	200	Presumed Middle Miocene	Ash yet to be dated	4796.1	131.9
DMS-97-28-D	Victoria Valley	-77.404	161.663	575 ± 50m	-5	200	Presumed Middle Miocene	Ash yet to be dated	4087.4	513.1
DMS-97-28-I	Victoria Valley	-77.404	161.663	575 ± 50m	-5	200	Presumed Middle Miocene	Ash yet to be dated	0.6	0
DMS-97-32	Victoria Valley	-77.404	161.655	575 ± 50m	-5	200	Presumed Middle Miocene	Ash yet to be dated	252.1	1575.3
DMS-97-34-A	Victoria Valley	-77.403	161.67	575 ± 50m	-5	200	Presumed Middle Miocene	Ash yet to be dated	4.2	0
DMS-02-7	Arena Valley	-77.857	160.964	1300 ± 50m	-11	75	11.27±0.12 Ma	Argon 40/39 date on interbedded ash	0	0
DMS-91-750-C	Arena Valley	-77.828	160.986	1300 ± 50m	-11	75	11.28±0.05 Ma	Argon 40/39 date on interbedded ash	0.8	0
DMS-10-8-A	Beacon Saddle	-77.823	160.854	1750 ± 50m	-20	75	Middle Miocene	Strat correlation	0.2	0
DMS-10-8-B	Beacon Saddle	-78.823	161.854	1750 ± 50m	-20	75	Middle Miocene	Strat correlation	0.6	0
DME-06-9	Beacon Valley - Mullins Glacier	-77.857	160.569	1350 ± 50m	-12	75	>7.69±0.01 Ma	Argon 40/39 date on interbedded ash	39.7	7.3
DME-97-7	Beacon Valley - Taylor Glacier	-77.852	160.601	1350 ± 50m	-12	75	>8.07±0.06 Ma	Argon 40/39 date on interbedded ash	69.7	0
DMS-99-2-A	Beacon Valley, Granite drift	-77.845	160.608	1350 ± 50m	-12	75	8.07±0.06 Ma	Argon 40/39 date on interbedded ash	0	0
DMS-97-7	Beacon Valley, Granite driftr	-77.852	160.601	1350 ± 50m	-12	75	>8.07±0.06 Ma	Argon 40/39 date on interbedded ash	0.2	0.5
EME-98-13	Beacon Valley, Mullins Glacier	-77.865	160.538	1350 ± 50m	-12	75	7.69±0.01 Ma	Argon 40/39 date on interbedded ash	131.8	0
NEST SITE ICE	Beacon Valley, Mullins Glacier nest site	-77.874	160.544	1350 ± 50m	-12	75	> 4 Ma	Average of multiple Argon 40/39 dates on overlying ash	17.7	15.3
DMS-98-13-A	Beacon Valley, Mullins till	-77.877	160.556	1350 ± 50m	-12	75	8.07±0.06 Ma	Argon 40/39 date on interbedded ash	0	0
DMS-06-2	Beacon Valley, nest site	-77.874	160.544	1400 ± 50m	-12	75	> 4 Ma	Average of multiple Argon 40/39 dates on overlying ash	8.3	0.3
DMI-97-14-2-DEBRIS	Central Beacon Valley	-77.851	160.595	1350 ± 50m	-12	75	>8.07±0.06 Ma	Argon 40/39 date on interbedded ash	675.3	0
DMI-97-14-2-MELTWATER	Central Beacon Valley	-77.851	160.595	1350 ± 50m	-12	75	>8.07±0.06 Ma	Argon 40/39 date on interbedded ash	0.4	0.3
BNS-97-15-C	Taylor Valley - Rhone	-77.702	162.082	1200 ± 50m	-4	50	>10.76±0.17	Strat correlation	0.4	0
BNS-97-37-C	Taylor Valley - Rhone	-77.704	162.072	1200 ± 50m	-4	50	>10.76±0.17	Strat correlation	1.1	0
BNS-97-41-B	Taylor Valley - Rhone	-77.71	162.066	1000 ± 50m	-4	50	10.76±0.17	Strat correlation	0	0
DMS-88-22-B	Taylor Valley - Rhone	-77.711	162.091	1000 ± 50m	-4	50	10.76±0.16	Strat correlation	0.7	0
DMS-88-23-C	Taylor Valley - Rhone	-77.711	162.082	1000 ± 50m	-4	50	10.76±0.16	Argon 40/39 date on interbedded ash	0.7	0
DMS-88-41	Taylor Valley - Rhone	-77.711	161.934	1000 ± 50m	-4	50	10.76±0.16	Strat correlation	1.4	0
DMS-88-49	Taylor Valley - Rhone	-77.712	161.665	1000 ± 50m	-4	50	10.76±0.16	Strat correlation	0.9	0
DMS-97-1-D	Taylor Valley - Rhone	-77.71	162.054	1000 ± 50m	-4	50	10.09±0.16	Argon 40/39 date on interbedded ash	0.5	0
DME-88-28	Rhone Platform	-77.709	162.088	1000 ± 50m	-4	50	10.76±0.16	Strat correlation	76.7	4.4

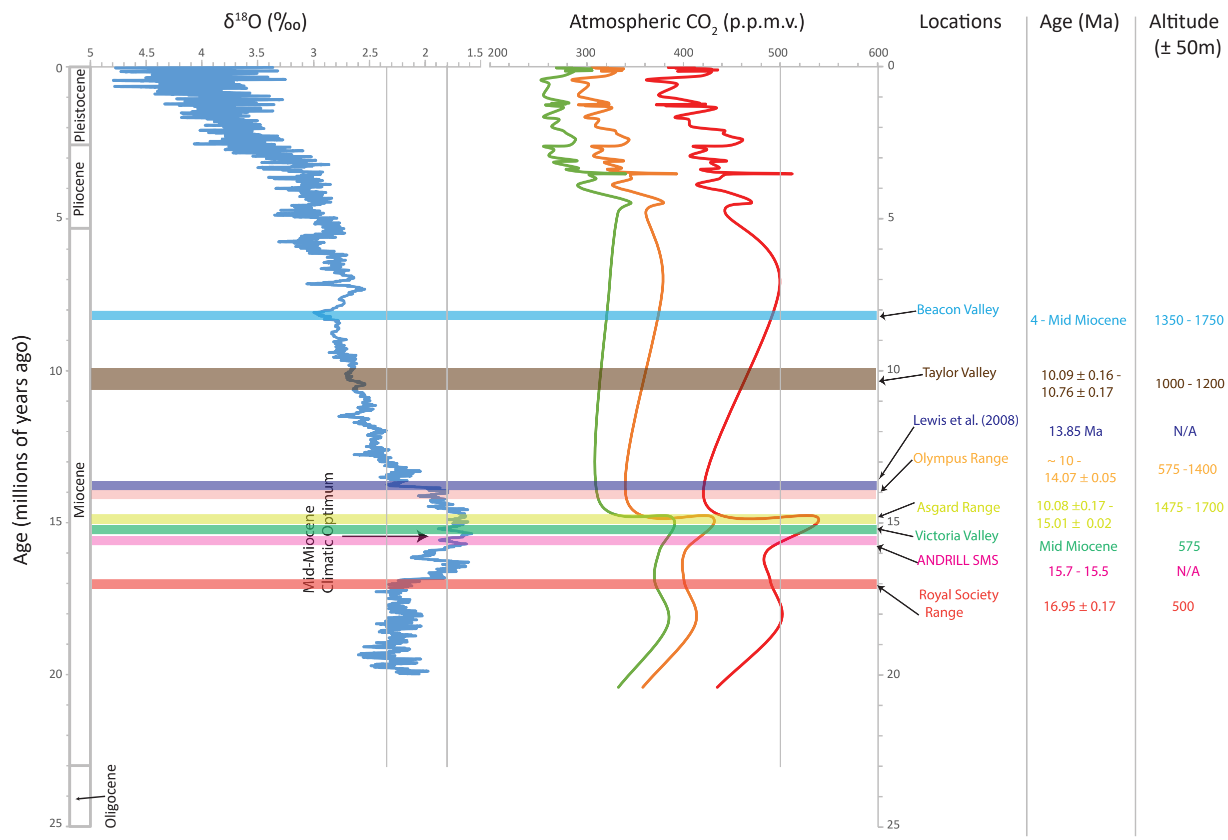

Figure 5: General sample regions with inferred age and altitude plotted on early Cenozoic history plots of Oxygen 18 isotope data and Atmospheric Carbon Dioxide data modified from Zachos et al. 2011 and Zhang et al. 2013. Oxygen 18 was plotted utilizing a running average of 15 of original data, and Carbon Dioxide was plotted using minimum, average, and maximum values of original data.

CHAPTER 3: RESULTS AND DISCUSSION

Figure 6, 7, 8, 9, 11, and 15, and Tables 2-7 present the results of the palynological tabulation completed. All 82 samples have been fully analyzed and all fossilized palynomorphs iden-

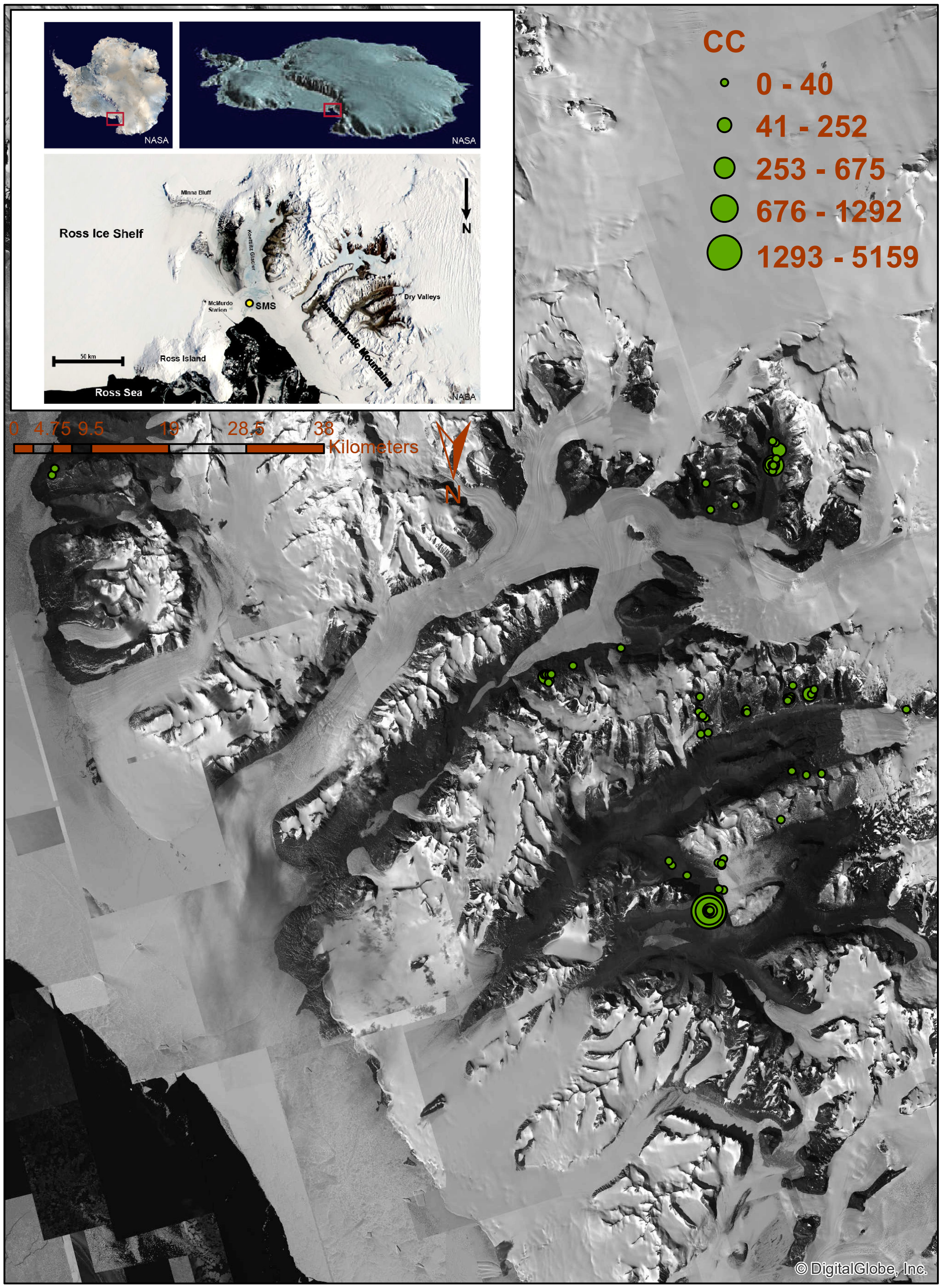

Figure 6: Sample spatial plot map of the McMurdo Dry Valley region utilizing WorldView-1, WorldView-2. QuickBird-2, and GeoEye-1 high resolution imagery. All samples' (with the exception of DMS-91-82-C) terrestrial sourced palynomorph concentration is plotted by circles with varying diameters based on concentration values (Polar Geospatial Center and DigitalGlobe, Inc., 2017).

tified and counted. Most of the samples required the examination of multiple slides as recovery was very low. Many of the locations studied turned out to be barren in palynomorphs. There are notable exceptions, 7 of the 82 samples provided an excellent recovery giving us details on what type of vegetation was growing, where, and when. These productive samples include samples DME-97-30, DME-97-31B, DMI-97-14-2 (debris), DMS-97-28D, DMS-97-28C, DMS-97-28A, DMS-97-32. Samples DME-97-30, DME-97-31B, DMS-97-28D, DMS-97-28C, DMS-97-28A, and DMS-97-32 were collected from Victoria Valley and have terrestrial derived palynomorph concentrations (i.e. pollen and spores) ranging from 252.1 to 5159.1 gdw^{-1} and nonterrestrial derived palynomorph (mostly acritarchs) concentrations ranging from 131.9 to 2386.1 gdw^{-1}. Samples DMI-97-14-2 (debris) was collected from Beacon Valley, which has a terrestrial derived palynomorph concentration of 675.3 gdw^{-1} and is barren in regards to nonterrestrial derived palynomorph.

The most abundant pollen genus recovered within the samples from Victoria Valley is an angiosperm pollen belonging to the *Nothofagus* (fusca group) genus. The *fusca* group's pollen morphology has been characterized as having thickened colpal margin and a peritreme outline that allows for identification from other types of *Nothofagus* pollen (Dettmann et al., 1990) with a high degree of confidence. *Nothofagus* specimens belonging to the fusca group grow in high latitudes and are known to be associated with cool climates (Hill and Scriven, 1994).
The nonterrestrial derived palynomorphs are dominated by *Leiosphaeridia* species which have been interpreted as an indicator for sea ice conditions (Warny et al, 2006, 2009; Griener et al, 2015). Zygnemataceae spores were identified in several samples. These palynomorphs are often observed in shallow and stagnant freshwater (Warny et al., 2009; Griener et al., 2015).

The following sections discuss the palynological data tabulated from each location analyzed in the context of age estimate received to date.

3.1 Royal Society Range

The Miers Divide region which can be seen in Figure 7 and Table 2 was the location for 5 samples. The age range of the samples collected here are from 16.95 ± 0.17 Ma and had an altitude ranging 500 to 599 ± 50 m (Marchant, pers. comm.). The samples collected here yielded results that were barren. Terrestrial palynomorph concentration ranges from 0 to 1.4 gdw^{-1} and completely lacked any nonterrestrial palynomorphs.

Table 2: Royal Society Range table containing code number for identification, Sample ID, Sample Region, Sample GIS Latitude/Longitude, modern values for altitude, temperature, and precipitation, the inferred age of each sample, the basis for the age inference,and the Terrestrial Palynomorph Concentration (TCC) and Marine and Freshwater Palynomorph Concentration (MCC).

Code #	Sample ID	Sample Region	Latitude	Longitude	Altitude (m)	Temp. (°C)	Precipitation (mm weq)	Inferred age	Basis	TCC	MCC
					Modern Val.	Modern Val.	Modern Val.			(GDW^-1)	(GDW^-1)
1	DMS-10-10-C	Royal Society Range	-78.09	164.269	500 ± 50m	-7	100	16.95 ± 0.17	Argon 40/39 date on interbedded ash	1.4	0
2	DMS-10-10-G	Royal Society Range	-78.09	164.269	500 ± 50m	-7	100	16.95 ± 0.17	Argon 40/39 date on interbedded ash	0	0
3	DMS-10-11-B	Royal Society Range	-78.09	164.269	500 ± 50m	-7	100	16.95 ± 0.17	Argon 40/39 date on interbedded ash	1.4	0
4	DMS-10-11-F	Royal Society Range	-78.09	164.269	599 ± 50m	-7	100	16.95 ± 0.17	Argon 40/39 date on interbedded ash	0.8	0
5	DMS-94-004	Miers Divide	-78.084	164.292	500 ± 50m	-7	100	16.95 ± 0.17	Argon 40/39 date on interbedded ash	0	0

3.2 Asgard Range

From different valleys within the Asgard Range including the Koenig, Njord, and Sessrumnir valleys (Figure 7 and Table 2) 27 samples were collected. Samples collected from this region spanned 10.08 ± 0.17 to 15.01 ± 0.02 Ma in age with altitudes ranging 1500 to 1700 ± 50 m (Marchant, pers. comm.). The samples from this region were dominated by reworked thermally metamorphosed specimens, with very few in situ identifable palynomorphs. This region may have had isolated pockets of very spares vegetation.

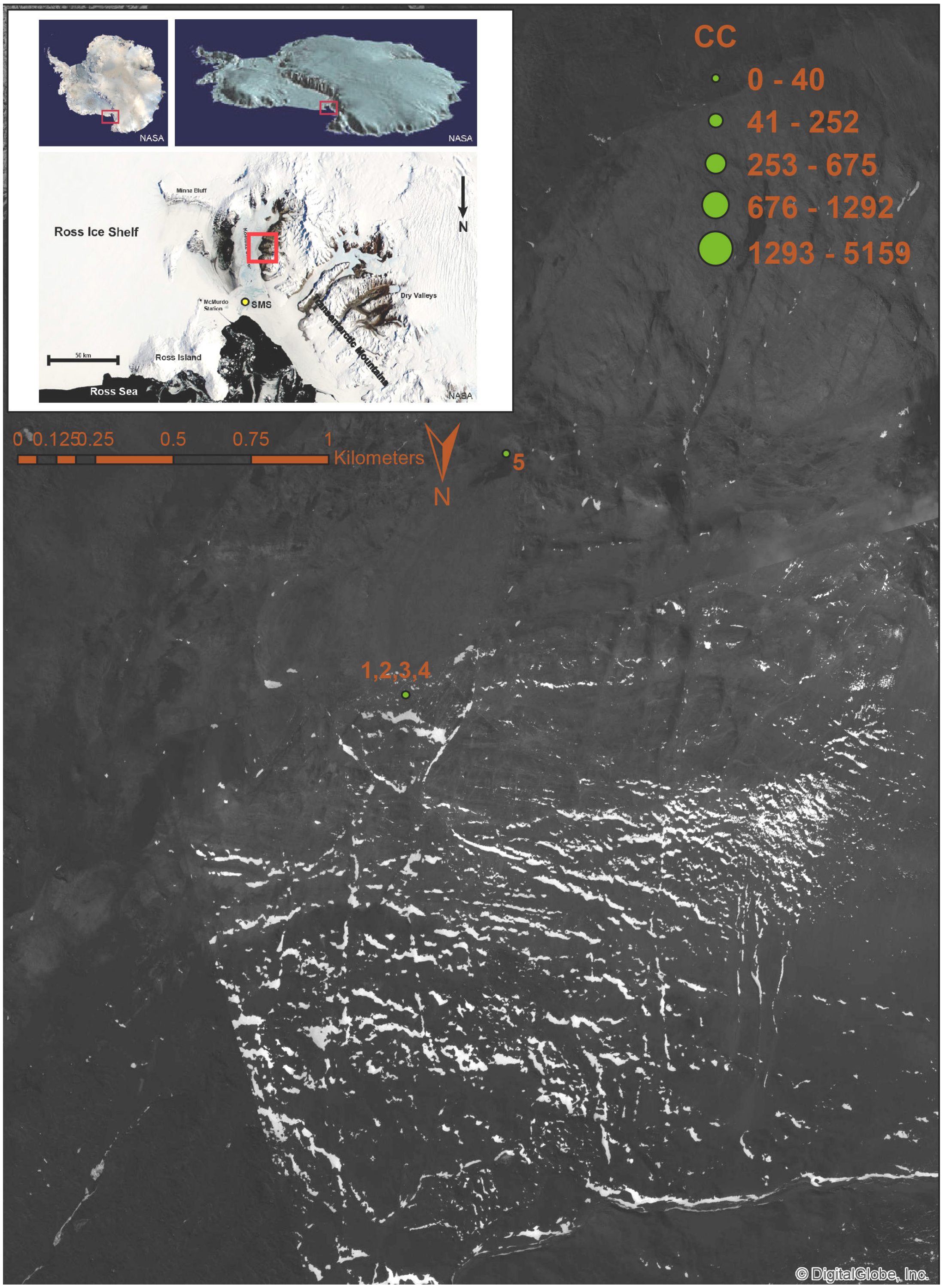

Figure 7: Sample spatial plot map of Royal Society Range samples utilizing WorldView-1, WorldView-2, QuickBird-2, and GeoEye-1 high resolution imagery. All samples' terrestrial sourced palynomorph concentration is plotted by circles with varying diameters based on concentration values (Polar Geospatial Center and DigitalGlobe, Inc., 2017).

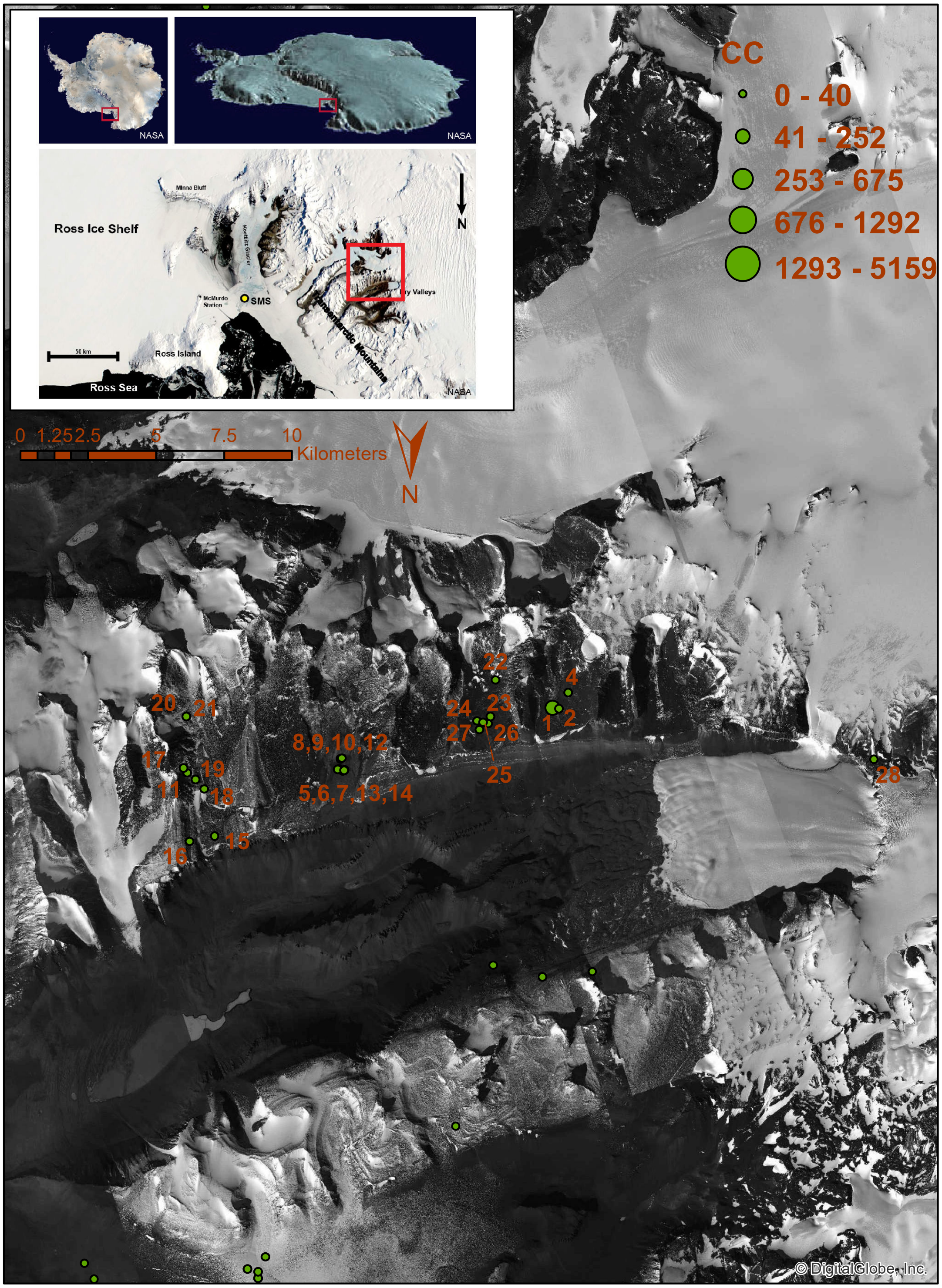

Figure 8: Sample spatial plot map of Asgard Range samples utilizing WorldView-1, WorldView-2. QuickBird-2, and GeoEye-1 high resolution imagery. All samples' (with the exception of DMS-91-82-C) terrestrial sourced palynomorph concentration is plotted by circles with varying diameters based on concentration values (Polar Geospatial Center and DigitalGlobe, Inc., 2017).

Table 3: Asgard Range table containing code number for identification, Sample ID, Sample Region, Sample GIS Latitude/Longitude, modern values for altitude, temperature, and precipitation, the inferred age of each sample, the basis for the age inference, and the Terrestrial Palynomorph Concentration (TCC) and Marine and Freshwater Palynomorph Concentration (MCC).

Code #	Sample ID	Sample Region	Latitude	Longitude	Altitude (m)	Temp. (°C)	Precipitation (mm weq)	Inferred age	Basis	TCC	MCC
					Modern Val.	Modern Val.	Modern Val.			(GDW^-1)	(GDW^-1)
1	DME-91-60	Asgard Range - Koenig Valley	-77.597	160.81	1475 ± 50m	-20	100	13.67±0.10	Correlated with Argon 40/39 date on nearby ash	107.9	0
2	DMS-91-62	Asgard Range - Koenig Valley	-77.596	160.801	1475 ± 50m	-20	100	>13.56 Ma	Strat correlation	0.9	0
3	DMS-91-82-C	Asgard Range - Koenig Valley	-77.597	160.805	1475 ± 50m	-20	100	>13.56 Ma	Strat correlation	642.7	304.6
4	DMS-91-92	Asgard Range - Koenig Valley	-77.6	160.779	1475 ± 50m	-20	100	>13.56 Ma	Strat correlation	1.3	0
5	DME-96-30	Asgard Range - Njord Valley	-77.6	161.151	1675 ± 50m	-20	100	13.67±0.10	Correlated with Argon 40/39 date on nearby ash	9.2	0
6	DME-96-31B	Asgard Range - Njord Valley	-77.6	161.148	1675 ± 50m	-20	100	13.67±0.10	Correlated with Argon 40/39 date on nearby ash	4.3	3.5
7	DME-96-33B	Asgard Range - Njord Valley	-77.6	161.151	1675 ± 50m	-20	100	13.67±0.10	Correlated with Argon 40/39 date on nearby ash	39.6	0
8	DME-96-38	Asgard Range - Njord Valley	-77.601	161.156	1675 ± 50m	-20	100	13.67±0.10	Correlated with Argon 40/39 date on nearby ash	4	0
9	DME-96-39	Asgard Range - Njord Valley	-77.601	161.158	1675 ± 50m	-20	100	13.67±0.10	Correlated with Argon 40/39 date on nearby ash	1.2	0.2
10	DME-96-53A	Asgard Range - Njord Valley	-77.604	161.149	1675 ± 50m	-20	100	13.67±0.10	Correlated with Argon 40/39 date on nearby ash	0.4	0.2
11	DMS-02-11-B	Asgard Range - Njord Valley	-77.616	161.382	1675 ± 50m	-20	100	>14.8 Ma	Strat correlation	0.3	0
12	DMS-89-211	Asgard Range - Njord Valley	-77.604	161.146	1675 ± 50m	-20	100	14.55 ± 0.06	Argon 40/39 date on interbedded ash	0.3	0
13	DMS-96-25-C	Asgard Range - Njord Valley	-77.6	161.149	1675 ± 50m	-20	100	13.67±0.10	Argon 40/39 date on interbedded ash	0.5	0
14	DMS-96-33-C	Asgard Range - Njord Valley	-77.6	161.149	1675 ± 50m	-20	100	13.67±0.10	Argon 40/39 date on interbedded ash	0	0
15	DMS-90-17	Asgard Range - Nibelungen Valley	-77.593	161.373	1675 ± 50m	-20	100	>14.8 Ma	Strat correlation	0	0
16	DMS-90-36	Asgard Range - Nibelungen Valley	-77.594	161.413	1675 ± 50m	-20	100	10.08 ± 0.17 Ma	Argon 40/39 date on interbedded ash	0.8	0
17	DMS-90-84	Asgard Range - Nibelungen Valley	-77.618	161.385	1675 ± 50m	-20	100	>13.56 Ma	Strat correlation	0.4	0
18	DMS-90-97-B	Asgard Range - Nibelungen Valley	-77.609	161.365	1675 ± 50m	-20	100	>13.56 Ma	Strat correlation	1.2	0
19	DMS-91-2-B	Asgard Range - Nibelungen Valley	-77.613	161.373	1675 ± 50m	-20	100	>14.8 Ma	Strat correlation	0.5	0
20	DMS-91-22	Asgard Range - Nibelungen Valley	-77.634	161.355	1675 ± 50m	-20	100	15.01 ± 0.02	Argon 40/39 date on interbedded ash	0.6	0
21	DMS-91-22-B	Asgard Range - Nibelungen Valley	-77.634	161.355	1675 ± 50m	-20	100	>15.01 ± 0.02	Argon 40/39 date on interbedded ash	0.7	0
22	DMS-89-132	Asgard Range - Sessrumnir Valley	-77.612	160.88	1500 ± 50m	-20	100	10.12 ± 0.13	Argon 40/39 date on interbedded ash	0.2	0
23	DMS-89-48-B	Asgard Range - Sessrumnir Valley	-77.601	160.906	1500 ± 50m	-20	100	>13.56 Ma	Strat correlation	0.9	0
24	DMS-89-58	Asgard Range - Sessrumnir Valley	-77.601	160.928	1500 ± 50m	-20	100	>13.56 Ma	Strat correlation	1.5	0
25	DMS-89-58-B	Asgard Range - Sessrumnir Valley	-77.6	160.92	1500 ± 50m	-20	100	>14.8 Ma	Strat correlation	0.4	0
26	DMS-89-58-C	Asgard Range - Sessrumnir Valley	-77.599	160.913	1500 ± 50m	-20	100	>14.8 Ma	Strat correlation	0.6	0
27	DMS-89-73-C	Asgard Range - Sessrumnir Valley	-77.598	160.929	1500 ± 50m	-20	100	>13.56 Ma	Strat correlation	0	0
28	DMS-91-78	Mt. Flemming	-77.545	160.365	1700 ± 50m	-20	100	>14.8 Ma	Strat correlation	4.1	0

3.2.1 Asgard Range - Koenig Valley

Koenig Valley within the Asgard Range provided 4 samples. Samples DMS-91-82C and DME-91-60 have the highest concentration of palynomorphs with respect to all of the other samples collected throughout the Asgard Range. Sample DMS-91-82C and DME-91-60 have concentrations ranging from 107.9 to 642.7 gdw^{-1} for terrestrially derived palynomorphs and concentrations ranging from 0 to 304.6 gdw^{-1} for palynomorphs derived from nonterrestrial sources. Sample DMS-91-82C and DMS-91-92 can be seen in Plates 1 and 2. Sample DMS-91-82C contained one *Leiosphaeridia* sp*, Nothofagidites* sp*.* (fusca), and *Coptospora* sp. grains. Sample DMS-91-92 contained one *Chenopodipollis* sp. grain with *Schizophacus* sp algae. Sample DME-91-60 contained penecontemporaneous assemblage is made up entirely of bryophyte spores, with a few lycophyte spores, and a *Chenopodipollis* pollen, and abundant mainly black and brownish-black organic matter, and corroded mostly unidentifiable black and brownish black reworked Beacon spores and pollen (see Plate 3 & 4). The reworked Beacon assemblage includes spores, monosaccate, bisaccate and taeniate bisaccate pollen, of likely Permian origin for most, consistent with the abundant coaly organic matter. DME-91-60 contained one laboratory contaminant (a pink-stained dinocyst) and a large triporate pollen that is also likely a laboratory contaminant. It is of the northern *Carya/Caryopollenites* type as shown on Plate 3, microphotograph 2.

3.2.2 Asgard Range - Nibelungen Valley

Nibelungen Valley from the Asgard Range was the location for 7 samples. The samples from this region were barren with samples concentration ranging from 0 to 1.2 gdw^{-1} for terrestrially derived palynomorphs and completely barren of palynomorphs derived from nonterrestrial sources.

3.2.3 Asgard Range - Njord Valley

The Njord Valley from the Asgard Range had 10 samples retrieved from this location. The samples from this region were barren with samples concentration ranging from 0 to 39.6 gdw^{-1} for terrestrially derived palynomorphs and 0 to 3.5 gdw^{-1} palynomorphs derived from nonterrestrial sources. Most samples from this region contained reworked thermally metamorphosed specimens, but samples DME-96-53A, DME-96-30, DME-96-31B, DME-96-38, and DME-96-39

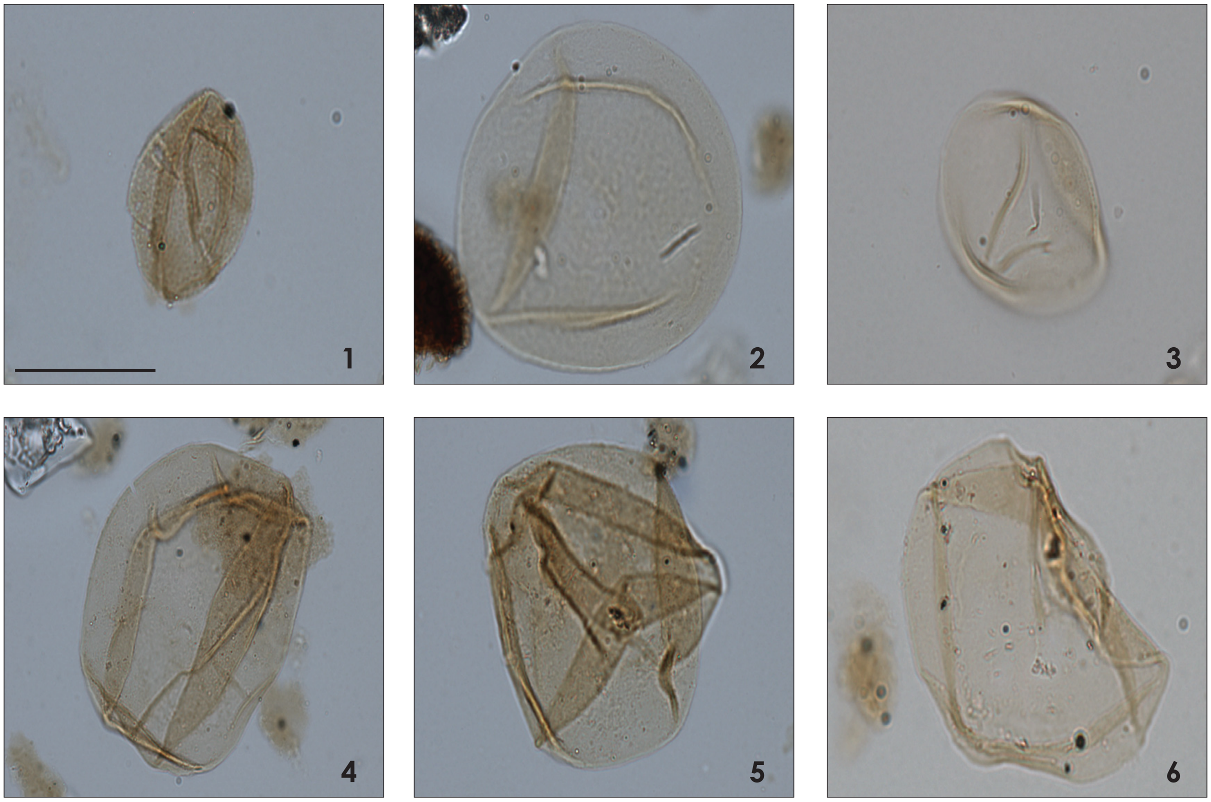

Plate 1. Light photomicrographs of key in situ specimens from sample DMS-91-82C, Asgard Range-Koenig Valley, Antarctica. All specimens are all shown at the same magnification with a 50 micrometer scalebar included. 1. *Nothofagidites* sp. (fusca). view #1. DMS-91-82C. 16.6x115. (60x). 2. *Coptospora* sp. view #1. DMS-91-82C. 12.5x137.8. (60x). 3. *Leiosphaeridia* sp. view #1. DMS-91-82C. 7.3x126.2. (60x). 4. *Leiosphaeridia* sp. view #1. DMS-91-82C. 16.6x118.2. (60x). 5. *Leiosphaeridia* sp. view #1. DMS-91-82C. 18.7x113. (60x). 6. *Leiosphaeridia* sp. view #1. DMS-91-82C. 10.1x133.7. (60x).

yielded interesting results. Sample DME-96-53A was very poor in palynomorphs and organic matter, it contains barely a trace of very small black organic matter, one small tricolpate pollen, two grains of *Chenopodipollis* sp. and one leiospherid alga (see Plate 5). The sample is characterized by overwhelming added *Lycopodium* which confirms that the assemblage was extremely sparse.

Sample DME-96-30 is composed of translucent nondescript tissue and dark brown-black organic matter. The recovered assemblage is sparse but relatively diverse containing penecontemporaneous moss *Coptospora* sp. and other bryophytes, possibly moss, hornwort or liverwort, lycophyte spores, and an assortment of angiosperm pollen including Poaceae (grass), Restionaceae (rush-like herbs), and several small triaperturate pollen. It also contains rare reworked spores and *Alisporites* sp. and a single pink-stained laboratory contaminant (see Plate 6).

Sample DME-96-31B contained sparse in situ paynomorphs that are mixed with abundant reworked palynomorphs of mostly Cretaceous age. It addition, abundant light-colored tissue and light-colored fluffy degraded material, including sheets of tissue and fragments that could be pieces of dinoflagellate cysts are noted, along with some dark brownish black and black organic matter. Palynomorphs in this sample are mainly Cretaceous dinocysts, and spores some of which were identifiable, reworked Triassic, but mostly indeterminate. Bisaccate pollen which might be part of the Cretaceous assemblage, but appeared to be reworked older Mesozoic forms.

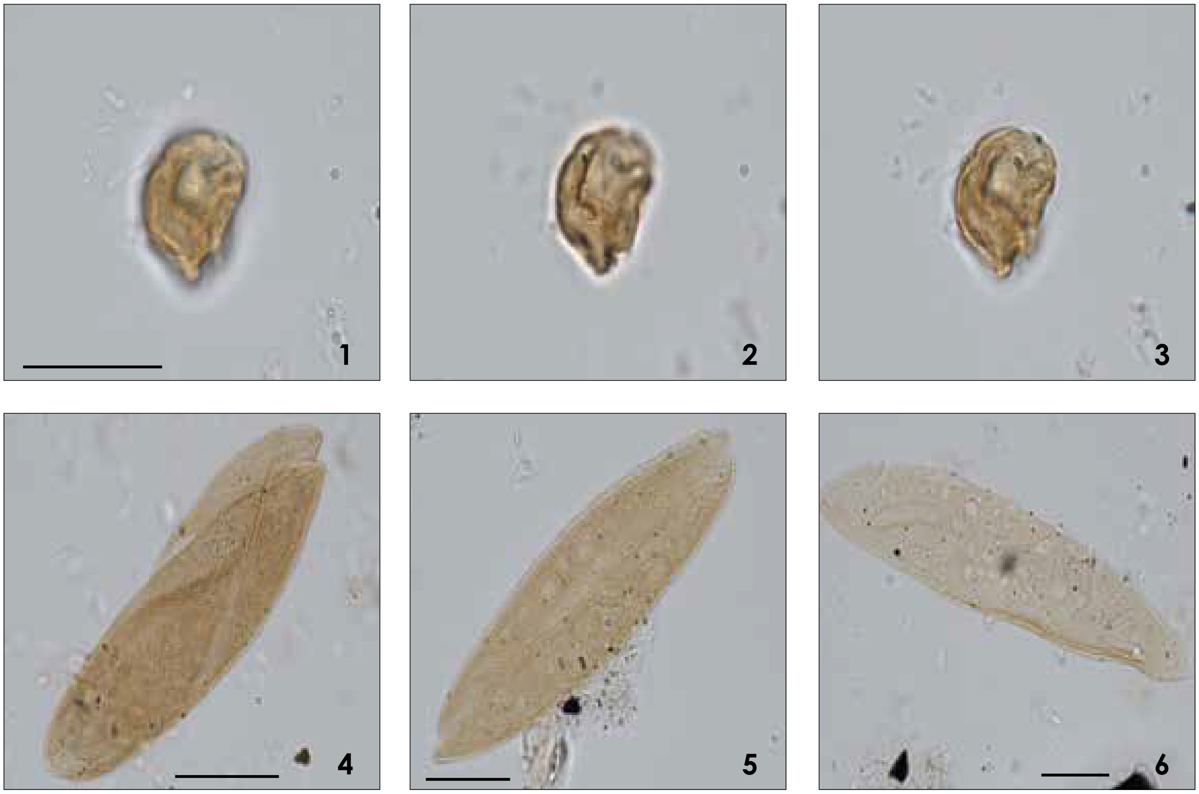

Plate 2. Light photomicrographs of key in situ specimens from sample DMS-91-92, Asgard Range-Koenig Valley, Antarctica. All specimens are all shown at the same magnification with a 50 micrometer scalebar included. 1. *Chenopodipollis* sp. view #1. DMS-91-92C. 4.6x125.9. (60x). 2. *Chenopodipollis* sp. view #2. DMS-91-92. 4.6x125.9. (60x). 3. *Chenopodipollis* sp. view #3. DMS-91-92. 4.6x125.9. (60x). 4. *Schizophacus* sp. view #1. DMS-91-92. 12x126.1. (60x). 5. *Schizophacus* sp. view #1. DMS-91-92. 3.5x134. (60x). 6. *Schizophacus* sp. view #1. DMS-91-92. 11.1x128. (60x).

No diagnostic Cretaceous terrestrial taxa were observed; the diagnostic Cretaceous taxa are all marine. There are also rare possibly penecontemporaneous palynomorphs including small triporate and tricolporate pollen, periporate pollen *Chenopodipollis* sp. and *Colobanthus* (Caryophyllaceae), and a single *Nothofagidites lachlaniae* and a few small *Leiosphaeridia* sp. The presence of these mixed with the other two assemblages suggests the Cretaceous and older specimens are reworked. The Cretaceous marine assemblage is intriguing. The relative abundance of these forms indicates the presence of nearby Cretaceous sediments, or at least a palynomorph-rich small clast within the Dry Valley region. This Cretaceous "outcrop" is likely presently sediment or ice-covered as no such strata have ever been encountered in this part of Antarctica, or, if they are not presently sediment or ice-covered, they could be completely eroded. Occasional reworked specimens (particularly of the easily recognized *Odontochitina*, typically *O. operculata*, as in this sample) have been reported from McMurdo Sound Eocene erratics (Askin, 2000), possibly derived from south of Mt. Discovery. No reworked *Odontochitina* or similar-aged dinocysts were reported from seaward in the ANDRILL cores (AND-SMS) or slightly further north reworked into the Cape Roberts Project cores (CRP-1, CRP-2/2A or CRP-3), off the mouth of the Mackay Glacier. This suggests that the Cretaceous sediment provenance is small and localized. The identification of the dinoflagellates is made difficult because of the corroded nature of the walls, and by the fact that most species are only represented by one or two specimens so the archeopyle and plate tabulation is not always visible. Thus, identifications presented here are tentative, but it is quite certain that most specimens recovered are of Cretaceous age, ranging most likely from the Aptian

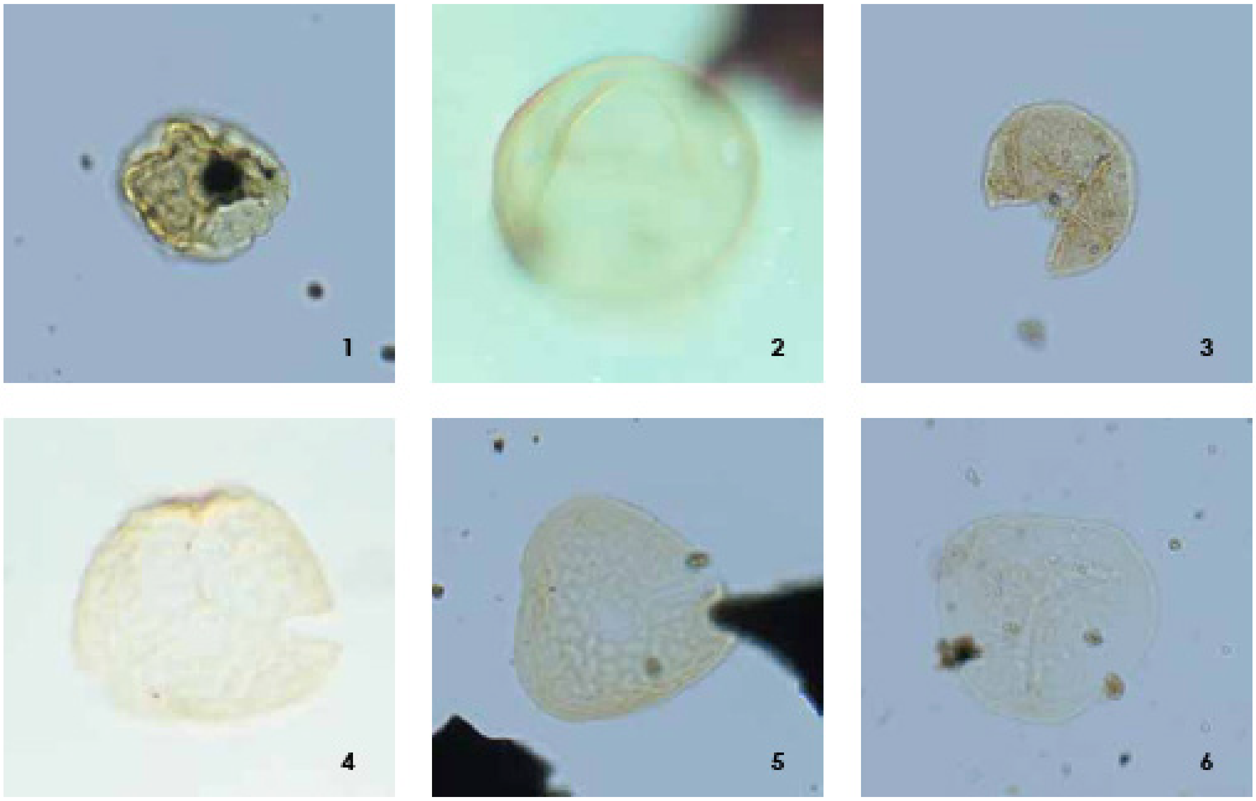

Plate 3. Light photomicrographs of key in situ pollen and spores species from sample DME-91-60, Asgard Range, Antarctica. 1. *Chenopodipollis* sp., view #4, 7.6 x 132.9, 60x. 2. *Caryopollenites* sp., DV3012, 100x (laboratory contaminant). 3. ?Gymnosperm pollen possibly reworked, view #3, 8.1 x 140.4, 60x. 4. *Triporoletes* sp./Bryophyte spore, DV301, 100x. 5. *Triporoletes* sp./Bryophyte spore, view #1, 11.0 x 129.0, 60x. 6. *Triporoletes* sp., view #3, 14.0 x 125.0, 60x.

to the Maastrichtian. More precise age could be proposed if we recovered better and more abundant specimens. *Odontochina operculata* was the most abundant and easily identificable species, but this species is believed to range from 129.93 - 67.33 Ma. The other tentatively identified genera include mainly Late Cretaceous genera such as *Areoligera* (range of 72.96 - 70.81 Ma), or *Glaphyrocysta* (range of 86 - ? Ma); *Spinidinium* sp. (range for genus of 87.44 - 71.69 Ma), *Spinidinium sverdrupianum* (range of 68.5 - 65.0 Ma), *Isabelidinium pellucidum* (range of 76.30 - 67.30 Ma), a genus possibly related to *Samlandia* (Late Cretaceous), and *Chatangiella triparta* (range of 85.60 - 65.0 Ma) see Plates 7-10.

Sample DME-96-33B contains sparse brownish black and black OM, and a penecontemporaneous assemblage of mainly bryophyte spores (including moss *Coptospora* spp., hornwort or liverwort spores, lycophyte spores, and assorted small angiosperm pollen, including Asteraceae and Chenopodiaceae. One reworked Cretaceous dinocyst, *Odontochitinaoperculata*, and some reworked bisaccate pollen likely Permian or Mesozoic were observed (see Plates 11 and 12). Sample DME-96-38 was sparse with rare small black organic matter and partially degraded orange brown organic matter. It contained Poaceae, *Chenopodipollis* sp. and small tricolporate angiosperm pollen, which also indicate sparse tundra vegetation. The most interesting recovery in this sample is what we believe is a fragment of an insect which can be seen in Plate 13. Dr. Sean Thomas O'Keefe, an entomologist, was asked for his opinion on this specimen. He noted that, given the size, that it might be part of a mite. It has foliose setae (those interesting leaf-

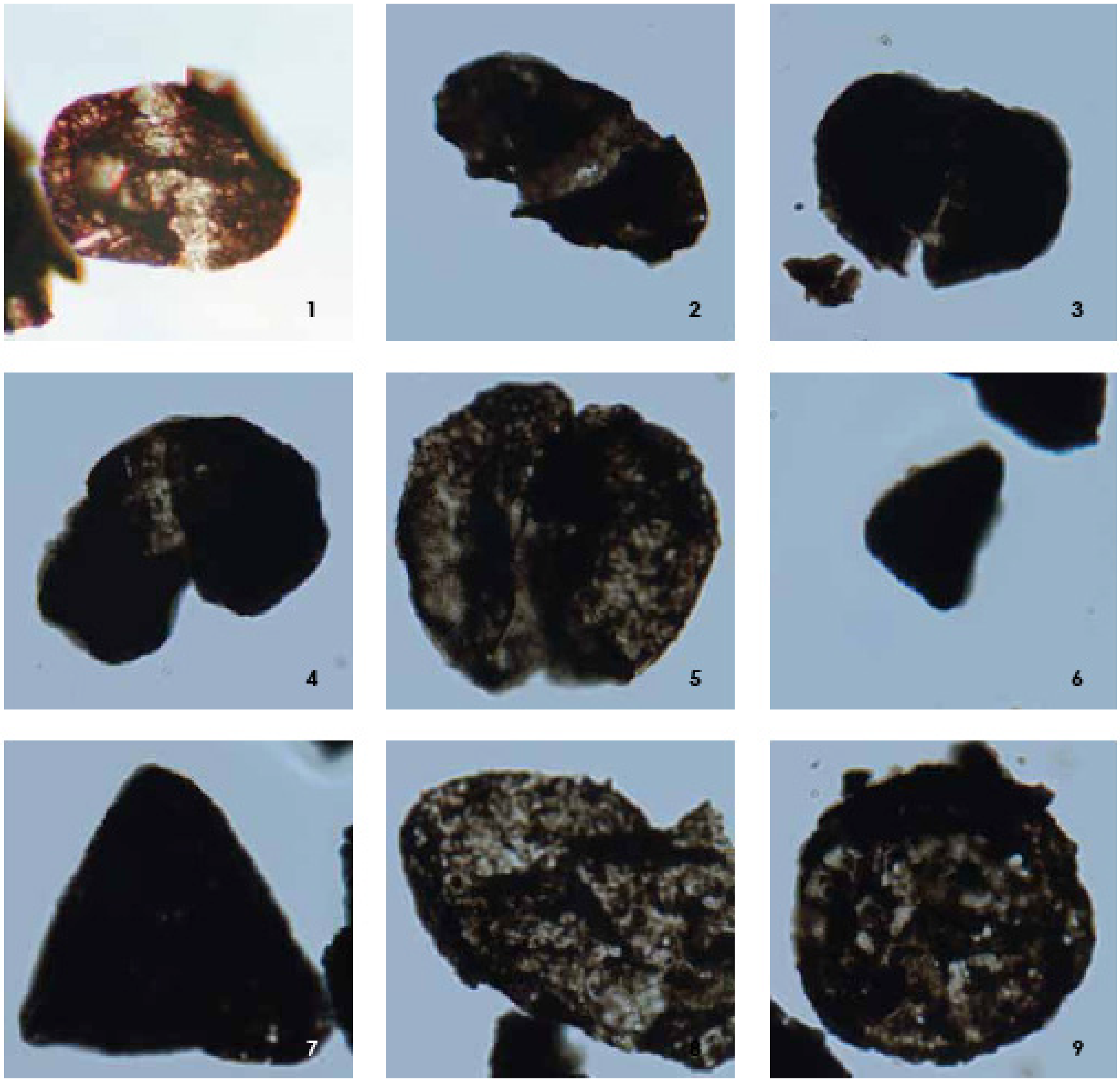

Plate 4. Light photomicrographs of reworked, thermally metamorphosed pollen and spore specimens from sample DME-91-60, Asgard Range, Antarctica. 1. Taeniate bisaccate pollen *Protohaploxypinus* sp. (Permian), DV3010. 2. Bisaccate pollen , view #3, 6.2 x 145.6, 60x. 3. Bisaccate pollen, possibly taeniate, view #2, 15.5 x 134.0, 60x. 4. Bisaccate pollen possibly taeniate, view #3, 19.0 x 145.0, 60x. 5. Bisaccate pollen, view #2, 19.0 x 117.0, 60x. 6. Indeterminate trilete spore, ?granulate, view #4, 15.5 x 114.5, 60x. 7. Trilete spore,, view #2, 7.0 x 117.7, 60x. 8. Bisaccate pollen, possibly taeniate, view #1, 11.0 x 145.8, 60x. 9. Trilete spore?, view #3, 20.0 x 129.5, 60x.

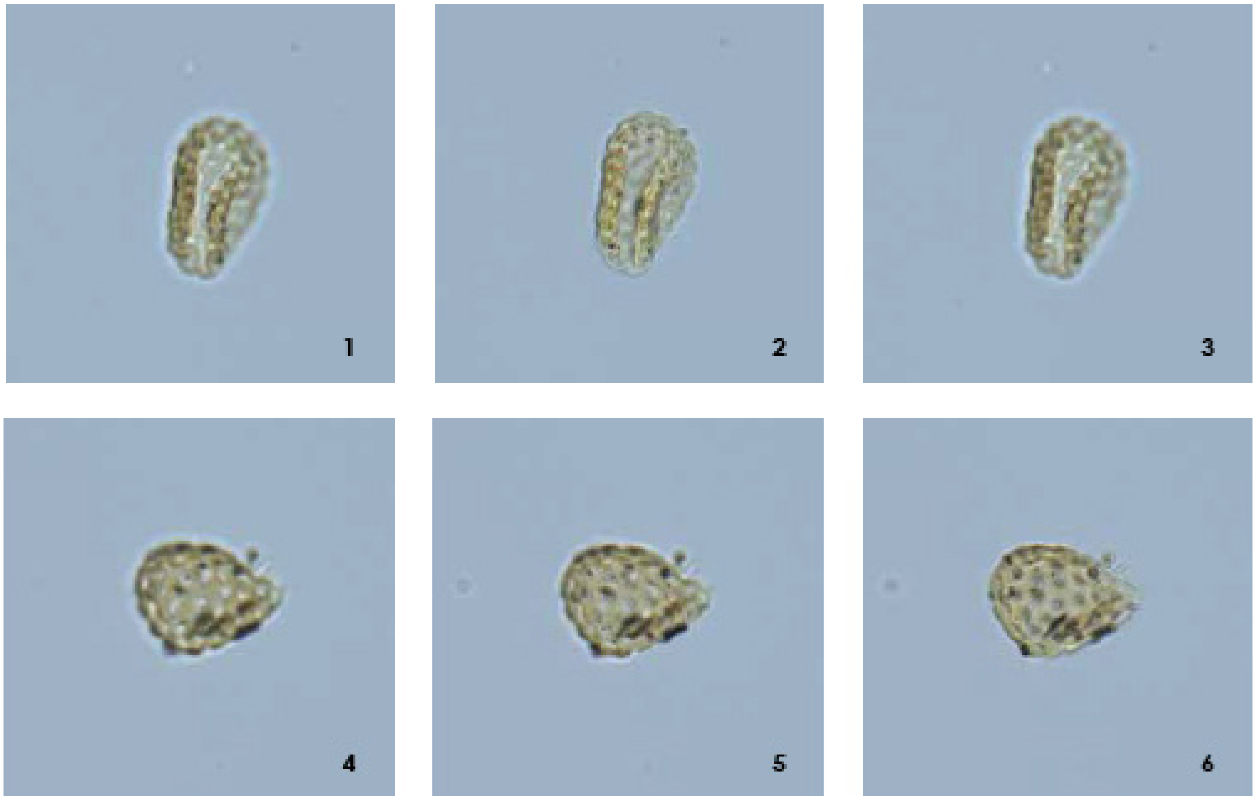

Plate 5. Light photomicrographs of key pollen species from sample DME-96-53-A, Asgard Range, Antarctica. 1-3. *Chenopodipollis* sp., views #1, 3, 5, 16.8x122.2, 60x. 4-6. *Chenopodipollis* sp., views #1, 3, 5, 20.3 x 134.8, 60x.

like portions projecting from the main body), which argue for something acarine (a mite). The "hole", or spiracle just before the portion that looks like a leg comes off of the body also argues for a mite (their spiracles are just in front of the last set of legs). Sample DME-96-39 contained another sparse slide with occasional black organic and partially degraded brown organic matter. Rare penecontemporaneous palynomoprhs, a moss spore (*Coptospora* sp.) and lycophyte spore (*Retitriletes*) and several *Chenopodipollis* spp. were found with one reworked corroded bisaccate pollen as shown in Plate 14.

3.2.4 Asgard Range - Sessrumnir Valley

The Asgard Range had 6 samples were collected from the Sessrumnir Valley. The samples from this region were barren with samples concentration ranging from 0 to 1.5 gdw^{-1} for terrestrially derived palynomorphs and are completely barren of palynomorphs derived from nonterrestrial sources. The samples from this region were completely dominated by reworked thermally metamorphosed specimens. *Chenopodipollis* sp. grains were observed in DMS-89-132 and DMS-89-58C. One unidentified triporate pollen grain was observed in DMS-89-58B.

3.2.5 Asgard Range – Mount Flemming

Mount Flemming near the Asgard Range provided only one sample for this study. The samples from this region were barren with samples concentration ranging from 0 to 4.1 gdw^{-1} for terrestrially derived palynomorphs and is completely barren of palynomorphs derived from nonterrestrial sources. DMS-91-78 was completely dominated by reworked thermally metamorphosed specimens. One unknown trilete spore was identified among mostly reworked thermally metamorphosed podocarp specimens.

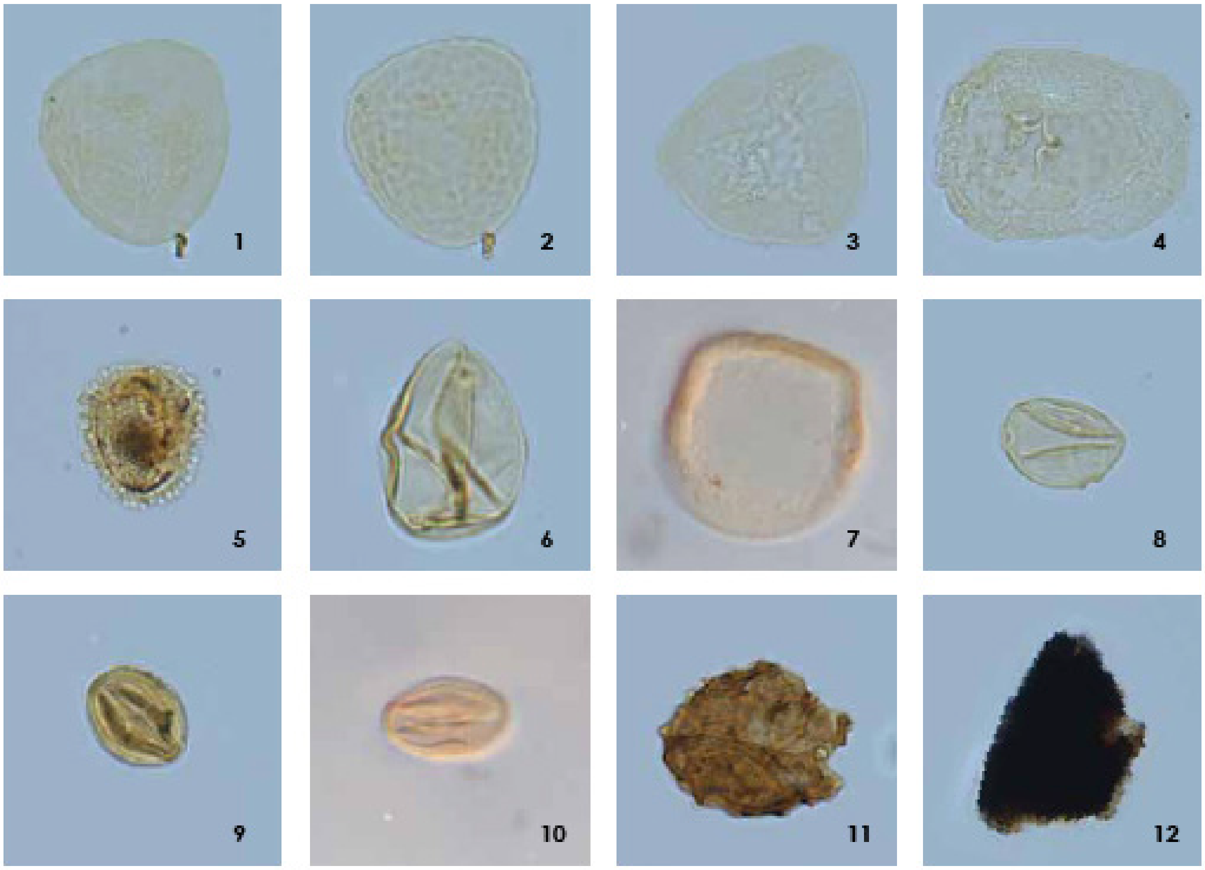

Plate 6. Light photomicrographs of key in situ pollen and spores species from sample DME-96-30-B, Asgard Range, Antarctica. 1. *Triporoletes* sp., view #2, 6.3 x 108.6, 60x. 2. *Triporoletes* sp., view #3, 6.3 x 108.6, 60x. 3. *Triporoletes* sp., view #3, 15.4 x 122.0, 60x. 4. Sacless gymnosperm?, view #2, 5.0 x 109.5, 60x. 5. Indeterminate pollen with clavate ornamentation, view #1, 18.0 x 140.3, 60x. 6. Monoporate, Poaceae, view #4, 8.9 x 116.5, 60x. 7. Monoporate, Restionaceae, DV2020 100x. 8. Triporate pollen, view #1, 10.0 x 110.1, 60x (potential contaminant). 9. Tricoloporate sp. A, view #6, 18.0 x 132.4, 60x. 10. Tricolporate sp. A, DV2021, 100x. 11. Unknown reworked spore, view #1, 6.3 x 127.6, 60x. 12. Thermally metamorphosed fragment of spore.

3.3 Olympus Range

The Olympus Range and the nearby regions of Bull Pass and Mckelvey Valley which can be seen in Figure 8, Table 4, and Plate 15 was the location for 14 samples. These 14 samples spanned an age range of 10 Ma to the Middle Miocene and were collected from altitudes ranging 575 to 1400 ± 50 m (Marchant, pers. comm.). This region is similar to the Asgard Range region being mostly composed of reworked thermally metamorphosed material, however this region has few freshwater and marine palynomorphs near the Bull Pass and McKelvey Valley area. This suggests that this region was exposed to freshwater and marine influence. Personal communication with Dr. David Marchant suggests that the age of the Olympus Range samples to be around 17 Ma.

3.3.1 Olympus Range – Bull Pass

Bull Pass near by the Olympus Range was the source location for 3 samples. The samples from this region were barren and had a terrestrial derived concentration of 1.1 gdw^{-1} and a non-

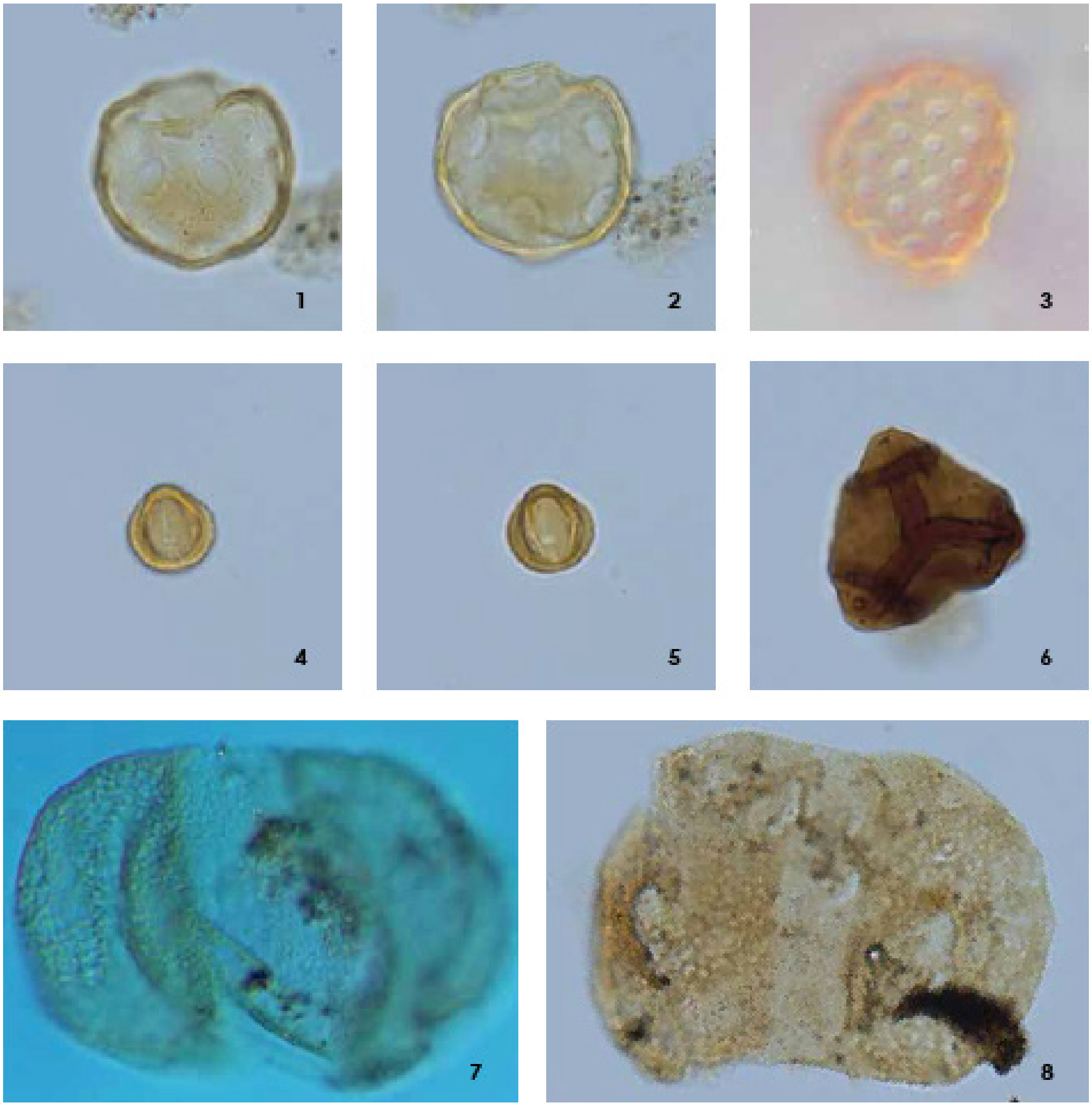

Plate 7. Light photomicrographs of key in situ pollen and spore species from sample DME-96-31-B, Asgard Range, Antarctica. 1. ?*Colobanthus* sp., view #2, 8.4 x 128.8, 60x. 2.? *Colobanthus* sp., view #4, 8.4 x 128.8, 60x. 3. *Chenopodipollis* sp., DV2023, 100x. 4.* Tricolporate, view #1, 6.2 x 139.6, 60x. 5.* Tricolporate, view #4, 6.2 x 139.6, 60x. 6. Reworked *Dictyophyllidites* sp. (Mesozoic), view #1, 6.7 x 133.0, 60x. 7. Reworked *Alisporites* sp. (Mesozoic), DV2022, 100x. 8. Reworked *Alisporites* sp. (Mesozoic), view #2, 8.4 x 131.0, 60x.

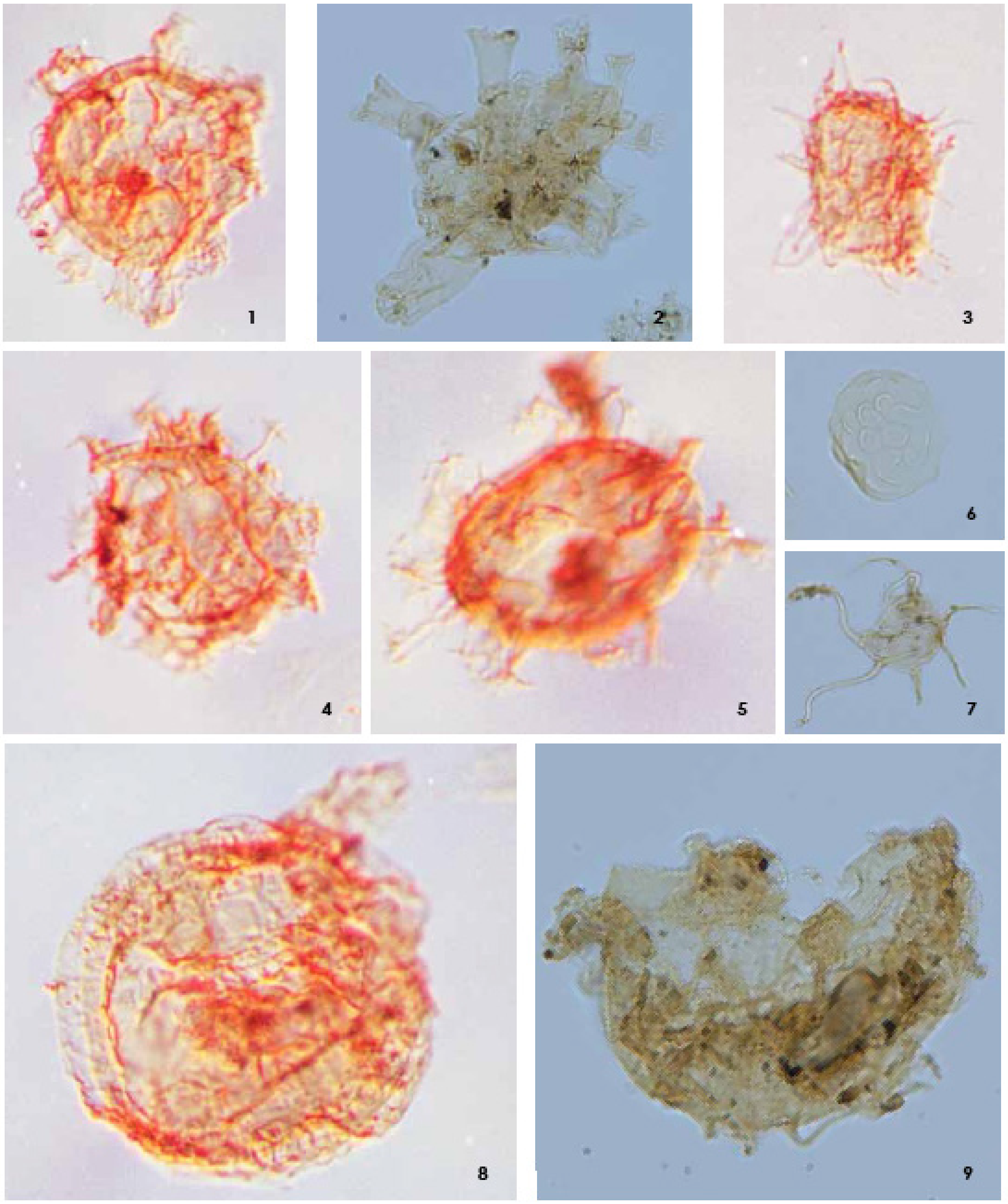

Plate 8. Light photomicrographs of key marine palynomorph species (dinoflagellates, *Zygnemaceae* and acritarch) from sample DME-96-31-B, Asgard Range, Antarctica. 1. Reworked unidentified dinoflagellate, DV1005. 2. Reworked dinoflagellate, possibly related to the genus *Hystrichokolpoma*, view #2, 14.3 x 111.4, 60x. 3. Reworked unidentified dinoflagellate, DV1006. 4. Reworked unidentified dinoflagellate, DV1007. 5. Reworked unidentified dinoflagellate, DV1013. 6. Spore of Zygnemaceae, view #1, 8.4 x 134.5, 60x. 7. Reworked ?acritarch, view #1, 11.3 x 146.1 (60x). 8. Dinoflagellate, possibly related to the genus *Samlandia* (range of Late Cretaceous), DV1017. 9. Dinoflagellate, possibly related to one of these Cretaceous genera; *Areoligera* (range of 72.96 - 70.81 Ma), *Cyclonephelum* (range of 117 - 94 Ma), or *Glaphyrocysta* (range of 86 - ? Ma), view #2, 11.0x 110.6, 60x.

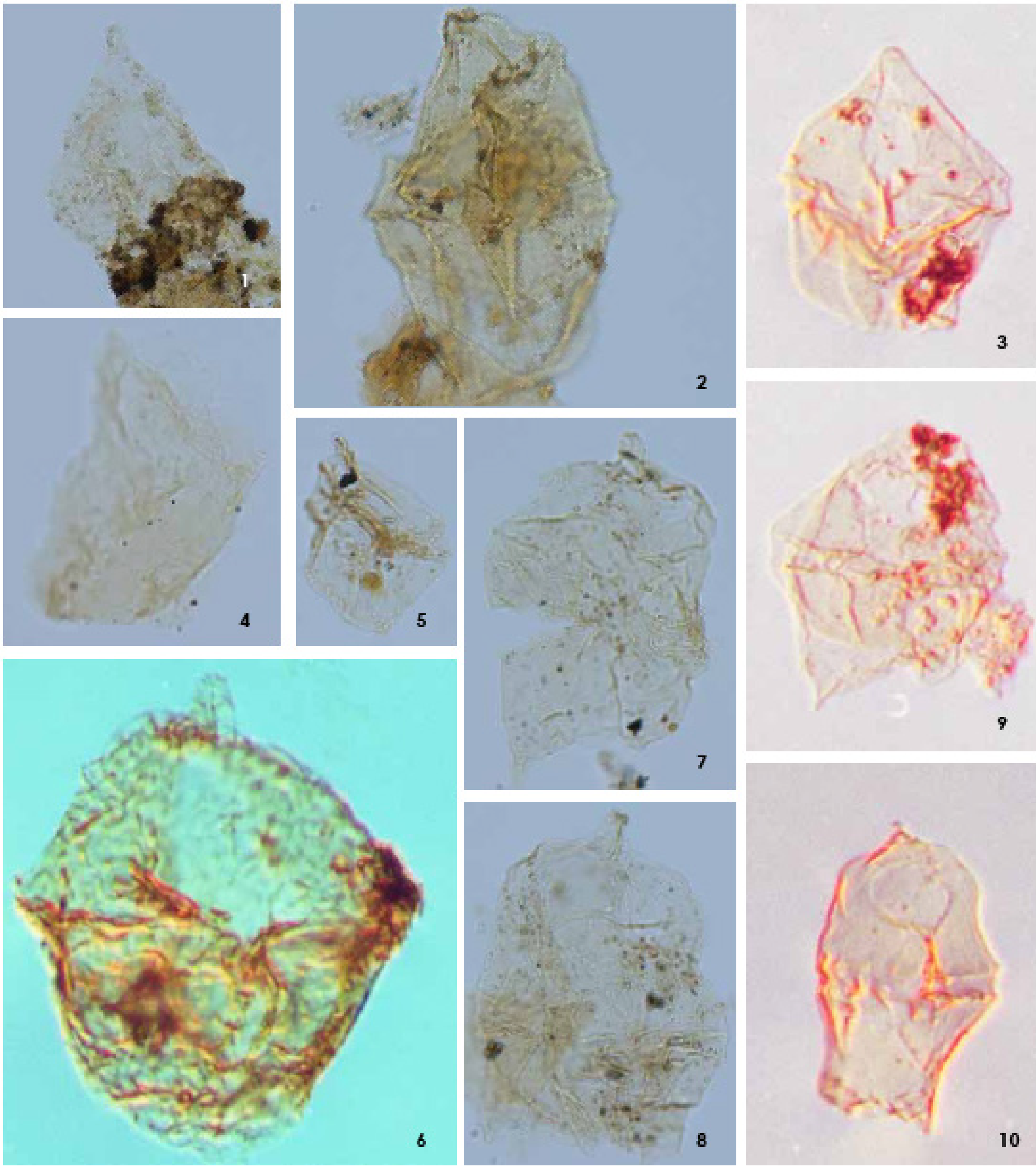

Plate 9. Light photomicrographs of key dinoflagellates from sample DME-96-31-B, Asgard Range, Antarctica. 1. ?*Spinidinium* sp. (range for genus of 87.44 - 71.69 Ma), view #2, 6.9 x 128.5, 60x. 2.?*Spinidinium* sp. (range for genus of 87.44 - 71.69 Ma), view #1, 8.4 x 131.9, 60x. 3. ?*Isabelidinium pellucidum* (range of 76.30 - 67.30 Ma), DV1003. 4. ?*Spinidinium* sp., view #2, 9.5 x128.4, 60x. 5. Unidentifiable dinoflagellate, view #2, 10.5 x 118.0, 60x. 6. Possibly related to *Samlandia* (Late Cretaceous genus), DV1016. 7. ?*Chatangiella triparta* (range of 85.60 - 65.0 Ma), view #2, 10.5 x 129.8, 60x. 8. ?*Chatangiella triparta* (range of 85.60 - 65.0 Ma), view #2, 9.5 x 124.2, 60x. 9. ?*Spinidinium sverdrupianum* (range of 68.5 - 65.0 Ma), DV1004. 10. ?*Chatangiella triparta* (range of 85.60 - 65.0 Ma), DV2014.

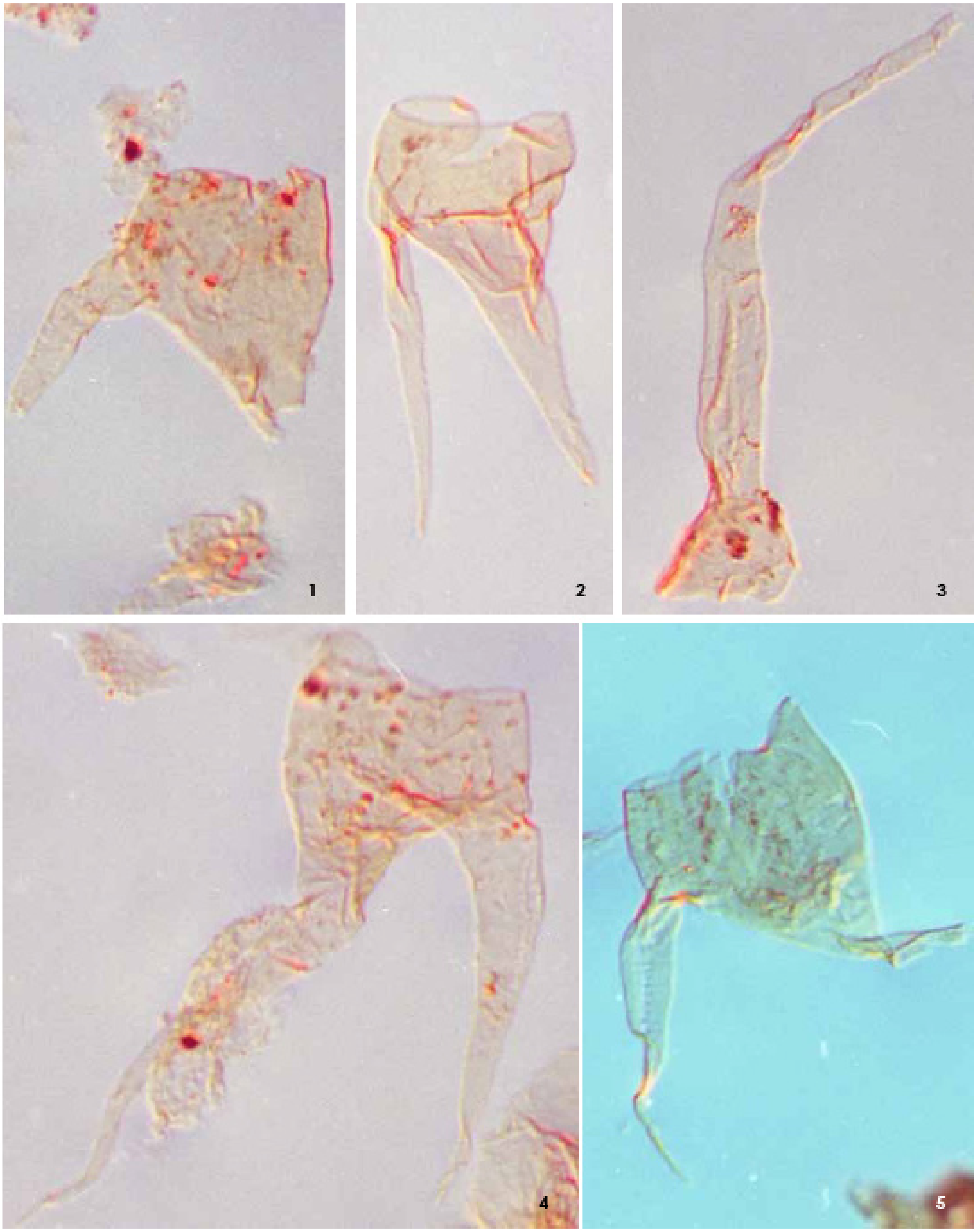

Plate 10. Light photomicrographs of key dinoflagellates from sample DME-96-31-B, Asgard Range, Antarctica. 1-5. Various specimens of the Cretaceous species *Odontochina operculata* (range from 129.93 - 67.33 Ma). 1. DV1001. 2. DV1002. 3. DV1009. 4. DV1010. 5. DV1011.

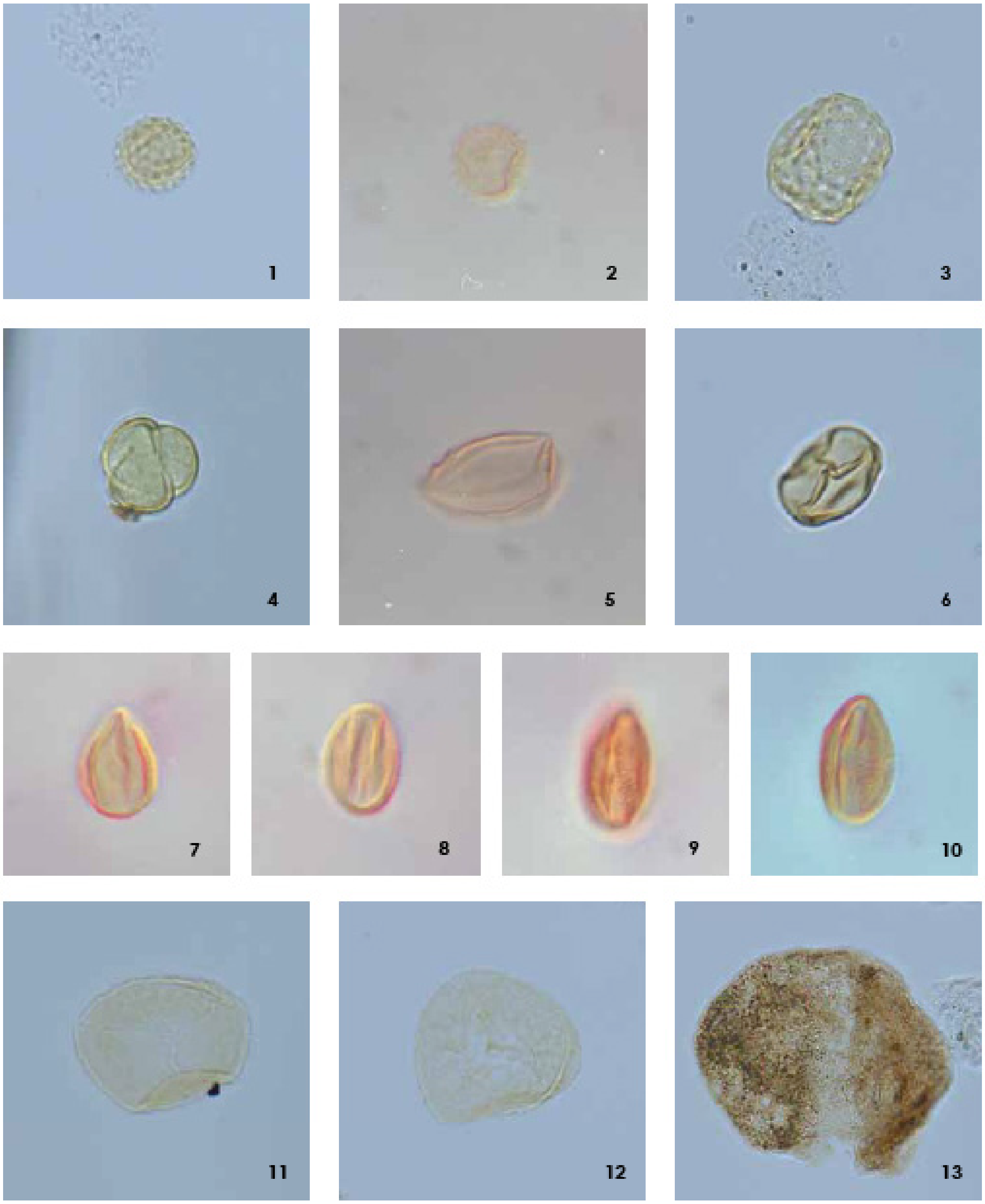

Plate 11. Light photomicrographs of key pollen and spore species from sample DME-96-33-B, Asgard Range, Antarctica. 1. Asteraceae, view #2, 8.1 x 137.7, 60x. 2. Asteraceae, DV3005, 100x. 3. *Chenopodipollis* sp., view #4, 10.0 x 134.6, 60x. 4. Tricolpate pollen, view #3, 10.0 x 147.3, 60x. Potential laboratory contaminant. 5. Triporate pollen,, DV3003, 100x. 6. Triporate pollen, view #2, 17.0 x 120.7, 60x. Potential laboratory contaminant. 7. Tricoloporate sp. A, DV2024, 100x. 8. Tricolporate sp. A, DV2025, 100x. 9. Tricolporate sp. A, DV3001, 100x. 10. Tricolporate sp. A, DV3002, 100x. 11. *Triporoletes* sp., view #4, 5.6 x 119.0, 60x. 12. *Triporoletes* sp., view #1, 8.1 x 144.6, 60x. 13. Reworked bisaccate pollen, looks vaguely taeniate, view #1, 8.5 x 115.4, 60x.

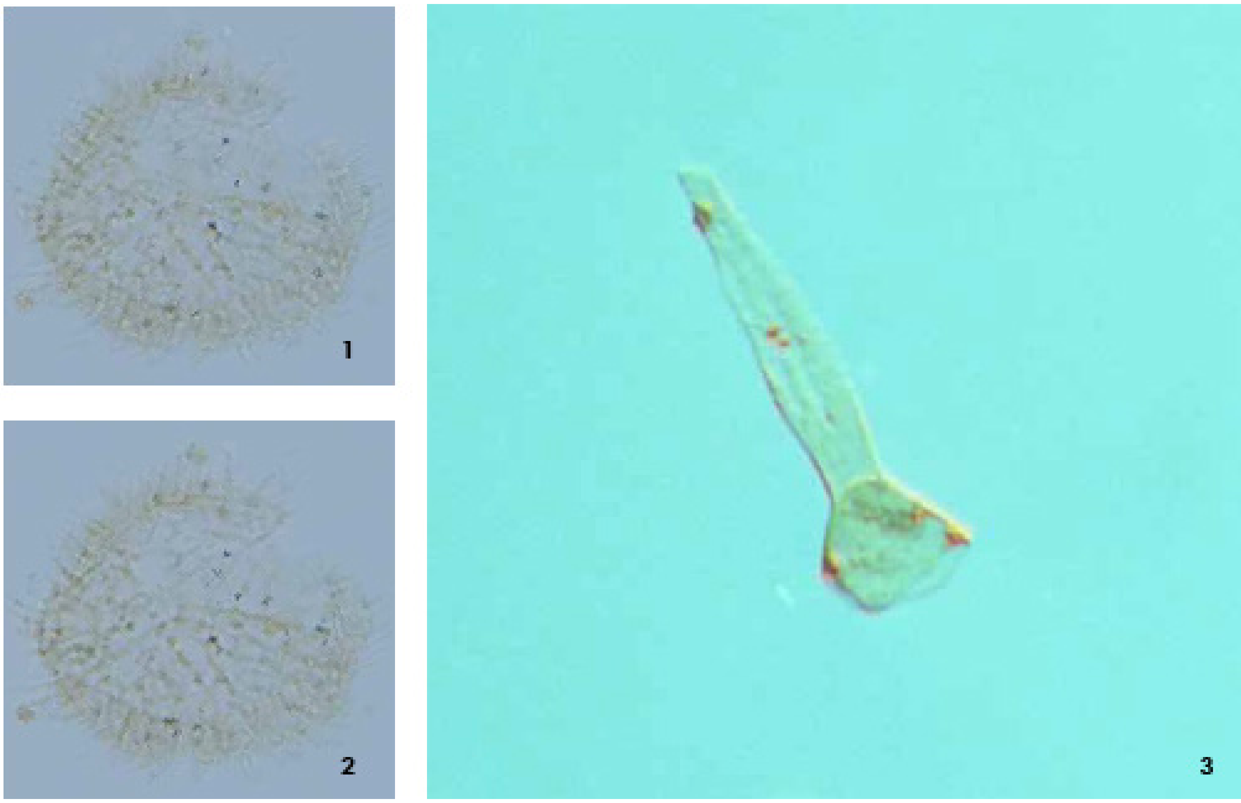

Plate 12. Light photomicrographs of key dinoflagellate species from sample DME-96-33-B, Asgard Range, Antarctica. 1-2. In situ? dinoflagellate cyst, views #2-4, 5.6 x 134.0, 60x. 3. Reworked archeopyle of *Odontochitina operculata* (range from 129.93 - 67.33 Ma), DV1018.

terrestrial derived concentration of 1.5. Samples from this region were composed primarily of thermally metamorphosed specimens. Two algal specimens were found including *Schizophacus* sp. and *Leiosphaeridia* sp. in sample DMS-95-35. These palynomorphs are indicative marine influence, and possibly some freshwater influence as indicated by the *Schizophacus* sp.

3.3.2 Olympus Range – Boreas Site

Boreas Site, which can be found in the Olympus Range, had only one sample. The sample was barren of palynomorphs and had a concentration of 0.9 and 1.6 gdw^{-1} for terrestrial and nonterrestrial sourced palynomorphs. Sample DMS-02-19 contained primarily reworked thermally metamorphosed specimens with two *Leiosphaeridia* sp. cysts and two *Nothofagidites* sp. (fusca) pollen grains.

3.3.3 Olympus Range – East

The Eastern portion of the Olympus Range provided 5 samples. The samples were barren having concentrations of 0 to 2.2 gdw^{-1} and 0 to 0.4 gdw^{-1} for terrestrial and nonterrestrial palynomorphs.

3.3.4 Olympus Range - West

The Western portion of the Olympus Range was the location for 3 samples. The samples collected here had concentrations that were barren ranging from 0.4 to 12.9 gdw^{-1} for terrestrial

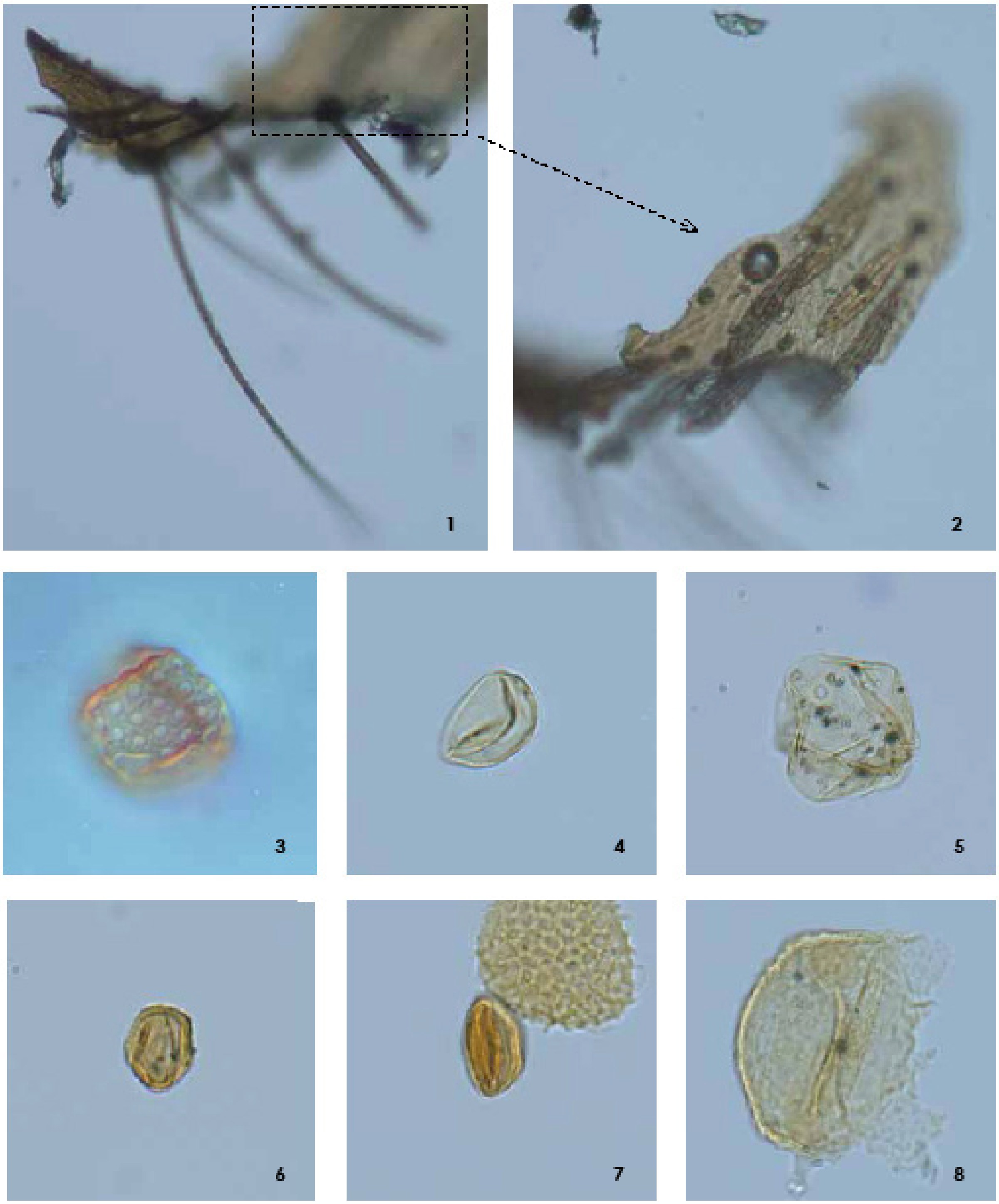

Plate 13. Light photomicrographs of key pollen and spore species and insect from sample DME-96-38, Asgard Range, Antarctica. 1-2. Insect fragment?, views #1 and 4, 23.3 x 110, 60x. 3. *Chenopodipollis* sp., DV3007, 100x. 4. Poaceae, view #2, 10.6 x 144.0, 60x. 5. Poaceae, view #4, 23.0 x 127.5, 60x. 6. Tricolporate sp. A, view #1, 12.5 x 140.4, 60x. 7. Tricolporate sp. A, view #3, 23.6 x 139.9, 60x. 8. Fragment of ?bisaccate pollen, ? reworked, view #2, 10.6 x 143.4, 60x.

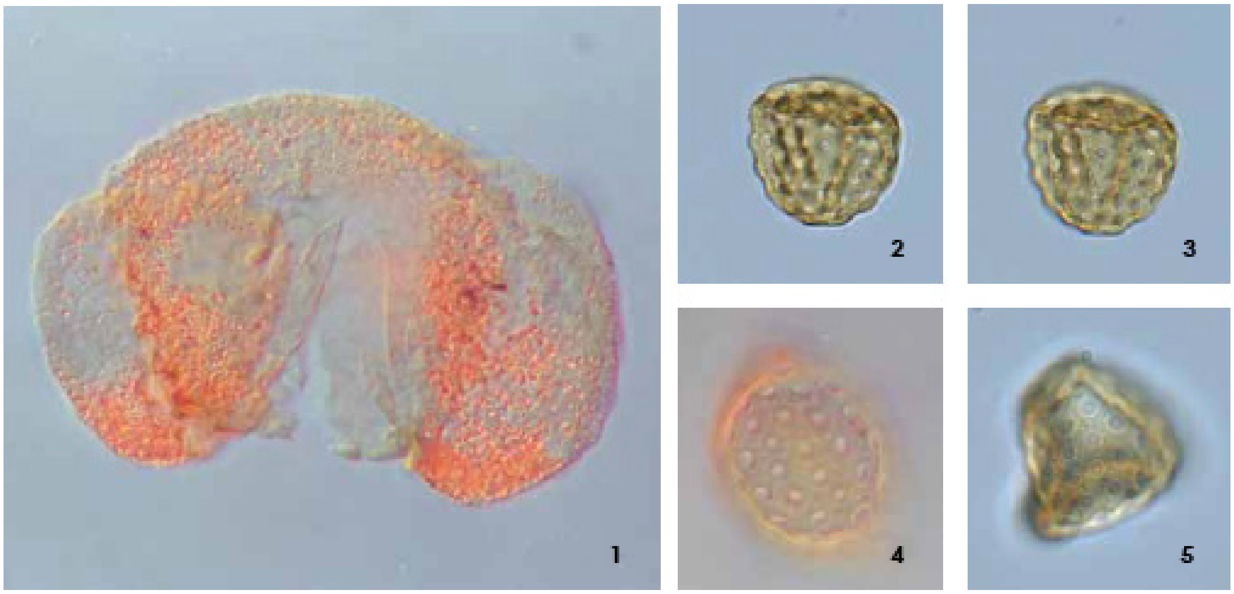

Plate 14. Light photomicrographs of key pollen species from sample DME-96-39, Asgard Range, Antarctica. 1. Reworked *Podocarpidites* sp., DV3009, 100x, 2-3. *Chenopodipollis* sp., views #3 and 4, 17.1 x 146.4, 60x. 4. *Chenopodipollis* sp., DV3008, 100x. 5. *Chenopodipollis* sp., view #5, 18.8 x 114.7, 60x.

palynomorphs.

3.3.5 Olympus Range – McKelvey Valley

Nearby McMelvey Valley, located close to the Olympus Range, 2 samples were collected. The samples collected here had concentrations ranging 0.6 to 4.2 gdw^{-1} and 0.3 to 0.4 gdw^{-1} for terrestrial and nonterrestrial derived palynomorphs. Sample DMS-91-43B is the first sample to have what appears to be an in situ dinoflagellate cysts which can be seen in plate 15. Dinoflagellate cysts can be indicative of a marine influence, so this region must have been exposed to marine influence previously.

3.4 Victoria Valley

Victoria Valley region was the site where 12 samples were collected, as shown in Figure 10 and Table 5. The interpreted ages of this region are thought to be Mid-Miocene in age, and the altitude of this region is 575 ± 50 m (Dr. Marchant, personal communication). This region has the highest ranges of concentrations for both terrestrial and nonterrestrial palynomorphs. The terrestrial concentration ranges from 0 to 5159.1 gdw^{-1} and the nonterrestrial component ranges from 0 to 2386.1 gdw$_{-1}$. Samples DME-97-30, DME-97-31B, DME-97-32, DME-97-33, DME-97-35, DMS-97-28A, DMS-97-28C, DMS-97-28D, and DMS-97-32 yielded interesting results. Sample DME-97-30, as seen in plates 16 and 17 contains abundant *Nothofagidites lachlaniae*, including several clumps. The presence of these clumps is important as it is a very clear indication that these specimens are penecontemporaneous, as reworking would break the clumps. The sample also contains some bryophyte spores (mosses *Coptospora*, and liverwort *Belgisporis*), and a single possible in-place podocarp conifer pollen. although pollen of the woody plant *Nothofagus* is abundant (though this may have resulted from a fortuitous pollen sac preservation), no other angiosperm pollen was observed. This suggests a slightly different habitat from those from the Asgard Range which have a more diverse angiosperm flora. This could also result from an age difference. The other unique characteristic of this sample is the abundant algal material recovered some *Leiosphaeridia* spp. (large and small types), and common *Botryococcus* (some partially de-

Table 4: Olympus Range table containing code number for identification, Sample ID, Sample Region, Sample GIS Latitude/Longitude, modern values for altitude, temperature, and precipitation, the inferred age of each sample, the basis for the age inference, and the Terrestrial Palynomorph Concentration (TCC) and Marine and Freshwater Palynomorph Concentration (MCC).

Code #	Sample ID	Sample Region	Latitude	Longitude	Altitude (m)	Temp. (°C)	Precipitation (mm weq)	Inferred age	Basis	TCC (GDW^-1)	MCC (GDW^-1)
					Modern Val.	Modern Val.	Modern Val.				
1	DMS-95-2	Bull Pass	-77.465	161.767	575 ± 50m	-8	100	Presumed Middle Miocene	Strat correlation	0	0
2	DMS-95-35	Bull Pass	-77.449	161.711	575 ± 50m	-8	100	Presumed Middle Miocene	Strat correlation	1.1	1.5
3	DMS-95-9	Bull Pass	-77.471	161.774	575 ± 50m	-8	100	Presumed Middle Miocene	Strat correlation	0	0
4	DMS-02-19	Olympus Range (Boreas site)	-77.475	161.163	1400 ± 50m	-20	200	14.07 ± 0.05 Ma	Strat correlation with dated ash in nearby lacustrine sediments	0.9	1.6
5	ALS-02-203-A	Olympus Range (East)	-77.448	161.527	1375 ± 50m	-20	200	14.07 ± 0.05 Ma	Strat correlation with dated ash in nearby lacustrine sediments	0.9	0
6	ALS-02-203-B	Olympus Range (East)	-77.448	161.527	1375 ± 50m	-20	200	14.07 ± 0.05 Ma	Strat correlation with dated ash in nearby lacustrine sediments	0.3	0
7	ALS-02-206	Olympus Range (East)	-77.452	161.538	1375 ± 50m	-20	200	14.07 ± 0.05 Ma	Strat correlation with dated ash in nearby lacustrine sediments	0	0.4
8	ALS-02-59	Olympus Range (East)	-77.454	161.506	1375 ± 50m	-20	200	14.07 ± 0.05 Ma	Strat correlation with dated ash in nearby lacustrine sediments	2.2	0
9	ALS-02-72	Olympus Range (East)	-77.45	161.524	1375 ± 50m	-20	200	14.07 ± 0.05 Ma	Strat correlation with dated ash in nearby lacustrine sediments	0.2	0
10	DMS-00-5-A	Olympus Range (West)	-77.509	160.886	1350 ± 50m	-15	100	> 10 Ma	Strat correlation	0.4	0
11	DMS-00-6-C	Olympus Range (West)	-77.513	160.962	1350 ± 50m	-15	100	> 10 Ma	Strat correlation	2.1	0
12	DMS-00-8-F	Olympus Range (West)	-77.522	161.028	1350 ± 50m	-6	50	> 10 Ma	Strat correlation	12.9	0
13	DMS-95-31	Insell Range/ McKelvey Valley	-77.421	161.555	575 ± 50m	-9	100	Presumed Middle Miocene	Strat correlation	4.2	0.4
14	DMS-95-43-B	Insell Range/ McKelvey Valley	-77.424	161.579	575 ± 50m	-9	100	Presumed Middle Miocene	Strat correlation	0.6	0.3

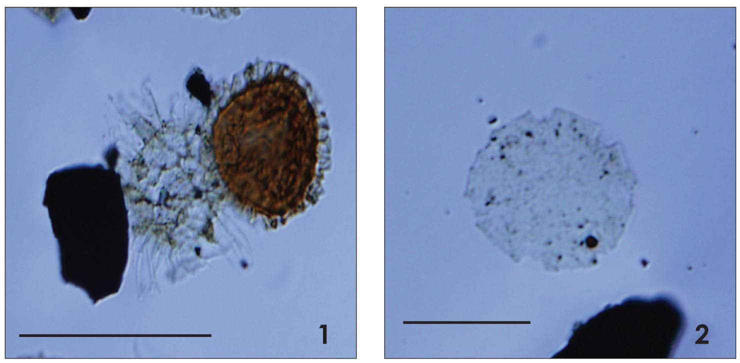

Plate 15. Light photomicrographs of various tricolpate pollen grains from sample DMS-91-43B McKelvey Valley, Antarctica. All specimens are all shown at the same magnification with a 50 micrometer scalebar for 1, and a 25 micrometer scalebar for 2-3. 1.*Micrhystridium* sp. view #1. DMS-91-43B. 2x141.1. (60x). 2. *Nothofagidites* sp. (fusca). view #1. DMS-91-43B. 15.9x124.7 (60x).

graded) plus some Zygnema-type algal cysts. The latter two are consistent with lacustrine depositional environment, although *Botryococcus* also grows in marginal brackish conditions. Sample DME-97-31B is characterized by abundant *Nothofagidites lachlaniae*, plus some other *Nothofagidites* spp. and angiosperm pollen, along with common moss (*Coptospora*) and other bryophyte (moss, hornwort, or liverwort) spores, and a few lycophyte spores (*Retitriletes*). It is a presumed penecontemporaneous flora reflecting low diversity tundra vegetation including bryophytes and *Nothofagus*. This sample also contains abundant algal material mostly *Leiosphaeridia* spp. (large and small types), with some larger thicker *Schizophacus*-type Zygnemataceae algae and common *Botryococcus* (some partially degraded). There are also rare fragments of light-colored, very corroded dinocysts, that are most likely reworked (see Plate 18). Sample DME-97-32 The sparse palynomorph assemblage is made of nicely preserved *Leiosphaeridia* spp. with a few bryophyte and lycophyte spores as shown in plate 19. Sample DME-97-33 contained a few light-colored bryophyte and lycophyte spores and angiosperm pollen, including one Poaceae were recovered. However, there was no *Nothofagidites*, but there was rare reworked Cretaceous dinocyst fragments (see Plate 20). Sample DME-97-35 contained rare specimens of moss spores (*Coptospora*), lycophyte spores, small angiosperm pollen and a slightly textured leiospherid alga which can be seen in Plate 21.

This large dominance of prostrate woody southern beech angiosperm pollen has been determined southern beech with a higher tolerance for a cooler range of temperatures as described in the study of Warny et al. (2009;2016). The high recovery of *Nothofagidites* sp. (fusca) indicates that this location might have served as an isolated region where tundra vegetation could survive. This vegetation may have been able to take advantage of pockets of freshwater indicated

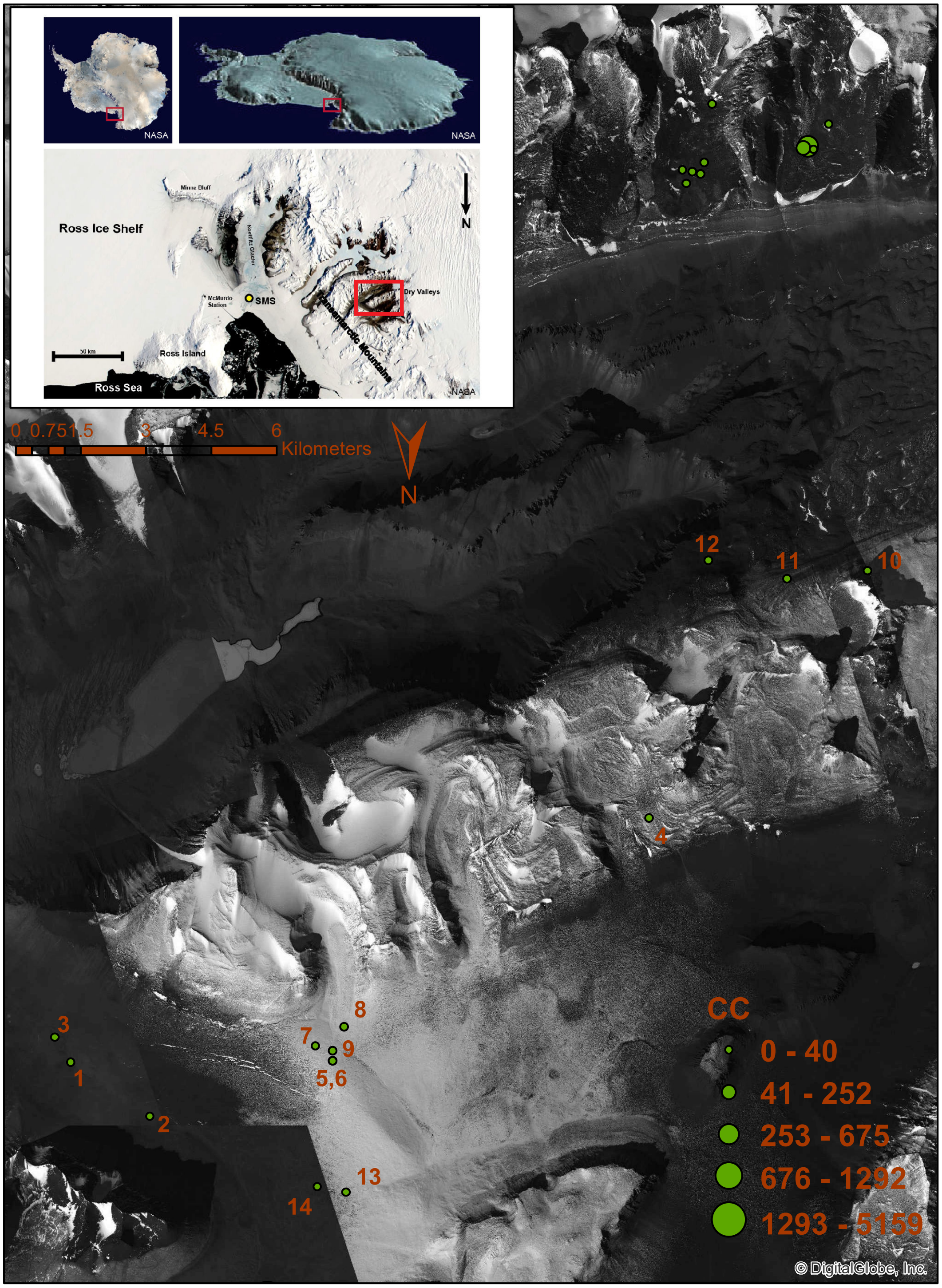

Figure 9: Sample spatial plot map of Olympus Range samples utilizing WorldView-1, WorldView-2. QuickBird-2, and GeoEye-1 high resolution imagery. All samples' terrestrial sourced palynomorph concentration is plotted by circles with varying diameters based on concentration values (Polar Geospatial Center and DigitalGlobe, Inc., 2017).

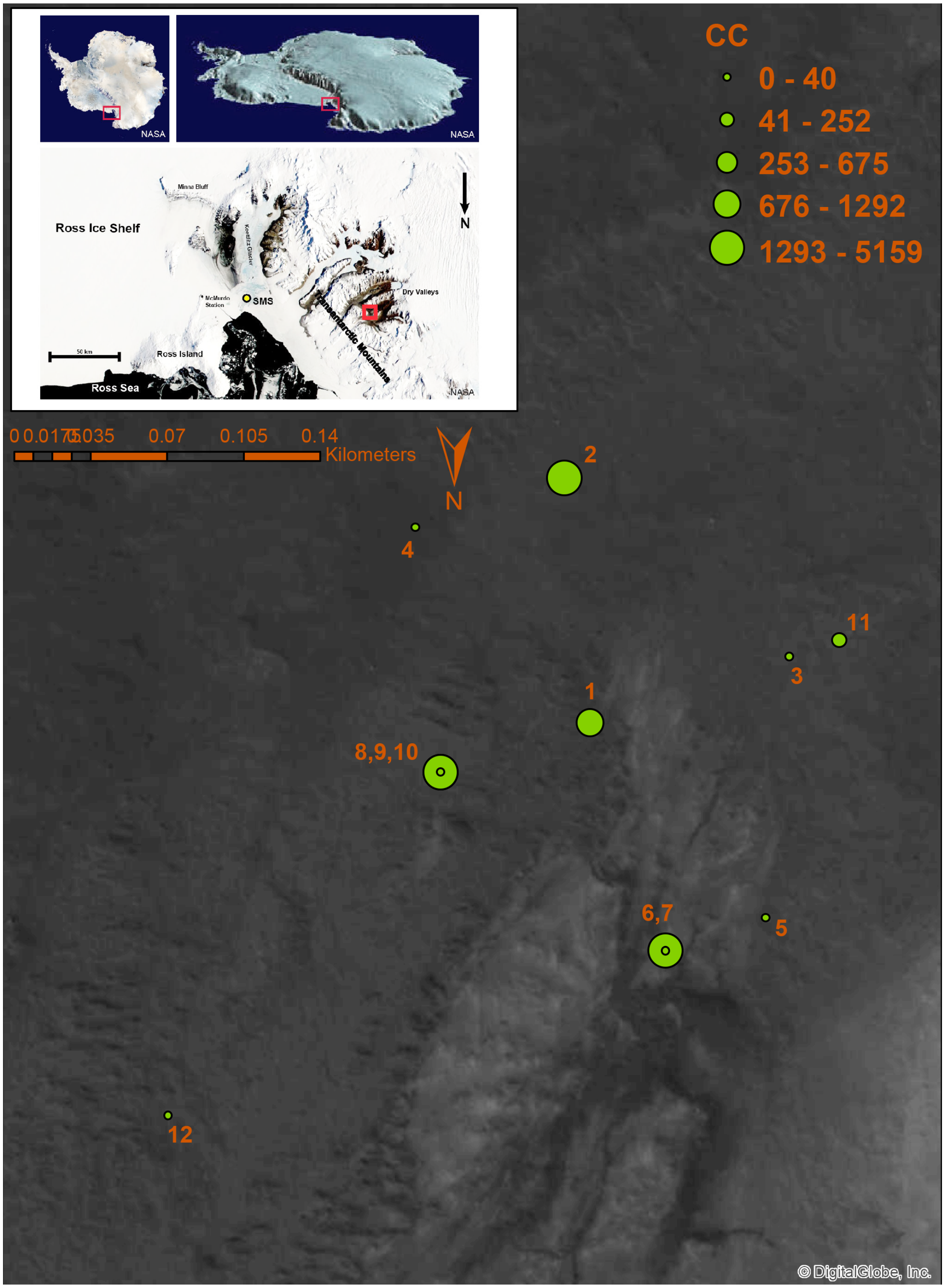

Figure 10: Sample spatial plot map of Victoria Valley samples utilizing WorldView-1, WorldView-2. QuickBird-2, and GeoEye-1 high resolution imagery. All samples' terrestrial sourced palynomorph concentration is plotted by circles with varying diameters based on concentration values (Polar Geospatial Center and DigitalGlobe, Inc., 2017).

Table 5: Victoria Valley table containing code number for identification, Sample ID, Sample Region, Sample GIS Latitude/Longitude, modern values for altitude, temperature, and precipitation, the inferred age of each sample, the basis for the age inference,and the Terrestrial Palynomorph Concentration (TCC) and Marine and Freshwater Palynomorph Concentration (MCC).

Code #	Sample ID	Sample Region	Latitude	Longitude	Altitude (m)	Temp. (°C)	Precipitation (mm weq)	Inferred age	Basis	TCC	MCC
					Modern Val.	Modern Val.	Modern Val.			(GDW^-1)	(GDW^-1)
1	DME-97-30	Victoria Valley	-77.404	161.66	575 ± 50m	-5	200	Presumed Middle Miocene	Ash yet to be dated	1292	735.6
2	DME-97-31B	Victoria Valley	-77.405	161.659	575 ± 50m	-5	200	Presumed Middle Miocene	Ash yet to be dated	5017.6	2247.5
3	DME-97-32	Victoria Valley	-77.404	161.656	575 ± 50m	-5	200	Presumed Middle Miocene	Ash yet to be dated	0	0
4	DME-97-33	Victoria Valley	-77.405	161.662	575 ± 50m	-5	200	Presumed Middle Miocene	Ash yet to be dated	31.4	1.4
5	DME-97-35	Victoria Valley	-77.403	161.658	575 ± 50m	-5	200	Presumed Middle Miocene	Ash yet to be dated	27.4	2
6	DMS-97-28-A	Victoria Valley	-77.403	161.66	575 ± 50m	-5	200	Presumed Middle Miocene	Ash yet to be dated	5159.1	2386.1
7	DMS-97-28-B	Victoria Valley	-77.403	161.66	575 ± 50m	-5	200	Presumed Middle Miocene	Ash yet to be dated	29	3
8	DMS-97-28-C	Victoria Valley	-77.404	161.663	575 ± 50m	-5	200	Presumed Middle Miocene	Ash yet to be dated	4796.1	131.9
9	DMS-97-28-D	Victoria Valley	-77.404	161.663	575 ± 50m	-5	200	Presumed Middle Miocene	Ash yet to be dated	4087.4	513.1
10	DMS-97-28-I	Victoria Valley	-77.404	161.663	575 ± 50m	-5	200	Presumed Middle Miocene	Ash yet to be dated	0.6	0
11	DMS-97-32	Victoria Valley	-77.404	161.655	575 ± 50m	-5	200	Presumed Middle Miocene	Ash yet to be dated	252.1	1575.3
12	DMS-97-34-A	Victoria Valley	-77.403	161.67	575 ± 50m	-5	200	Presumed Middle Miocene	Ash yet to be dated	4.2	0

Figure 11: Photograph of Nothofagus gunnii alpine shrubbery during autumn in modern day Tasmania which is similar to what existed in Victoria Valley (Greg Jordan, 2011).

by the presence of Zygnemataceae and *Schizophacus* algae. Figure 11 represents southern beech vegetation found in modern day Tasmania that would provide a similar vegetation to what this study expects to find.

3.5 Beacon Valley

Beacon Valley and the surrounding area including Arena Valley had 14 samples collected from those regions as shown in Figure 12, Table 6. Ages from these samples range from around 4 Ma to Mid-Miocene. And the altitude of these samples range from 1300 to 1750 ± 50 m (Marchant, pers. comm.). The samples from this region are predominately barren with the exception of sample DMI-97-14-2 Debris, and EME-98-13. This suggests that the locations of DMI-14-2 Debris within the Central Beacon Valley and EME-98-13 at Mullins Glacier may have been isolated locations with sparse vegetation survived.

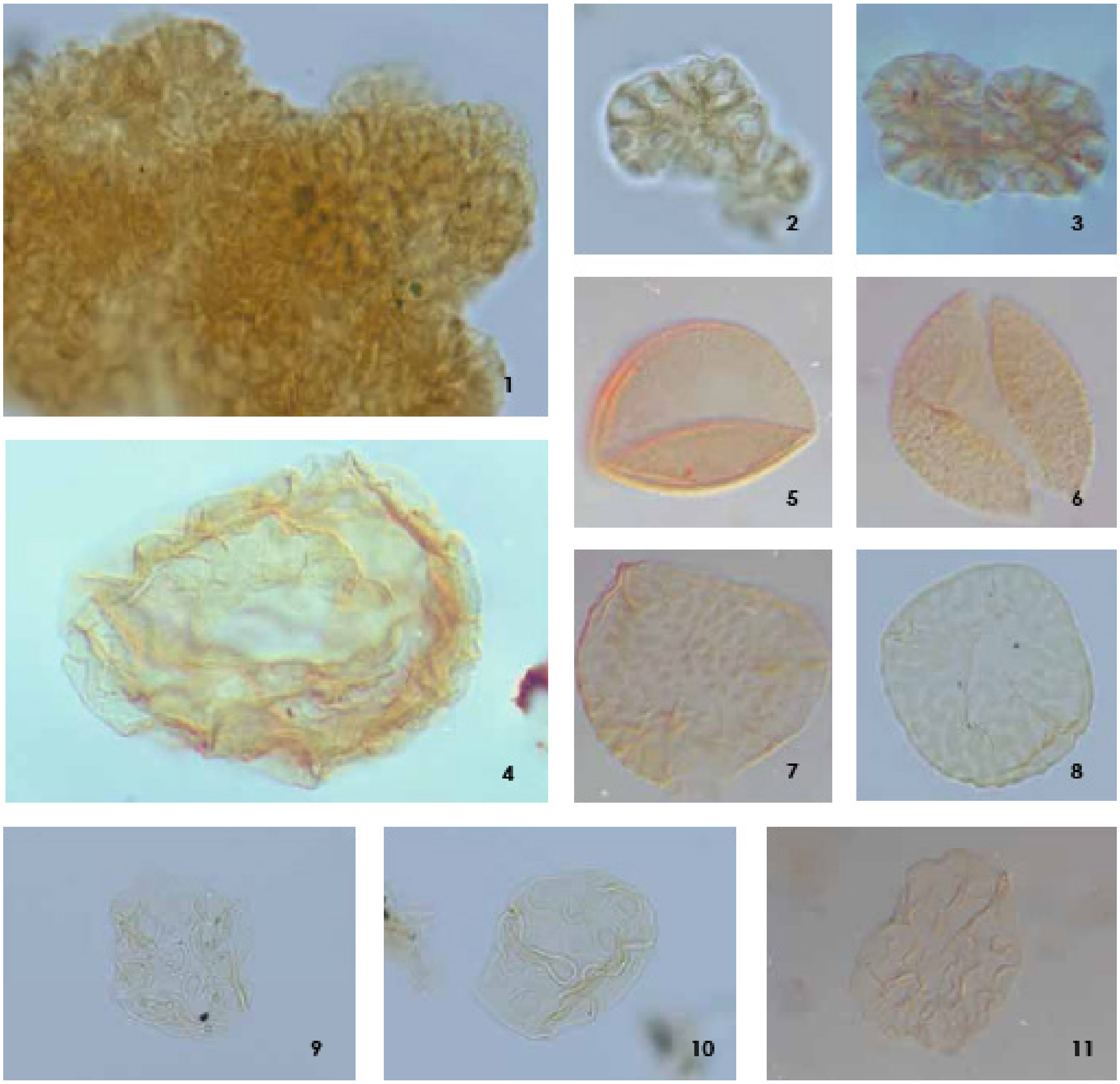

Plate 16. Light photomicrographs of key in situ algae and spore species from sample DME-97-30, Victoria Valley, Antarctica. All specimens are shown at the same magnification. 1. Large colony of *Botryococcus* sp., view #2, 5.0 x 124.9, 60x. 2. *Botryococcus* sp., view #1, 2.9 x 128.0, 60x. 3. *Botryococcus* sp., DV3020, 100x. 4. *Belgisporis* sp., DV2005, 100x. 5-8. Various specimens of *Coptospora* spp. showing variation in ornamentation, from fine to large. 5. DV2006,100x. 6. DV3021,100x. 7. DV2003,100x. 8. View #2, 2.9 x 118.5, 60x. 9-11. Various specimens of spores of Zygnemaceae. 9. View #2, 2.9 x 121.9, 60x. 10. View #1, 5.6 x 126.9, 60x. 11. DV2004, 100x.

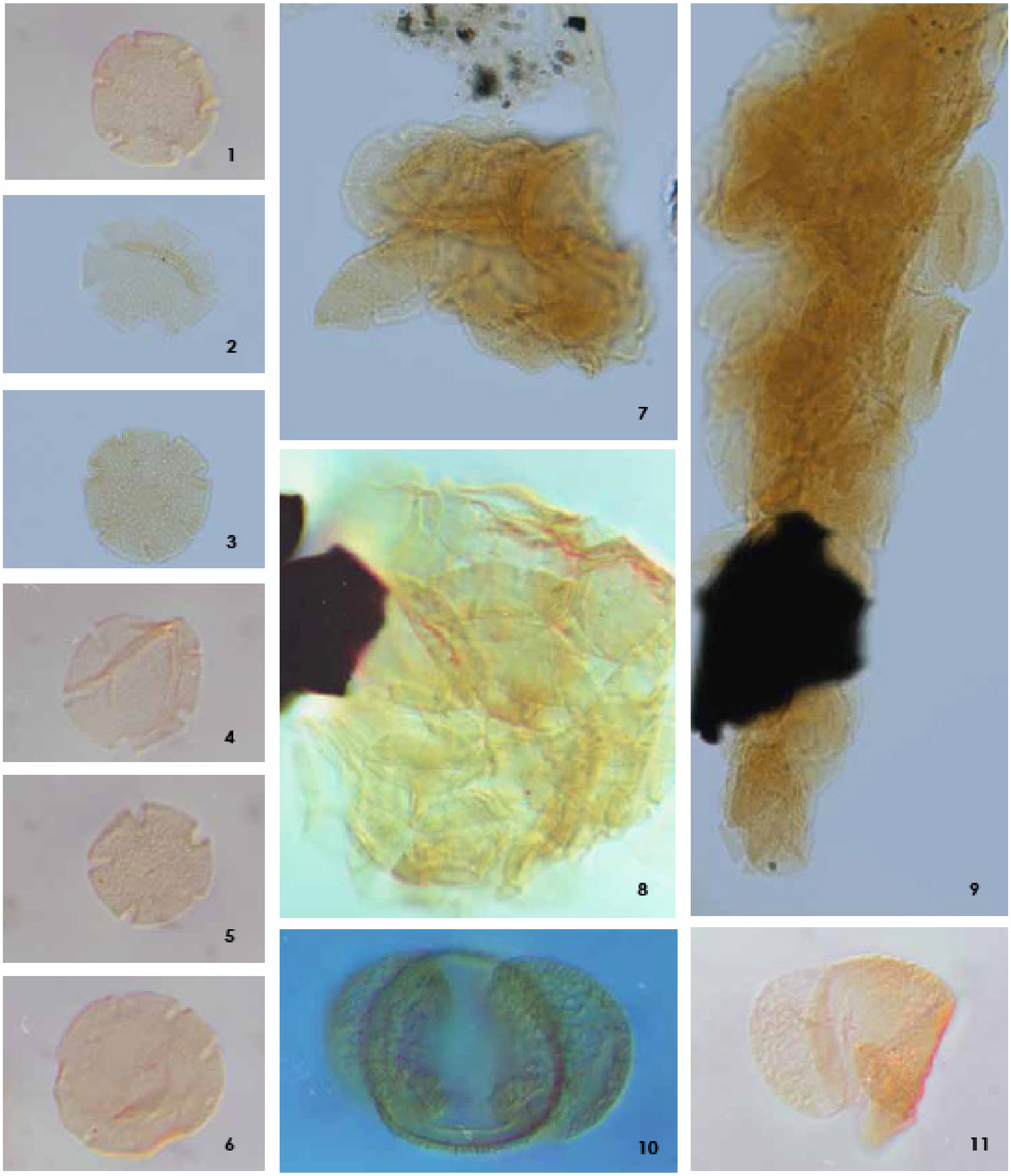

Plate 17. Light photomicrographs of key in situ pollen species from sample DME-97-30, Victoria Valley, Antarctica.   1-9. Various specimens of *Nothofagidites lachlaniae*, including numerous clumps of adherent pollen (7-9) confirming that these specimens are definitely penecontemporaneous. 1. DV3019, 100x. 2. View #1, 3.4 x 127.8. 3. View #1, 5.6 x 131.5, 60x. 4. DV3025, 100x. 5. DV3018, 100x. 6. DV3024, 100x. 7. View #3, 3.4 x 129.2, 60x. 8. DV2007, 100x. 9. View #2, 7.4 x 128.2, 60x. 10. Likely contaminant conifer pollen, DV2001, 100x. 11. *Podocarpidites* sp., DV2002.

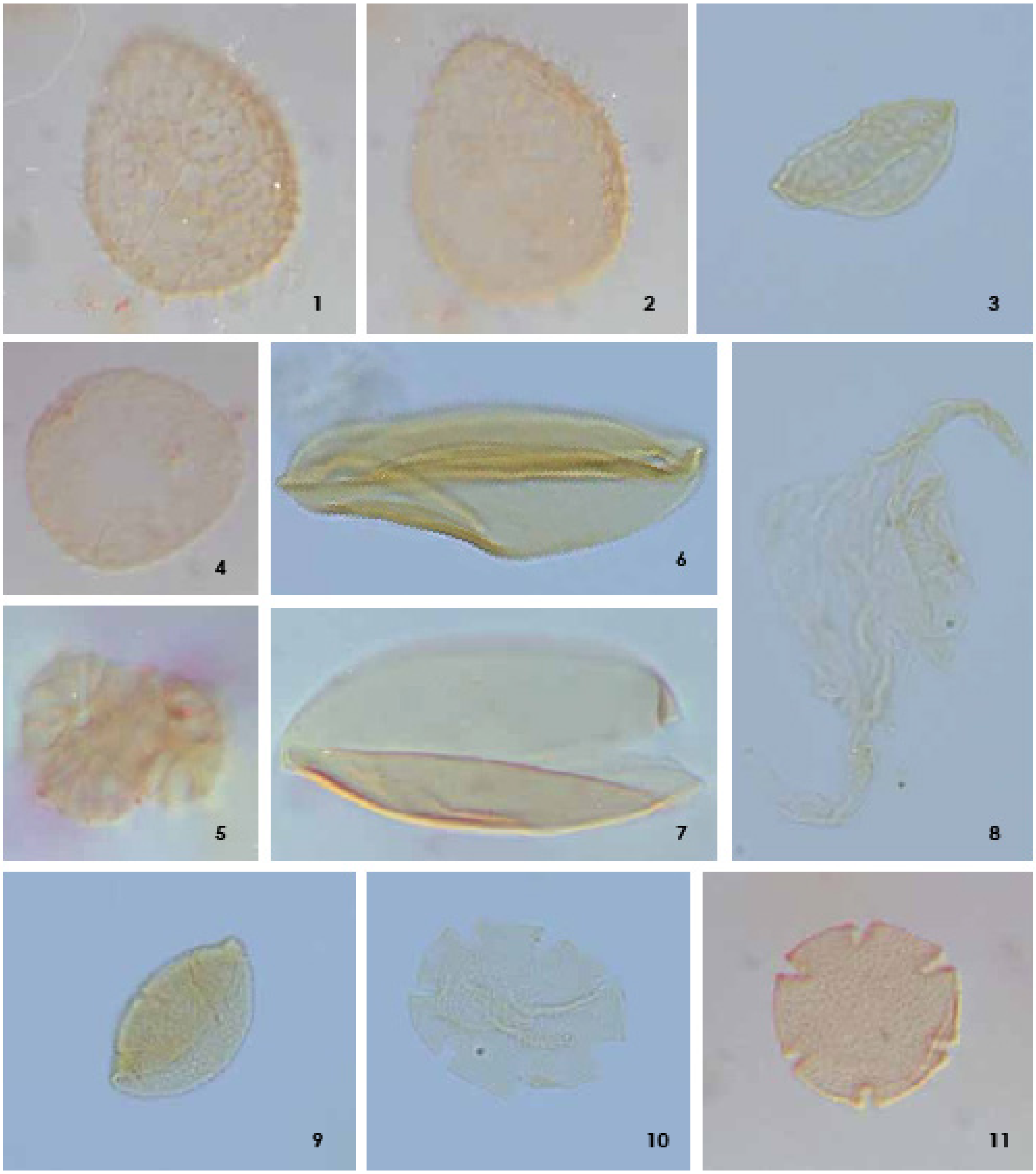

Plate 18. Light photomicrographs of key in situ pollen, spores, and dinoflagellate cyst species from sample DME-97-31-B, Victoria Valley, Antarctica.
1-2. Trilete bryophyte spore with indistinct incomplete reticulate ornamentation, DV2009 and DV2010 100x. 3. Coptospora sp., view #1, 4.1 x 125.6, 60x. 4. *Triporoletes* sp., DV3023, x100. 5. *Botryococcus* sp., DV2008, 100x. 6. *Schizophacus parvus*, view #2, 4.9x 142.5, 60x. 7. *Schizophacus parvus*, DV2011, 100x. 8. Dinoflagellate, possibly related to *Palaeocystodinium benjaminii* (range of 68.5 - 61.5 Ma), view #2, 4.1 x 140.5, 60x. 9. *Nothofagidites lachlaniae*, view #4, 8.6 x 143.4, 60x. 10. *Nothofagidites lachlaniae*, view #2, 5.7 x 144, 60x. 11. *Nothofagidites lachlaniae*, DV3022, 100x.

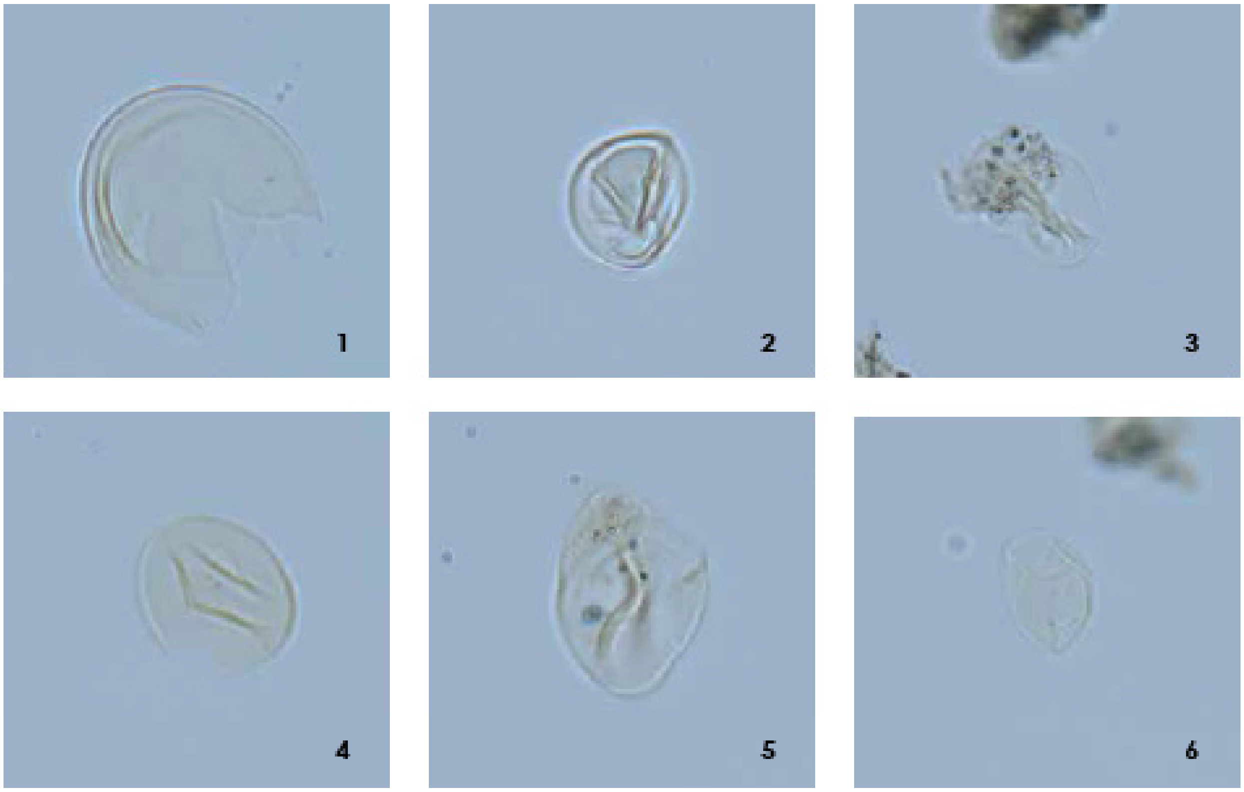

Plate 19. Light photomicrographs of various leiospheres from sample DME-97-32, Victoria Valley, Antarctica.1-6. Various specimens of *Leiosphaeridia* spp. 1. View #1, 5.0 x 114.8, 60x. 2. View #2, 6.4 x 109.5, 60x. 3. View #2, 7.3 x 146.2, 60x. 4. View #4, 7.9 x 125.7, 60x. 5. View #2, 8.5 x 125.4, 60x. 6. View #3, 8.5 x 131.5, 60x.

3.5.1 Beacon Valley – Arena Valley

Arena Valley nearby the Beacon Valley provided the location for 2 samples. The samples from this region were barren with concentrations ranging from 0 to 0.8 gdw^{-1} for terrestrial palynomorphs.

3.5.2 Beacon Valley – Beacon Saddle

Beacon Saddle nearby the Beacon Valley was the location where 2 samples were collected. The samples from this region are barren with concentrations ranging 0.2 to 0.6 gdw^{-1} for terrestrial palynomorphs. Sample DMS-10-08A contained what appears to be a *Chenopodipollis* sp. grain. Sample DMS-10-08B contains two fungal spores and one unidentified angiosperm pollen grain.

3.5.3 Beacon Valley – Mullins/Taylor/Granite/NEST

Mullins Glacier, Taylor Glacier, Granite drift, Mullins Glacier nest site, and Mullins Glacier till had 8 samples collected from these locations. The samples collected from these regions ranged from 0.2 to 131.8 gdw^{-1} for terrestrial sourced palynomorphs and 7.3 to 15.3 gdw^{-1} nonterrestrial sourced palynomorphs. Most of the samples contain opaque reworked thermally matamorphosed specimens. Sample EME-98-13 has the highest concentration of terrestrial palynormophs of 131.8 gdw^{-1}. This sample contains few unidentified tricolpate pollen grains. Sample DME-06-009 also contained some tricolporate pollen grains and one *Leiosphaeridia* sp.

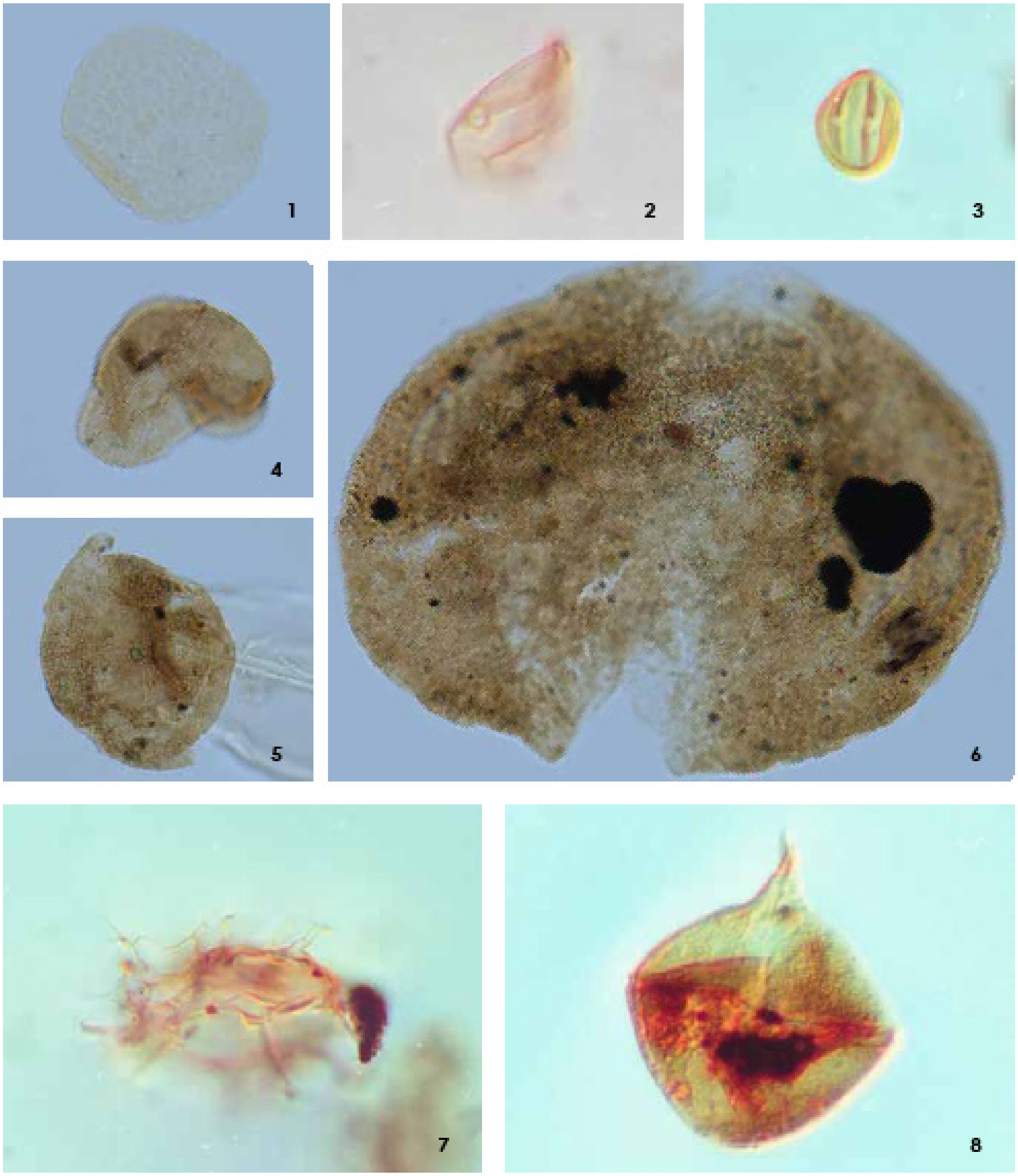

Plate 20. Light photomicrographs of key in situ pollen, spores and dinoflagellate cyst species from sample DME-97-33, Victoria Valley, Antarctica. 1. *Triporoletes* sp., view #2, 8.5 x 144.5, 60x. 2. Poaceae, DV2014, 100x. 3. Tricolporate pollen, DV2013, 100x. 4. Reworked gymnosperm pollen grain, view #2, 8.5 x 130.7, 60x. 5. Reworked gymnosperm pollen grain, view #2, 6.5 x 147.7, 60x. 6. Reworked gymnosperm pollen grain, view #2, 11.0 x 144.8, 60x. 7. Reworked *Spiniferites* sp., DV2012, 100x. 8. Reworked corroded Cretaceous dinoflagellate *Cribroperidinium* sp., DV2015, 25x.

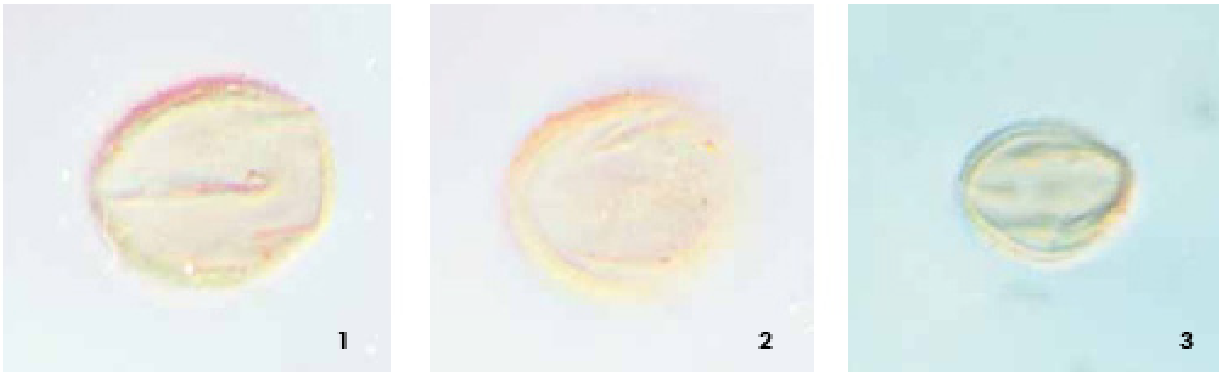

Plate 21. Light photomicrographs of key in situ pollen species from sample DME-97-35, Victoria Valley, Antarctica. 1-2. Tricolpate pollen, DV2017 and DV2018, 100x. 3. Tricolporate pollen sp. A, DV2019, 100x.

Table 6: Beacon Valley table containing code number for identification, Sample ID, Sample Region, Sample GIS Latitude/Longitude, modern values for altitude, temperature, and precipitation, the inferred age of each sample, the basis for the age inference, and the Terrestrial Palynomorph Concentration (TCC) and Marine and Freshwater Palynomorph Concentration (MCC).

Code #	Sample ID	Sample Region	Latitude	Longitude	Altitude (m) Modern Val.	Temp. (°C) Modern Val.	Precipitation (mm weq) Modern Val.	Inferred age	Basis	TCC (GDW^-1)	MCC (GDW^-1)
1	DMS-02-7	Arena Valley	-77.857	160.964	1300 ± 50m	-11	75	11.27±0.12 Ma	Argon 40/39 date on interbedded ash	0	0
2	DMS-91-750-C	Arena Valley	-77.828	160.986	1300 ± 50m	-11	75	11.28±0.05 Ma	Argon 40/39 date on interbedded ash	0.8	0
3	DMS-10-8-A	Beacon Saddle	-77.823	160.854	1750 ± 50m	-20	75	Middle Miocene	Strat correlation	0.2	0
4	DMS-10-8-B	Beacon Saddle	-78.823	161.854	1750 ± 50m	-20	75	Middle Miocene	Strat correlation	0.6	0
5	DME-06-9	Beacon Valley - Mullins Glacier	-77.857	160.569	1350 ± 50m	-12	75	>7.69±0.01 Ma	Argon 40/39 date on interbedded ash	39.7	7.3
6	DME-97-7	Beacon Valley - Taylor Glacier	-77.852	160.601	1350 ± 50m	-12	75	>8.07±0.06 Ma	Argon 40/39 date on interbedded ash	69.7	0
7	DMS-99-2-A	Beacon Valley, Granite drift	-77.845	160.608	1350 ± 50m	-12	75	8.07±0.06 Ma	Argon 40/39 date on interbedded ash	0	0
8	DMS-97-7	Beacon Valley, Granite driftr	-77.852	160.601	1350 ± 50m	-12	75	>8.07±0.06 Ma	Argon 40/39 date on interbedded ash	0.2	0.5
9	EME-98-13	Beacon Valley, Mullins Glacier	-77.865	160.538	1350 ± 50m	-12	75	7.69±0.01 Ma	Argon 40/39 date on interbedded ash	131.8	0
10	NEST SITE ICE	Beacon Valley, Mullins Glacier nest site	-77.874	160.544	1350 ± 50m	-12	75	> 4 Ma	Average of multiple Argon 40/39 dates on overlying ash	17.7	15.3
11	DMS-98-13-A	Beacon Valley, Mullins till	-77.877	160.556	1350 ± 50m	-12	75	8.07±0.06 Ma	Argon 40/39 date on interbedded ash	0	0
12	DMS-06-2	Beacon Valley, nest site	-77.874	160.544	1400 ± 50m	-12	75	> 4 Ma	Average of multiple Argon 40/39 dates on overlying ash	8.3	0.3
13	DMI-97-14-2-DEBRIS	Central Beacon Valley	-77.851	160.595	1350 ± 50m	-12	75	>8.07±0.06 Ma	Argon 40/39 date on interbedded ash	675.3	0
14	DMI-97-14-2-MELTWATER	Central Beacon Valley	-77.851	160.595	1350 ± 50m	-12	75	>8.07±0.06 Ma	Argon 40/39 date on interbedded ash	0.4	0.3

3.5.4 Beacon Valley – Central Beacon Valley

The Central Beacon Valley had 2 samples collected from this location. The sample concentration ranges from 0.4 to 675.3 gdw^{-1} for terrestrial palynomorphs and 0 to 0.3 gdw^{-1} for non-terrestrial palynormorph concentration. Sample DMI-97-14-2 Meltwater mainly contains black organic matter, with some very light plant tissue and orange-brown partially degraded organic matter. It contains overwhelming numbers of added *Lycopodium*. It only contains two specimens of *Nothofagidites lachlaniae*, one *Coptospora* sp. and two *Leiosphaeridia* sp. which could possibly possibly penecontemporaneous with the sediment. A laboratory contaminant, *Alnus* specimen, was found plus one large, thick-walled algal body.Sample DMI-97-14-2 Debris contains *Coptspora* sp. moss spores and low diversity of angiosperms such as Poaceae, Asteraceae, and *Chenopodipollis* (see Plate 22 and 23).

This low assemblage of bryophyte spores and angiosperm pollen grains may indicate that this location may have allowed for slightly more substantial vegetation to survive while the rest of the surrounding region was too inhospitable. Examples of the ground covering vegetation that would be similar to what we would see in region can be seen in figures 14 – 16. This is important because the sample from this region are thought to be some of the youngest samples in the study with an age of 8.07±0.06 Ma, which makes this site even younger than the Lewis et al. (2009) study site.

3.6 Taylor Valley

The Rhone Platform in Taylor Valley was the site for 9 samples as shown in figure 16, Ta-

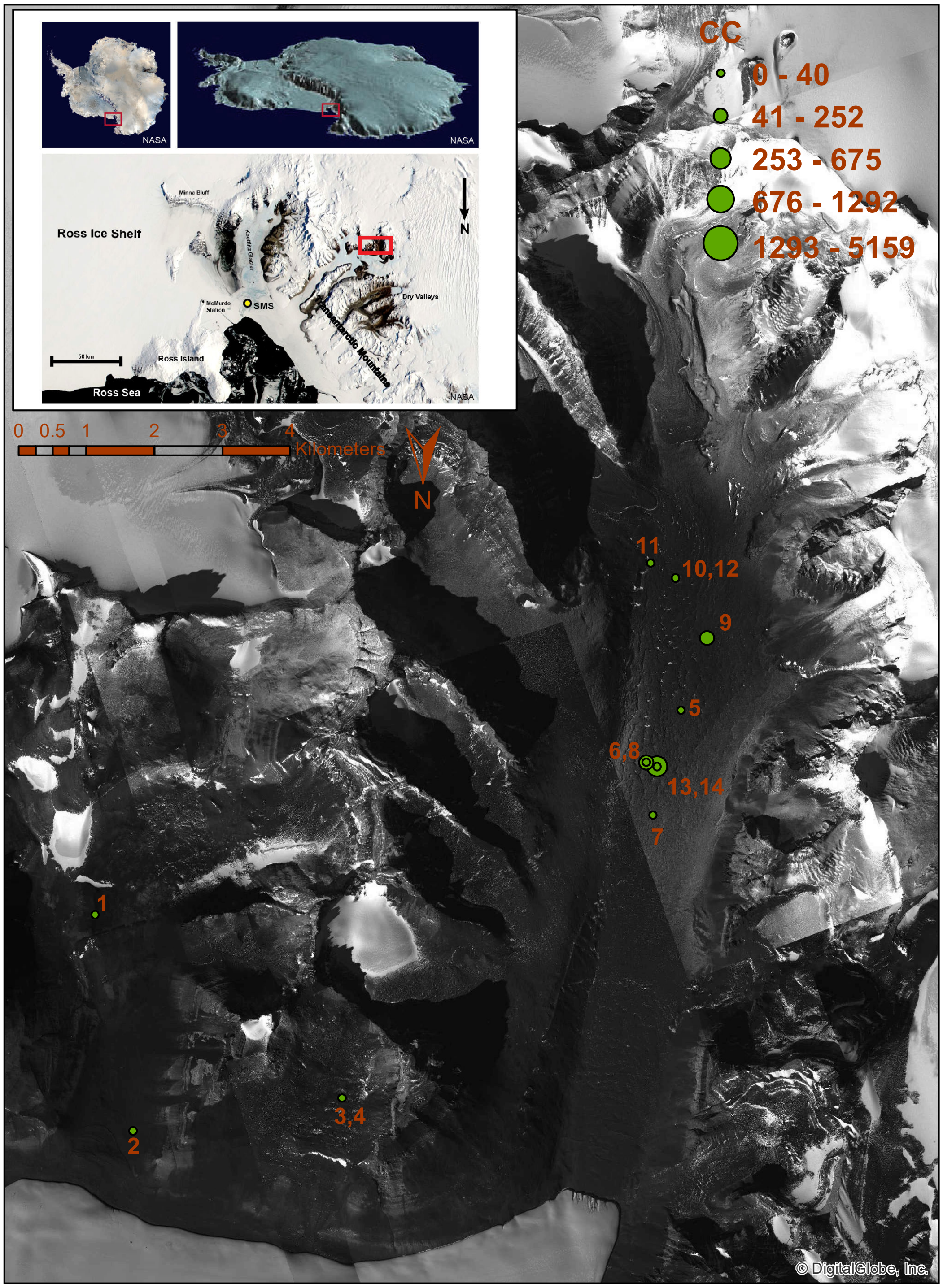

Figure 12: Sample spatial plot map of Beacon Valley samples utilizing WorldView-1, WorldView-2. QuickBird-2, and GeoEye-1 high resolution imagery. All samples' terrestrial sourced palynomorph concentration is plotted by circles with varying diameters based on concentration values (Polar Geospatial Center and DigitalGlobe, Inc., 2017).

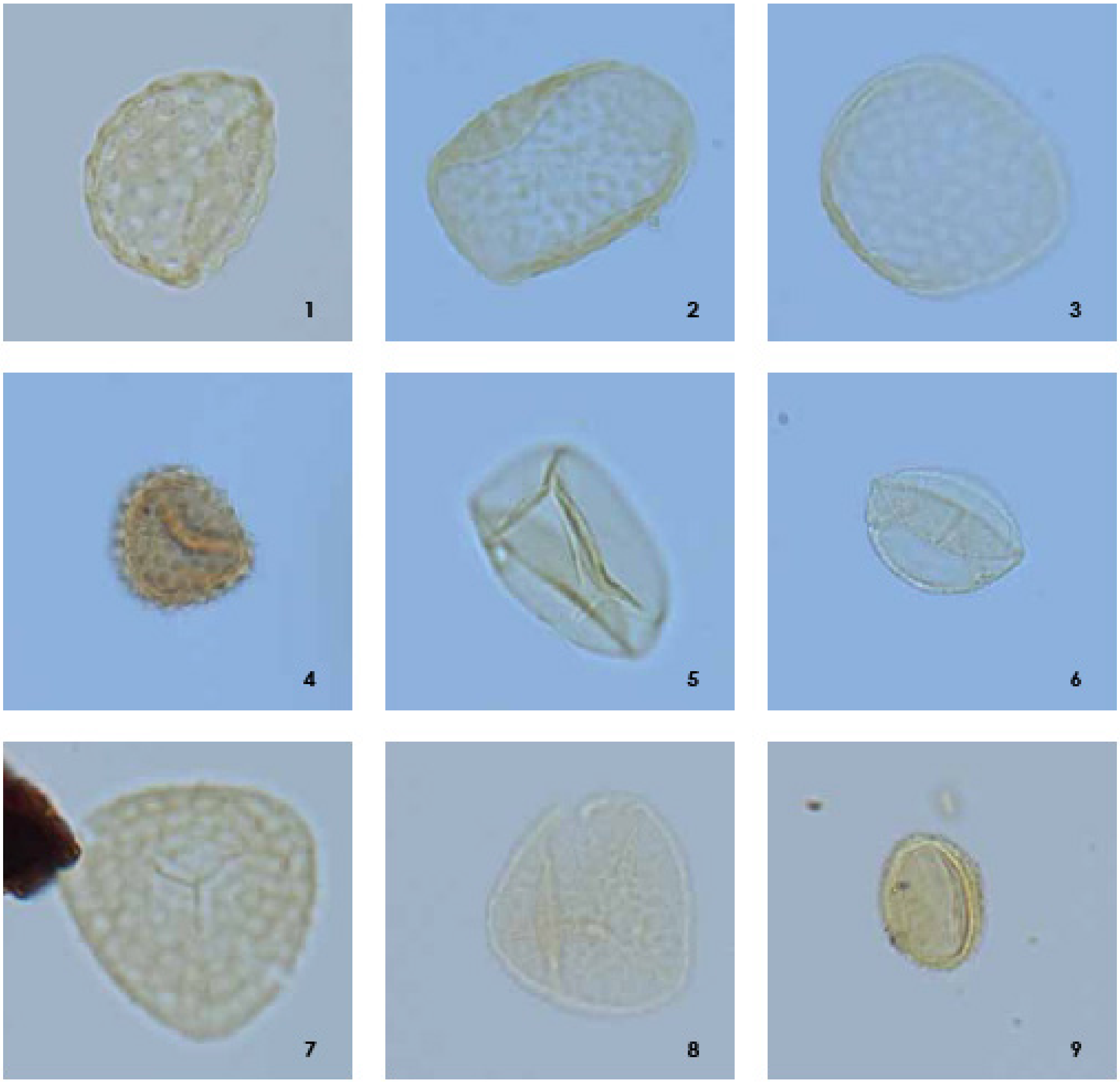

Plate 22. Light photomicrographs of key in situ pollen and spores species from sample DMI-97-14-2 (debris), Beacon Valley, Antarctica. 1. *Chenopodipollis* sp., view #4, 11.1 x 120.8, 60x. 2. *Coptospora* sp., view #3, 9.4 x 139.6, 60x. 3. *Coptospora* sp., view #3, 8.1 x 139.6, 60x. 4. Asteraceae, view #4, 9.4 x 132.7, 60x. 5. *Poaceae*, view #2, 4.8 x 136.3, 60x. 6. *Nothofagidites* sp., view #4, 8.9 x 122.9, 60x. 7. *Retitriletes* sp., view #4, 15.4 x 138.8, 60x. 8. *Triporoletes* sp., view #3, 14.7 x 147.5, 60x. 9. Tricolporate sp. A, view #3, 14.7 x 13.0, 60x.

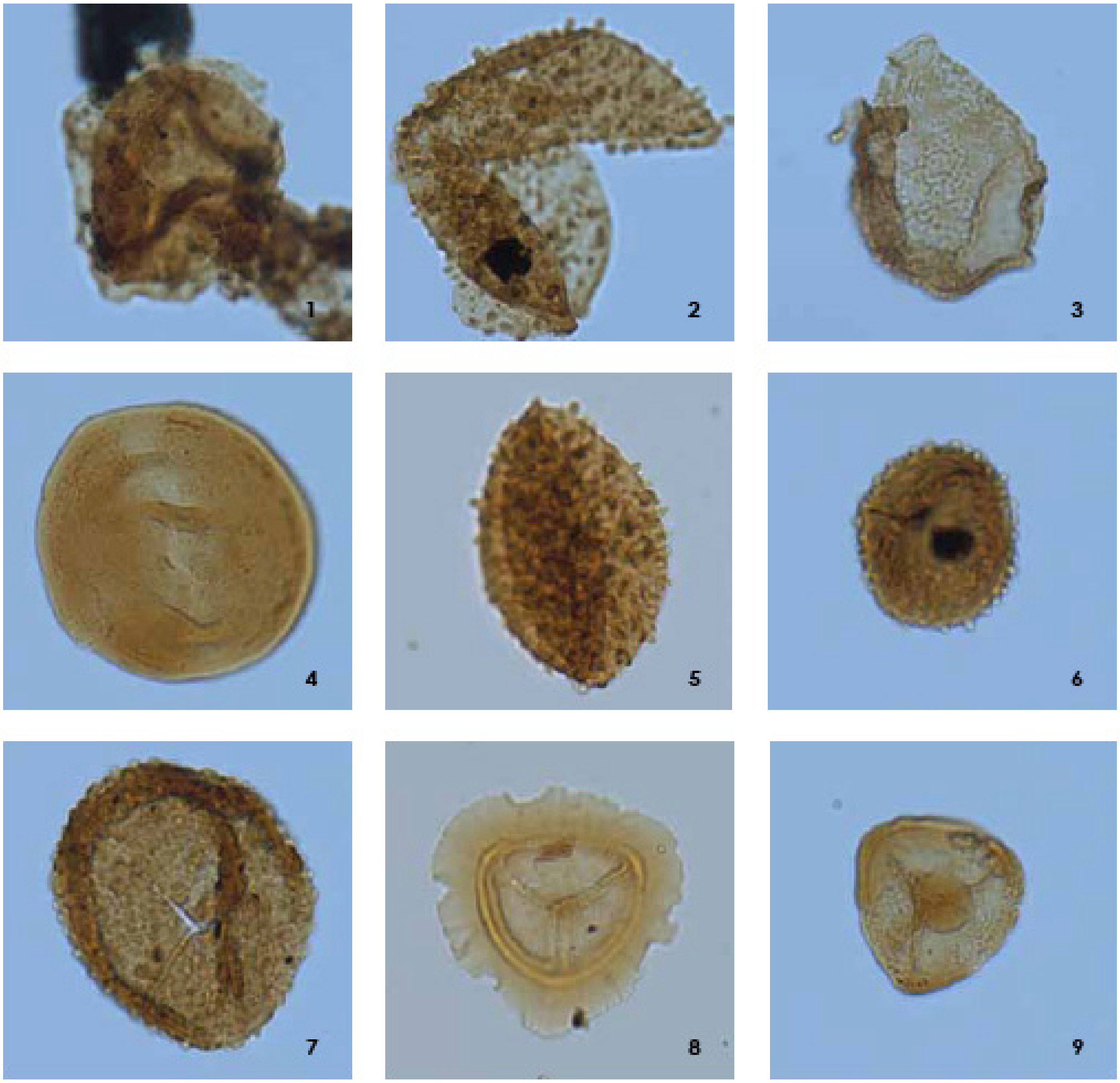

Plate 23. Light photomicrographs of key reworked spore species from sample DMI-97-14-2 (debris), Beacon Valley, Antarctica. 1. *Aequitriradites cf spinulosus*, view #2, 10.0 x 142.6, 60x. 2. *Baculatisporites* sp., view #2, 4.8 x 133.0, 60x. 3. TBA, view #3, 9.4 x 128.7, 60x. 4. *Classopollis* ?*classoides*, view #1, 7.4 x 129.9, 60x. 5. *Baculatisporites* sp., view #2, 6.8 x 124.7, 60x. 6. *Baculatisporites* sp., view #3, 6.8 x 140.8, 60x. 7. *Osmundacidites - Baculatisporites* complex, view #3, 15.9 x 123.8, 60x. 8. *Murospora florida*, view #4, 12.4 x 128.8, 60x. 9. *Stereisporites antiquasporites*, view #3, 5.2 x 131.9,, 60x.

ble 7, and Plate 24 and 25. Samples from this region range in ages from 10.09±0.16 to 10.76±0.17 Ma and spanned altitude ranges from 1000 to 1200 ± 50 m (Marchant, pers. comm.). Terrestrial palynomorph concentration ranges from 0 to 776.7 gdw^{-1} and 0 to 4.4 gdw^{-1} for nonterrestrial palynomorph concentration for this region. The samples from this region were mostly barren except DME-88-28. It contains a sparse possibly penecontemporaneous flora of mainly moss spores *Coptospora* sp. with other bryophyte and lycophyte spores and various small angiosperm pollen

including Poaceae. Common reworked dark brown to black corroded spore and pollen remnants, mostly unidentifiable are noted throughout the slides. These include mainly specimens derived from the Beacon, with some younger and lighter colored Mesozoic reworked specimens. The sample also contains reworked Cretaceous dinocysts, that possibly include taxa such as *Circu-*

Figure 13: Photograph of Antarctic Pearlwort at St. Andrews Bay, South Georgia. This ground covering wild flower vegetation is similar to the type of angiosperm pollen observed in Beacon Valley (Wikimedia commons, 2011).

Figure 14: Photograph of Antarctic hair grass at Peterman Island. This ground covering grass vegetation is similar to the type of angiosperm pollen observed in Beacon Valley (Wikimedia commons, 2011).

lodinium distinctum (range from 90.14 - 68.5 Ma), *Diconodinium* sp. (range from 122.10 - 70.0 Ma), *Isabelidinium cooksoniae* (range from 82 - 67.7 Ma), Subtilisphaera symperlucida (range from 133 - 92 Ma), *Apteodinium* sp. (range of genus from 143 - 68.80 Ma), or *Cribroperidinium* sp. laboratory contaminants were found as well including large pink-stained spore, *Tilia*, *Alnus*, and *Betula*.

Figure 15: Photograph of Schistidium antarctici mosses near Casey Station. The moss shown here is similar to the type of bryophyte spore observed in the Beacon Valley (Sharon Robinson, 2012).

Table 7: Taylor Valley table containing code number for identification, Sample ID, Sample Region, Sample GIS Latitude/Longitude, modern values for altitude, temperature, and precipitation, the inferred age of each sample, the basis for the age inference, and the Terrestrial Palynomorph Concentration (TCC) and Marine and Freshwater Palynomorph Concentration (MCC).

Code #	Sample ID	Sample Region	Latitude	Longitude	Altitude (m)	Temp. (°C)	Precipitation (mm weq)	Inferred age	Basis	TCC	MCC
					Modern Val.	Modern Val.	Modern Val.			(GDW^-1)	(GDW^-1)
1	BNS-97-15-C	Taylor Valley - Rhone	-77.702	162.082	1200 ± 50m	-4	50	>10.76±0.17	Strat correlation	0.4	0
2	BNS-97-37-C	Taylor Valley - Rhone	-77.704	162.072	1200 ± 50m	-4	50	>10.76±0.17	Strat correlation	1.1	0
3	BNS-97-41-B	Taylor Valley - Rhone	-77.71	162.066	1000 ± 50m	-4	50	10.76±0.17	Strat correlation	0	0
4	DMS-88-22-B	Taylor Valley - Rhone	-77.711	162.091	1000 ± 50m	-4	50	10.76±0.16	Strat correlation	0.7	0
5	DMS-88-23-C	Taylor Valley - Rhone	-77.711	162.082	1000 ± 50m	-4	50	10.76±0.16	Argon 40/39 date on interbedded ash	0.7	0
6	DMS-88-41	Taylor Valley - Rhone	-77.711	161.934	1000 ± 50m	-4	50	10.76±0.16	Strat correlation	1.4	0
7	DMS-88-49	Taylor Valley - Rhone	-77.712	161.665	1000 ± 50m	-4	50	10.76±0.16	Strat correlation	0.9	0
8	DMS-97-1-D	Taylor Valley - Rhone	-77.71	162.054	1000 ± 50m	-4	50	10.09±0.16	Argon 40/39 date on interbedded ash	0.5	0
9	DME-88-28	Rhone Platform	-77.709	162.088	1000 ± 50m	-4	50	10.76±0.16	Strat correlation	76.7	4.4

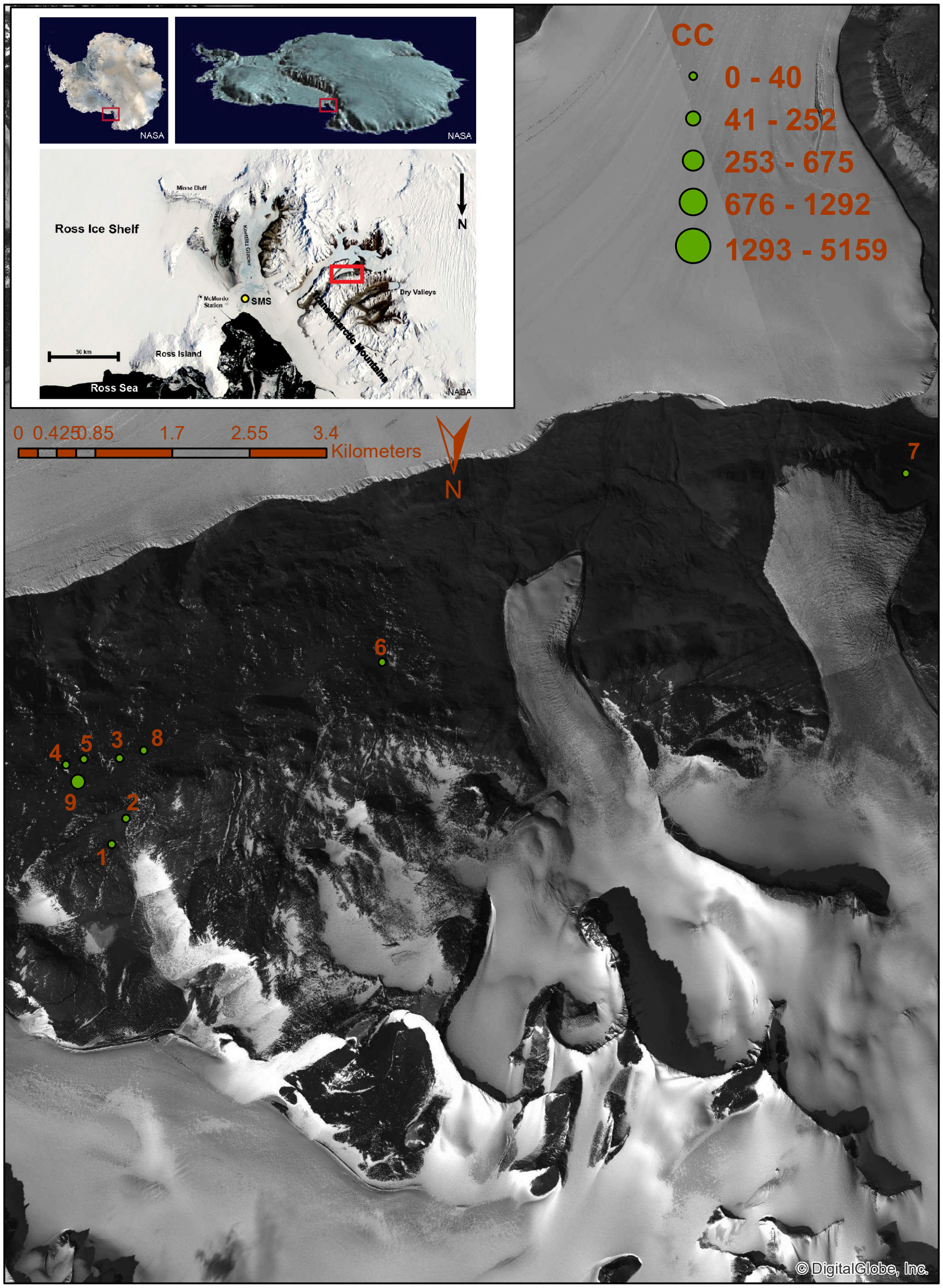

Figure 16: Sample spatial plot map of Taylor Valley samples utilizing WorldView-1, WorldView-2. QuickBird-2, and GeoEye-1 high resolution imagery. All samples' terrestrial sourced palynomorph concentration is plotted by circles with varying diameters based on concentration values (Polar Geospatial Center and DigitalGlobe, Inc., 2017).

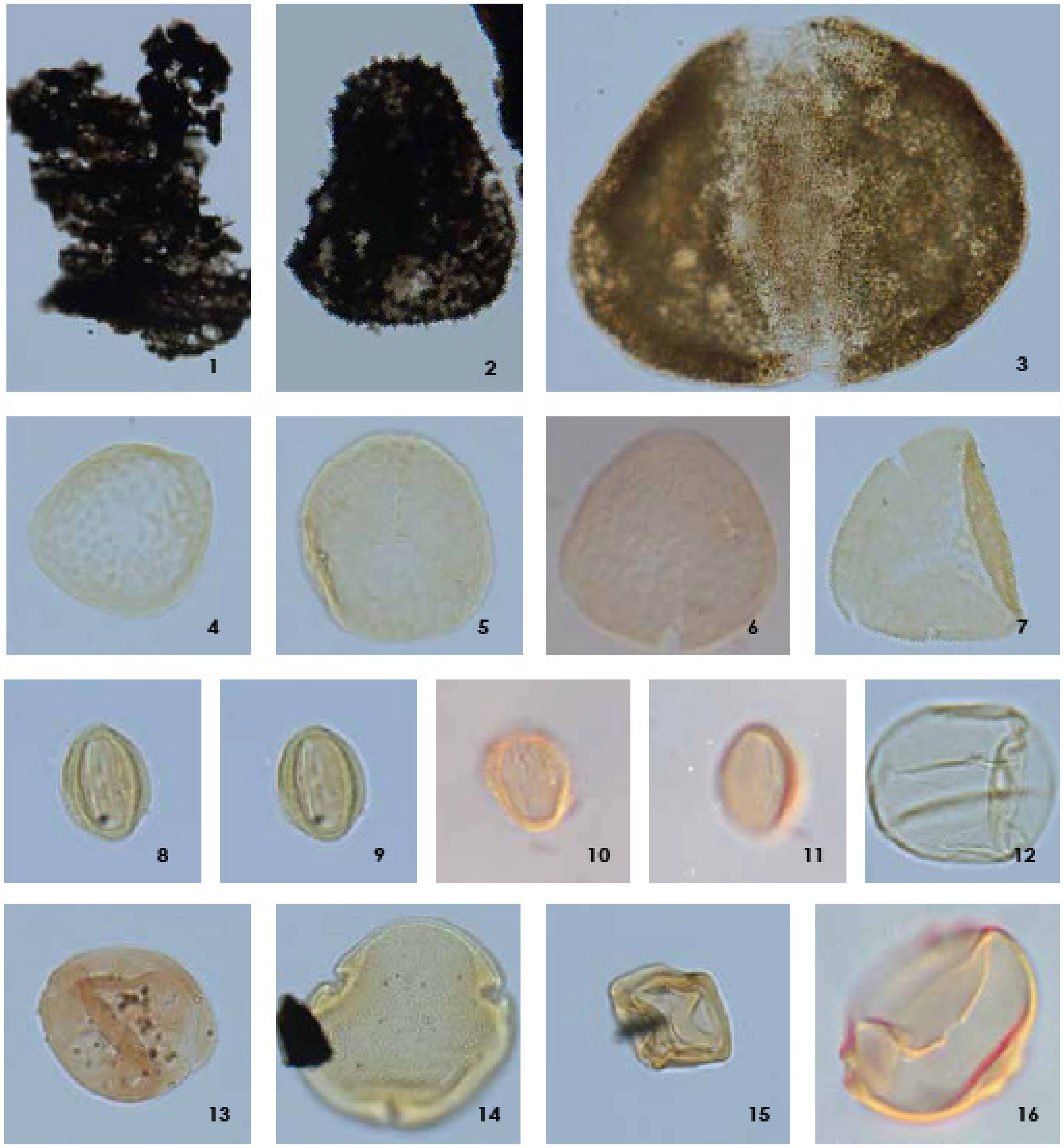

Plate 24. Light photomicrographs of key in situ pollen and spores species from sample DME-88-28, Taylor Valley, Antarctica. 1. Burnt organic matter, view #2, 9.6 x 125.2, 60x. 2. Thermally altered apiculate spore, reworked, view #1, 14.0 x 126.1, 60x. 3. Oxidized, reworked gymnosperm pollen, , view #2, 7.1 x 142.4, 60x. 4. *Coptospora* sp., view #2, 6.3 x 108.6, 60x. 5. *Triporoletes* sp., view #3, 7.4 x 135.3, 60x. 6. *Coptospor*a sp. DV3014, 100x. 7. *Triporoletes* sp., view #4, 10.9 x 142.0, 60x. 8-9. Tricolporate sp. A, views #1 and 4., 10.4 x 126.5, 60x. 10. Tricolporate sp. A, DV3015, 100x. 11. Tricolporate sp. A., DV3017, 100x. 12. Poaceae, view #5, 28.9 x 125.2, 60x. 13. Reworked Triporate pollen, view #1, 12.0 x 134.0, 60x. 14. *Tilia* sp., view #4, 10.9 x 137.7, 60x, laboratory contaminant. 15. *Alnus* sp., view #3, 12.0 x 145.5, 60x, laboratory contaminant. 16. *Betula* sp., DV3016, 100x, laboratory contaminant.

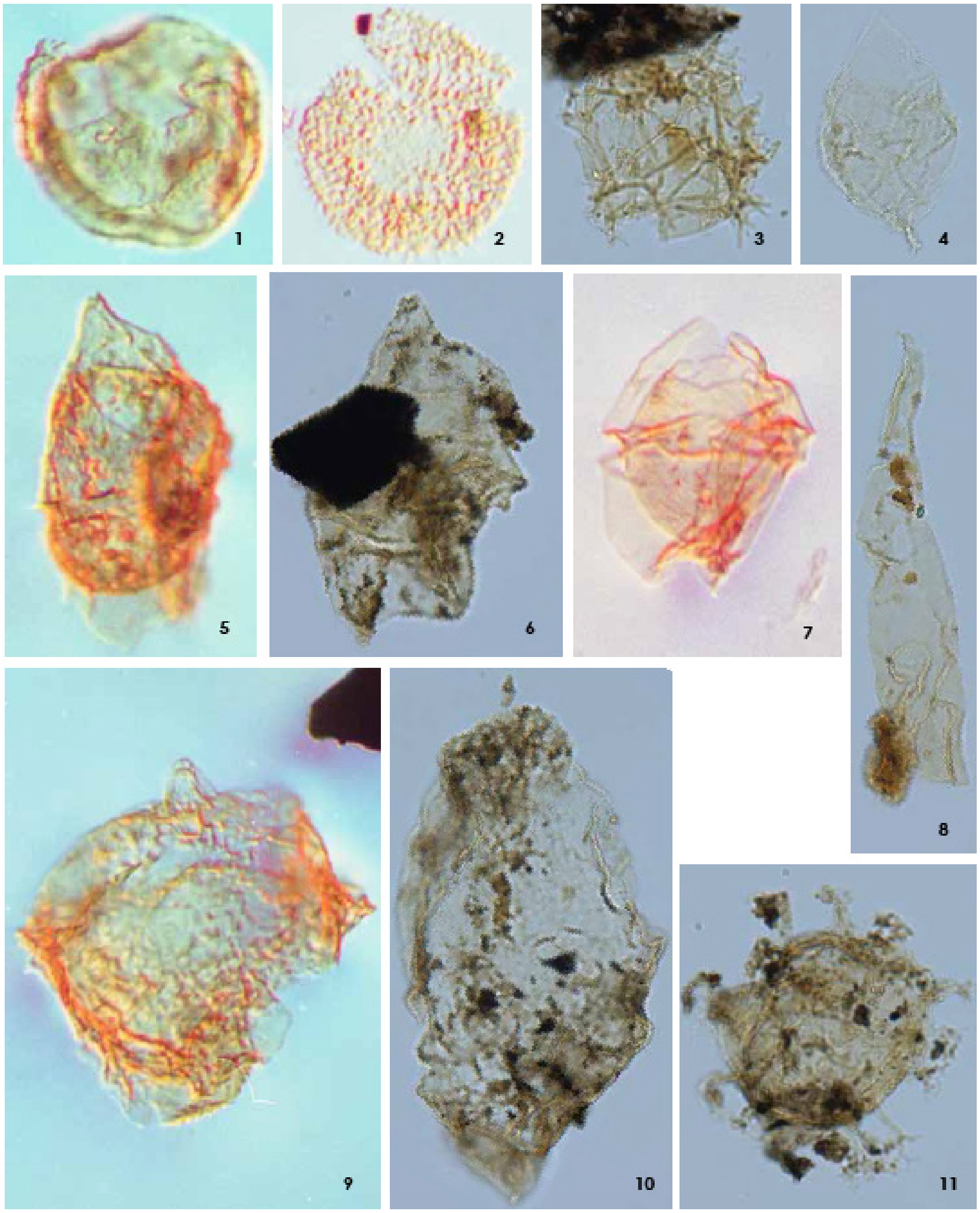

Plate 25. Light photomicrographs of key in situ marine palynomorph species from sample DME-88-28, Taylor Valley, Antarctica. 1. Unidentified dinoflatellate cyst, DV1023. 2. Possibly Circulodinium distinctum (range from 90.14 - 68.5 Ma), DV1022. 3. Unidentified dinoflatellate cyst, view #5, 15.5 x 130.6, 60x. 4. Possibly *Diconodinium* sp. (range from 122.10 - 70.0 Ma), view #3, 15.0 x 135.8, 60x. 5. Possibly *Isabelidinium cooksoniae* (range from 82 - 67.7 Ma), or *Chatangiella victoriensis*?, DV1019. 6. Possibly *Isabelidinium cooksoniae* (range from 82 - 67.7 Ma), view #1, 11.5 x 130.8, 60x. 7. Possibly *Subtilisphaera symperlucida* (range from 133 - 92 Ma), DV1020. 8. *Palaeocystodinium* ?*australiense*, view #1, 7.4 x 133.7, 60x. 9. Possibly *Apteodinium* sp. (range of genus from 143 - 68.80 Ma) or *Cribroperidinium* sp., DV2021. 10. Unidentified dinoflatellate cyst, view #1, 10.4 x 146.3, 60x. 11. Unidentified dinoflatellate cyst, view #3, 12.7 x 126.6, 60x.

CHAPTER 4: CONCLUSION

The results provided by this thesis aid in uncovering the vegetation and paleoclimate history of Antarctic history during the Miocene through the Pliocene by providing insight into where, what type of, and when vegetation existed in the Cenozoic around the Miocene to Pliocene. Observed palynological sample concentrations within the McMurdo Dry Valleys were predominantly barren or low values. Areas with large concentrations of palynomorphs are potential locations for where vegetation may have taken refuge. Samples DMI-97-14-2 Debris from Beacon Valley and samples DME-97-30, DME-97-31B, DME-97-32, DME-97-33, DME-97-35, DMS-97-28A, DMS-97-28C, DMS-97-28D, and DMS-97-32 from Victoria Valley have much higher concentrations than all the other samples and the locations from where these samples were collected may be locations for refugia. The type of vegetation that existed in these isolated pockets of refugia in Beacon Valley and Victoria Valley can be answered by looking at the palynological assemblage from each sample. DMI-97-14-2 Debris contains Coptospora sp. similar to the Victoria Valley samples, however DMI-97-14-2 Debris had a different angiosperm assemblage composed of Poaceae, Asteraceae, and *Chenopodipollis* sp. and lacked a marine or freshwater palynomorph assemblage. This assemblage indicates an environment predominantly experiencing low ground coverage including grasses and wild flowers with mosses. Victoria Valley samples have low diversity of terrestrial palynomorphs including bryophyte *Coptospora* sp. spores and angiosperm pollen grains including *Nothofagidites* sp. (fusca group) and Poaceae. This palynomorph assemblage consists of a low diversity tundra vegetation. The nonterrestrial palynomorph diversity of the Victoria Valley region was dominated by *Leiosphaeridia* sp. and Zygnemaceae sp. algal palynomorphs. *Leiospaeridia* sp. have been interpreted as sea ice indicators while Zygnemaceae have been interpreted as fresh water indicators. These results indicate that these samples were deposited when climate was cold and glaciated, as indicated by the presence of *Leiosphaeridia* sp., with vegetation limited to a tundra as indicated by the strong presence of in situ *Nothofagidities* sp. (fusca group) pollen. Meltwater pockets of freshwater existed in which in situ Zygnemaceae algae could grow. Radiometric dating and correlation between volcanic ash beds provide the basis for age control for this study and answer when vegetation existed in these refugia. From the previously mentioned dating methods, the potential refugia located in the Central Beacon Valley existed around 8.07 ± 0.06 Ma and around Mid-Miocene for Victoria Valley.

The results from this study may have been influenced by at least three factors. The first factor is that the locations within Beacon Valley and Victoria Valley may indeed have been refugia and provided hospitable environments for vegetation to survive while other locations investigated by this study could not support vegetation. The second factor is that Beacon Valley and Victoria Valley are the only locations where the recent geologic record has been preserved. Other locations might have been refugia as well, and sediments containing palynomorph rich sediment was eroded away. The third factor is that Beacon Valley and Victoria Valley results are artifacts of transportation processes depositing palynomorph rich sediment into these regions. However, three observations tend to refute this possibility. If the third factor were true, we would expect to see higher reworked assemblages within the samples, more varied assemblages and potential mixing between Beacon Valley and Victoria Valley sample assemblages, and the large clusters of *Nothofagus* pollen would be absent from the samples or broken up.

This study provides guidance for where future expeditions and studies should focus on when researching the McMurdo Dry Valleys. Beacon Valley and Victoria Valley appear promising in regards to being ideal locations additional studies. In order to further understand the timing of vegetation decimation within the McMurdo Dry Valleys more in depth investigations of these two regions is necessary.

REFERENCES:

Acton, G., Crampton, J., Di Vincenzo, G., Fielding, C. R., Florindo, F., Hannah, M., ... & Levy, R. (2008). Preliminary integrated chronostratigraphy of the AND-2A core, ANDRILL Southern McMurdo Sound project, Antarctica.

Anderson, J. B. (1999). *Antarctic marine geology*. Cambridge University Press.

Anderson, J. B., Warny, S., Askin, R. A., Wellner, J. S., Bohaty, S. M., Kirshner, A. E., ... & Lawver, L. A. (2011). Progressive Cenozoic cooling and the demise of Antarctica's last refugium. *Proceedings of the National Academy of Sciences*, 108(28), 11356-11360.

Armstrong, R. L. (1978). K-Ar dating: Late Cenozoic McMurdo volcanic group and dry valley glacial history, Victoria Land, Antarctica. *New Zealand Journal of Geology and Geophysics*, 21(6), 685-698.

Askin, R. A. (1992). Late Cretaceous–early Tertiary Antarctic outcrop evidence for past vegetation and climates. *The Antarctic Paleoenvironment: a perspective on global change: Part One*, 61-74.

Askin, R. A. (1997). Eocene–? earliest oligocene terrestrial palynology of Seymour Island, Antarctica. *The Antarctic Region: Geological Evolution and Processes*, 993(199), 7.

Askin, R. A. (2000). Spores and pollen from the McMurdo Sound erratics, Antarctica. *Paleobiology and Paleoenvironments of Eocene Rocks: McMurdo Sound, East Antarctica*, 161-181.

Askin, R. A., & Raine, J. I. (2000). Oligocene and Early Miocene terrestrial palynology of the Cape Roberts Drillhole CRP-2/2A, Victoria Land Basin, Antarctica. *Terra Antartica*, 7(4), 493-501.

Raine, J. I., & Askin, R. A. (2001). Terrestrial palynology of Cape Roberts Project Drillhole CRP-3, Victoria Land Basin, Antarctica. *Terra Antartica*, 8(4), 389-400.

Barrett, P. J. (1981). History of the Ross Sea region during the deposition of the Beacon Supergroup 400-180 million years ago. *Journal of the Royal Society of New Zealand*, 11(4), 447-458.

Behrendt, J. C., & Cooper, A. (1991). Evidence of rapid Cenozoic uplift of the shoulder escarpment

of the Cenozoic West Antarctic rift system and a speculation on possible climate forcing. *Geology*, 19(4), 315-319.

Cooper, A. K., & Davey, F. J. (Eds.). (1987). *The Antarctic continental margin: geology and geophysics of the western Ross Sea* (Vol. 5). Circum-Pacific Council for.

DeConto, R.M., and Pollard, D. (2003). Rapid Cenozoic glaciation of Antarctica induced by declining atmospheric CO_2. *Nature*, 421, 245–249.

Dettmann, M. E., Pocknall, D. T., Romero, E. J., Zamaloa M. D. C., 1990, *Nothofagidities* Erdtmanex Potonié, 1960; a catalogue of species with notes on the paleogeographic distribution of *Nothofagus* Bl. (Southern Beech): New Zealand, New Zealand Geological Survey, 1-52.

Doran, P. T., McKay, C. P., Clow, G. D., Dana, G. L., Fountain, A. G., Nylen, T., & Lyons, W. B. (2002). Valley floor climate observations from the McMurdo Dry Valleys, Antarctica, 1986–2000. *Journal of Geophysical Research: Atmospheres*, 107(D24).

Doran, P. T., Wharton Jr, R. A., & Lyons, W. B. (1994). Paleolimnology of the McMurdo dry valleys, Antarctica. *Journal of Paleolimnology*, 10(2), 85-114.

Elliot, D. H., & Fleming, T. H. (2004). Occurrence and dispersal of magmas in the Jurassic Ferrar large igneous province, Antarctica. *Gondwana Research*,7(1), 223-237.

Feakins, S., Warny, S., and DeConto, R., (2014). Snapshot of cooling and drying before onset of Antarctic Glaciation. Earth and Planetary Science Letters, 404: 154-166.

Feakins, S. J., Warny, S., & Lee, J. E. (2012). Hydrologic cycling over Antarctica during the middle Miocene warming. *Nature Geoscience*, 5(8), 557-560.

Fitzgerald, P. G. (1992). The Transantarctic Mountains of southern Victoria Land: the application of apatite fission track analysis to a rift shoulder uplift. *Tectonics*, 11(3), 634-662.

Fitzgerald, P. G. (1994). Thermochronologic constraints on post-Paleozoic tectonic evolution of the central Transantarctic Mountains, Antarctica.*Tectonics*, 13(4), 818-836.

Fitzgerald, P. G., & Gleadow, A. J. (1988). Fission-track geochronology, tectonics and structure of the Transantarctic Mountains in northern Victoria Land, Antarctica. *Chemical Geology: Isotope Geoscience section*, 73(2), 169-198.

Fitzgerald, P. G., & Gleadow, A. J. (1990). New approaches in fission track geochronology as a tectonic tool: Examples from the Transantarctic Mountains. *International Journal of Radiation Applications and Instrumentation. Part D. Nuclear Tracks and Radiation Measurements*, 17(3), 351-357.

Fitzgerald, P. G., Sandiford, M., Barrett, P. J., & Gleadow, A. J. (1986). Asymmetric extensionassociated with uplift and subsidence in the Transantarctic Mountains and Ross Embayment. *Earth and Planetary Science Letters*, 81(1), 67-78.

Fountain, A. G., Nylen, T. H., Monaghan, A., Basagic, H. J., & Bromwich, D. (2010). Snow in the McMurdo Dry Valleys, Antarctica. *International Journal of Climatology*, 30(5), 633-642.

Francis, J. E., Ashworth, A., Cantrill, D. J., Crame, J. A., Howe, J., Stephens, R., ... & Thorn, V. (2008, August). 100 million years of Antarctic climate evolution: evidence from fossil plants. In Antarctica: *A Keystone in a Changing World. Proceedings of the 10th International Symposium on Antarctic Earth Sciences*. The National Academies Press, Washington, DC, 19-27.

Gleadow, A. J. W., & Fitzgerald, P. G. (1987). Uplift history and structure of the Transantarctic Mountains: new evidence from fission track dating of basement apatites in the Dry Valleys area, southern Victoria Land. *Earth and Planetary Science Letters*, 82(1), 1-14.

Griener, K. W., Nelson, D. M., & Warny, S. (2013). Declining moisture availability on the Antarctic Peninsula during the Late Eocene. *Palaeogeography, Palaeoclimatology, Palaeoecology*, 383, 72-78.

Griener, K. and Warny, S., (2015). *Nothofagus* pollen grain size as a proxy for long-term climate change: an applied study on Antarctic Eocene, Oligocene, and Miocene cores. Review of Palaeobotany and Palynology, 221:138–143

Griener, K. W., Warny, S., Askin, R., & Acton, G. (2015). Early to middle Miocene vegetation history of Antarctica supports eccentricity-paced warming intervals during the Antarctic icehouse phase. *Global and Planetary Change*, 127, 67-78.

Harwood, D. M., Bohaty, S., & Scherer, R. (1998). Lower Miocene diatom biostratigraphy of theCRP-1 drillcore, McMurdo Sound, Antarctica. *Terra Antartica*, 5(3), 499-514.

Hill, R. S., & Scriven, L. J., 1995, The angiosperm-dominated woody vegetation of Antarctica: a

review. *Review of Palaeobotany and Palynology*, 86 (3), 175-198.

Levy, J. (2013). How big are the McMurdo Dry Valleys? Estimating ice-free area using Landsat image data. *Antarctic Science*, 25(1), 119-120.

Levy, R., Harwood, D., Florindo, F., Sangiorgi, F., Tripati, R., von Eynatten, H., ... & Fielding, C. (2016). Antarctic ice sheet sensitivity to atmospheric CO2 variations in the early to mid-Miocene. *Proceedings of the National Academy of Sciences*, 201516030.

Lewis, A. R., Marchant, D. R., Ashworth, A. C., Hedenäs, L., Hemming, S. R., Johnson, J. V., ... & Willenbring, J. K. (2008). Mid-Miocene cooling and the extinction of tundra in continental Antarctica. *Proceedings of the National Academy of Sciences*, 105(31), 10676-10680.

Marchant, D. R., Denton, G. H., Swisher, C. C., & Potter, N. (1996). Late Cenozoic Antarctic paleoclimate reconstructed from volcanic ashes in the Dry Valleys region of southern Victoria Land. *Geological Society of America Bulletin*, 108(2), 181-194.

Marchant, D. R., & Head, J. W. (2007). Antarctic dry valleys: Microclimate zonation, variable geomorphic processes, and implications for assessing climate change on Mars. *Icarus*, 192(1), 187-222.

Pagani, M., Huber, M., Liu, Z., Bohaty, S. M., Henderiks, J., Sijp, W., ... & DeConto, R. M. (2011). The role of carbon dioxide during the onset of Antarctic glaciation. *Science*, 334(6060), 1261-1264.

Prebble, J. G., Raine, J. I., Barrett, P. J., & Hannah, M. J. (2006). Vegetation and climate from two Oligocene glacioeustatic sedimentary cycles (31 and 24 Ma) cored by the Cape Roberts Project, Victoria Land Basin, Antarctica. *Palaeogeography, Palaeoclimatology, Palaeoecology*, 231(1), 41-57.

Pross, J., Contreras, L., Bijl, P. K., Greenwood, D. R., Bohaty, S. M., Schouten, S., ... & Huck, C. E. (2012). Persistent near-tropical warmth on the Antarctic continent during the early Eocene epoch. *Nature*, 488(7409), 73-77.

Raine, J. I. (1998). Terrestrial palynomorphs from Cape Roberts Project drillhole CRP-1, Ross Sea, Antarctica. *Terra Antartica*, 5(3), 539-548.

Roberts, A. P., Wilson, G. S., Harwood, D. M., & Verosub, K. L. (2003). Glaciation across the Oligocene–Miocene boundary in southern McMurdo Sound, Antarctica: new chronology from the CIROS-1 drill hole.*Palaeogeography, Palaeoclimatology, Palaeoecology*, 198(1), 113-130.

Stern, T. A., & ten Brink, U. S. (1989). Flexural uplift of the Transantarctic Mountains. *Journal of Geophysical Research: Solid Earth*, 94(B8), 10315-10330.

Thomson, M. R. A., Crame, J. A., & Thomson, J. W. (1991). *Geological evolution of Antarctica* (Vol. 1). Cambridge University Press.

Ten Brink, U. S., Bannister, S., Beaudoin, B. C., & Stern, T. A. (1993). Geophysical investigations of the tectonic boundary between East and West Antarctica. *SCIENCE-NEW YORK THEN WASHINGTON-*, 261, 45-45.

Truswell, E. M., & Macphail, M. K. (2009). Polar forests on the edge of extinction: what does the fossil spore and pollen evidence from East Antarctica say?. *Australian Systematic Botany*, 22(2), 57-106.

Warny, S., Wrenn, J. H., Bart, P. J., & Askin, R. (2006). Palynology of the NBP03–01A transect in the Northern Basin, western Ross Sea, Antarctica: A late Pliocene record. *Palynology*, 30(1), 151-182.

Warny, S., Askin, R. A., Hannah, M. J., Mohr, B. A., Raine, J. I., Harwood, D. M., & Florindo, F. (2009). Palynomorphs from a sediment core reveal a sudden remarkably warm Antarctica during the middle Miocene. *Geology*, 37(10), 955-958.

Warny, S., & Askin, R. (2011a). Vegetation and Organic-Walled Phytoplankton at the End of the Antarctic Greenhouse World: Latest Eocene Cooling Events. *Tectonic, climatic, and cryospheric evolution of the Antarctic peninsula*, 193-210.

Warny, S., & Askin, R. (2011b). Last Remnants of Cenozoic Vegetation and Organic-Walled Phytoplankton in the Antarctic Peninsula's Icehouse World. *Tectonic, climatic, and cryospheric evolution of the Antarctic peninsula*, 167-192.

Warny, S., Kymes, C. M., Askin, R. A., Krajewski, K. P., & Bart, P. J. (2016). Remnants of Antarctic vegetation on King George Island during the early Miocene Melville Glaciation. *Palynology*, 40(1), 66-82.

Zachos, J., Pagani, M., Sloan, L., Thomas, E., & Billups, K. (2001). Trends, rhythms, and aberrations in global climate 65 Ma to present. *Science*, 292(5517), 686-693.

Zachos, J. C., Dickens, G. R., & Zeebe, R. E. (2008). An early Cenozoic perspective on green¬house warming and carbon-cycle dynamics. Nature, 451(7176), 279-283.

VITA

David Rau was born in Lafayette, Louisiana in 1991, and has spent most of his formative years in Slidell, Louisiana. Since 2010 he has lived in Baton Rouge, Louisiana pursuing higher education. He graduated from Louisiana State University in Baton Rouge, Louisiana in 2014 with a B.S. in Geology. After completing his undergraduate career, he went on to pursue his Master's degree in Geology at Louisiana State University. Upon Completing his Master's, he plans on pursuing a career in the oil and gas industry.